

Phase Equilibria at High Temperatures

Michael E. Fleet

*Department of Earth Sciences
University of Western Ontario
London, Ontario N6A 5B7, Canada
e-mail: mfleet@uwo.ca*

INTRODUCTION

The wide variety of metal sulfide structures and their accommodation of atomic substitution, non-stoichiometry and metal-metal (*M-M*) and ligand-ligand interactions allows for diverse physical, chemical and electronic properties. The energy band structure of 3*d* transition-metal sulfides, in particular, is strongly influenced by the covalence of metal-S bonds, which results in hybridization of S 3*p* and metal 3*d* bonding states and direct or indirect *M-M* bonding interactions in favorable cases. Differences in the phase relations of isostructural metal sulfides are often attributable to subtle changes in electronic states. The literature on metal sulfide phase relations relevant to the earth sciences is very extensive and could not possibly be summarized in a single chapter. Therefore, following Craig and Scott (1974), this chapter focuses on the base metal (Fe, Co, Ni, Cu, and Zn) sulfides, with the literature for other metal chalcogenides and pnictides and some sulfosalts summarized in a single table (Table 1). The relevant phase relations of the platinum-group element (PGE) chalcogenides and pnictides have been comprehensively reviewed in Makovicky (2002). A section on the halite structure sulfides (ninningerite, alabandite and oldhamite) is also included in this chapter. The material presented here relates closely to that discussed in other chapters, in particular the chapter on sulfide thermochemistry (Sack and Ebel 2006). The importance of understanding phase equilibria in the context of electronic and magnetic properties and, hence, electronic structure is also emphasized, thereby reinforcing material presented in several other chapters (Pearce et al. 2006; Vaughan and Rosso 2006).

Abbreviations used for mineral/phase names include: tr- troilite; po- pyrrhotite; hpo- hexagonal pyrrhotite; mpo- monoclinic pyrrhotite; py- pyrite; pn- pentlandite; hpn- high pentlandite; vs- vaesite; *mss*- (Fe,Ni) monosulfide solid solution; cv- covellite; al- anilite; ya- yarrowite; dg- digenite; cc- chalcocite; bn- bornite; nk- nukundamite; cp- chalcopyrite; tal- talnakhite; mh- mooihoekite; hc- haycockite; cb- cubanite; *iss*- intermediate solid solution; sp- sphalerite; wz- wurtzite; and *nss*- niningerite solid solution.

Fe, Co AND Ni SULFIDES AND THEIR MUTUAL SOLID SOLUTIONS

The sulfides of the ferrous metal triad (Fe, Co and Ni) include pyrite (the most common sulfide in the crust), troilite (the most common sulfide in the solar system), pyrrhotite (important in magmatic and massive sulfide ore bodies), and the ternary Fe-Ni-S monosulfide solid solution (*mss*) (important in the genesis of magmatic sulfide ores). The numerous low-temperature iron sulfide phases, which are of particular importance in aqueous and environmental geochemistry, are discussed in detail in other chapters. The progression of solid state properties and similarity in crystal structures and phase relations necessitates some degree of parallel discussion for equivalent phases in the Fe-S, Co-S and Ni-S binary systems.

Table 1. Summary of studies on sulfide phase relations relevant to Earth sciences.

System	Compound	Mineral/(Notes)	Stability, T_{\max} (°C)	References
Ag-S	Ag ₂ S	acanthite	177	Kracek (1946); Roy et al. (1959);
	Ag ₂ S	argentite	586-622	Taylor (1969); Bell and Kullerud
	Ag ₂ S		838	(1970)
As-S	AsS	realgar	307	Clark (1960a,b); Barton (1969);
	AsS		265	Kirkinskiy et al. (1967); Hall (1966);
	As ₂ S ₃	orpiment	315	Nagao (1955)
	As ₂ S ₃		170	
	As ₄ S ₃	dimorphite (a)		
Bi-S	Bi ₂ S ₃	bismuthinite	760	Van Hook (1960); Cubicciotti (1962,
	BiS ₂	(high <i>P</i>)		1963); Silverman (1964); Craig et al. (1971)
Ca-S	see text			
Cd-S	CdS	hawleyite		Corrl (1964); Miller et al. (1966);
	CdS	greenockite	1475	D'sugi et al. (1966); Trail and Boyle (1955); Yu and Gidisse (1971); Boer and Nalesnik (1969)
Co-S	Co ₃ S ₃		780-930	Rosenqvist (1954); Curlook and
	Co ₉ S ₈	cobalt pentlandite	832	Pidgeon (1953); Kuznetsov et al.
	Co ₁₋₃ S	jaipurite	460-1181	(1965)
	Co ₃ S ₄	linnaeite	660	
	CoS ₂	cattierite	950	
Cr-S	CrS		330	Bunch and Fuchs (1969); Jellinek
	CrS		570	(1957); Hansen and Anderko (1958)
	CrS		~1650	
	Cr ₃ S ₄	brezinaite		
	Cr ₂ S ₃		~1100	
Cu-S	see text			
Fe-S	see text			
Hg-S	HgS	(high <i>P</i>)		Dickson and Tunell (1959); Potter
	Hg ₁₋₃ S	cinnabar	316-345	and Barnes (1971); Kullerud (1965b);
	Hg ₁₋₃ S	metacinnabar	572	Mariano and Warekois (1963); Scott and Barnes (1969); Barnes (1973); Potter (1973)
Mg-S	see text			
Mn-S	MnS	alabandite	1610	Skinner and Luce (1971); Keil and
	MnS	(high <i>P</i>)		Snetsinger (1967)
	MnS ₂	haverite	423	
Mo-S	Mo ₂ S ₃		>610	Bell and Herfert (1957); Morimoto
	MoS ₂	molybdenite (h)	~1350	and Kullerud (1962); Clark (1970b,
	MoS ₂	molybdenite (r)	~1350	1971); Zelikman and Belyaerskaya (1956); Graeser (1964)
MoS ₂	jordisite (a)			
Ni-S	see text			
Os-S	OsS ₂	erlichmanite		Snetsinger (1971); Sutarno et al. (1967); Ying-chen and Yu-jen (1973)
Pb-S	PbS	galena	1115	Kullerud (1969); Bloem and Kroger (1956); Stubbles and Birchenall (1959)
Pt-S	PtS	cooperite		Richardson and Jeffes (1952);
	PtS ₂			Hansen and Anderko (1958); Cabri (1972); Grønvold et al. (1960)
Ru-S	RuS ₂	laurite		Ying-chen and Yu-jen (1973); Leonard et al. (1969); Sutarno et al. (1967)

table continued on following page

Table 1. continued from previous page

System	Compound	Mineral/(Notes)	Stability, T_{\max} (°C)	References
Sb-S	Sb ₂ S ₃	stibnite	556	Pettit (1964); Barton (1971); Clark (1970d)
	Sb ₂ S _{3-x}	meta-stibnite (a)		
Sn-S	β-SnS	herzenbergite	600	Moh (1969); Albers and Schol (1961); Karakhanova et al. (1966);
	α-SnS		880	Rau (1965); Moh and Berndt (1964);
	δ-Sn ₂ S ₃	ottemannite	661-675	Mootz and Puhl (1967)
	δ-Sn ₂ S ₃		710-715	
	β-Sn ₂ S ₃		744-753	
	α-Sn ₂ S ₃		760	
	β-SnS ₂	berndtite	680-691	
	α-SnS ₂		865	
Ti-S	Ti ₂ S			Franzen et al. (1967); Viaene and
	TiS		>800	Kullerud (1971); Wiegers and
	Ti ₈ S ₉			Jellinek (1970)
	Ti ₄ S ₅			
	Ti ₃ S ₄			
	TiS ₂			
	TiS ₃		>610	
V-S	V ₃ S			Chevreton and Sapet (1965);
	VS			Baumann (1964); Shunk (1969)
	V ₃ S ₄			
	~V ₂ S ₃			
	VS ₄	patronite		
Zn-S	See text			
Ag-As-S	Ag ₇ AsS ₆	As-billingsleyite	575	Toulmin (1963); Hall (1966, 1968);
	Ag ₅ AsS ₄	As-stephanite	361	Roland (1968, 1970); Wehmeier et al. (1968)
	Ag ₃ AsS ₃	proustite	495	
	Ag ₃ AsS ₃	xanthocanite	192	
	δ-AgAsS ₂	smithite	415	
	δ-AgAsS ₂	trechmannite	225	
	α-AgAsS ₂		415-421	
Ag-Au-S	Ag ₃ AuS ₂		181	Graf (1968); Barton and Toulmin (1964)
Ag-Bi-S	β-AgBiS ₂	matildite	195	Schenck et al. (1939); Van Hook (1960); Craig (1967); Karup-Møller (1972)
	α-AgBiS ₂		195-801	
	AgBi ₃ S ₅	pavonite	732	
Ag-Cu-S	Cu _{0.45} Ag _{1.55} S	jalpaite	117	Djurle (1958); Skinner (1966); Graf (1968); Skinner et al. (1966); Suhr (1965); Krestovnikov et al. (1968); Valverde (1968); Werner (1965)
	Cu _{0.8} Ag _{1.2} S	mckinstiyite	94	
	AgCu _{1+x} S	stromeyerite	93	
Ag-Cu-Pd-Bi-S		pavonite, benjaminit ¹		Chang et al. (1988)
Ag-Fe-S	AgFe ₂ S ₃	argentopyrite	152	Czamanske (1969); Czamanske and Larson (1969); Taylor (1970a,b)
	AgFe ₂ S ₃	sternbergite	152	
	Ag ₃ Fe ₇ S ₁₁	argyropyrite		
	Ag ₂ Fe ₅ S ₈	frieseite		
Ag-Pb-S				Vogel (1953); Van Hook (1960); Craig (1967).
Ag-Sb-S	Ag ₇ SbS ₆	Sb-billingsleyite	475	Barstad (1959); Somanchi (1963);
	Ag ₅ SbS ₄	stephanite	197	Toulmin (1963); Chang (1963);
	Ag ₃ SbS ₃	pyrargyrite	485	Cambi and Elli (1965); Hall (1966, 1968); Keighin and Honea (1969);
	Ag ₃ SbS ₃	pyrostilpnite	192	Wehmeier et al. (1968)
	AgSbS ₂	miargyrite	380	
	β-AgSbS ₂		510	
Ag-Sn-S				Sugaki et al. (1985)
As-Co-S	CoAsS	cobaltite		Bayliss (1969); Gammon (1966); Klemm (1965)

table continued on following page

Table 1. continued from previous page

System	Compound	Mineral/(Notes)	Stability, T_{\max} (°C)	References
As-Cu-S	Cu ₃ AsS ₄	luzonite	275-320	Maske and Skinner (1971); Gaines (1957)
	Cu ₃ AsS ₄	enargite	671	
	Cu ₂₄ As ₁₂ S ₃₁		578	
	Cu ₆ As ₄ S ₉	sinnerite	489	
	Cu ₁₂ AsS ₁₃	tennantite	665	
	CuAsS	lautite		
As-Fe-S	FeAsS	arsenopyrite	702	Clark (1960a,b); Morimoto and Clark (1961); Barton (1969); Kretschmar and Scott (1976)
As-Ni-S	NiAsS	gersdorffite	>700	Yund (1962); Klemm (1965); Bayliss (1968)
As-Pb-S	Pb ₉ As ₄ S ₁₅	gratonite	250	Rosch and Hellner (1959); Le Bihan (1963); Kutoglu (1969); Burkart-Baumann et al. (1972); Chang and Bever (1973)
	Pb ₉ As ₄ S ₁₅	jordanite	549	
	Pb ₂ As ₂ S ₅	dufrenoyite	485?	
	Pb ₁₉ As ₂₆ S ₅₈	rathite II	474	
	PbAs ₂ S ₄	sartorite	305	
As-Sb-S	AsSbS ₃	getchellite	345	Weissberg (1965); Moore and Dixon (1973); Craig et al. (1974); Dickson et al. (1974); Radtke et al. (1973)
	(As,Sb) ₁₁ S ₁₈	wakabayashilite		
	AsSb ₂ S ₂		538	
As-Tl-S	Tl ₃ AsS ₃			Canneri and Fernandes (1925); Graeser (1967); Radtke et al. (1974a,b)
	Tl ₄ As ₂ S ₅			
	Tl ₆ As ₄ S ₉			
	TlAsS ₂	lorandite	~300	
Bi-Cu-S	Cu ₉ BiS ₆		~375-650	Vogel (1956); Buhlmann (1965); Sugaki and Shima (1972); Godovikov and Ptit'syn (1968); Godovikov et al. (1970); Buhlmann (1971); Sugaki et al. (1972)
	Cu ₃ BiS ₃	wittichenite	527	
	Cu ₆ Bi ₄ S ₉			
	Cu ₂₄ Bi ₂₆ S ₅₁	empletite	~360	
	Cu ₂₄ Bi ₂₆ S ₅₁	cuprobismutite	474	
	Cu ₃ Bi ₅ S ₉		442-620	
	CuBi ₃ S ₅		649	
Cu ₃ Bi ₃ S ₇		~498		
Bi-Fe-S	FeBi ₄ S ₇		608-719	Urazov et al. (1960); Sugaki et al. (1972); Ontoev (1964)
Bi-Mo-S				Stemprok (1967)
Bi-Ni-S	Ni ₃ Bi ₂ S ₂	parkerite	>400	Schenck and von der Forst (1939); Fleet (1973); DuPreez (1945); Peacock and McAndrew (1950); Brower et al. (1974)
Bi-Pb-S	Pb ₁₀ AgBi ₅ S ₁₈	heyrovskyite	829	Schenck et al. (1939); Van Hook (1960); Craig (1967); Salanci (1965); Otto and Strunz (1968); Salanci and Moh (1969); Klominsky et al. (1971); Chang and Bever (1973)
	Pb ₃ Bi ₂ S ₆	lillianite	816	
	PbBi ₂ S ₄	galenobismutite	750	
	Pb ₂ Bi ₂ S ₅	cosalite	<450	
	Pb ₅ Bi ₄ S ₁₁	bursaite		
	PbBi ₄ S ₇	bonchevite		
	PbBi ₆ S ₁₀	ustarasite		
Bi-Sb-S	(Bi,Sb) ₂ S ₃		>200	Hayase (1955); Springer (1969); Springer and LaFlamme (1971)
Bi-Se-S	Bi ₄ (S,Se) ₃	ikunolite		Kato (1959); Markham (1962); Godovikov and Il'yasheva (1971)
Bi-Te-S	Bi ₂ Te _{1.5+x} S _{1.5-x}	δ-tetradymite		Beglaryan and Abrikasov (1959); Godovikov et al. (1970); Yusa et al. (1979)
	Bi ₂ Te _{2+x} S _{1-x}	β-tetradymite		
	Bi ₈ Te ₇ S ₅			
	Bi ₁₈ (TeS ₃) ₃	joseite-C		
	Bi ₉ (Te ₂ S ₂)			
	Bi ₁₅ (TeS ₄)			

table continued on following page

Table 1. continued from previous page

System	Compound	Mineral/(Notes)	Stability, T_{\max} (°C)	References
Ca-Fe-S	see text			
Ca-Mg-S	see text			
Ca-Mn-S	see text			
Cd-Mn-S	(Pb,Cd)S			Bethke and Barton (1961, 1971)
Cd-Zn-S	(Zn,Cd)S			Hurlbut (1957); Bethke and Barton (1971)
Co-Cu-S	CuCo ₂ S ₄	carrollite	>600	Williamson and Grimes (1974); Clark (1974)
Co-Fe-S	see text			
Co-Ni-S	(Co,Ni) _{1-x} S (Co,Ni) ₃ S ₄ (Co,Ni)S ₂			Klemm (1962, 1965); Delafosse and Can Hoang Van (1962); Bouchard (1968)
Co-Sb-S	CoSbS CoSbS	paracostibite costibite	876 <100?	Lange and Schlegel (1951); Cabri et al. (1970a,b)
Cr-Fe-S	Cr ₂ FeS ₄ (Cr,Fe) _{1-x} S	daubreelite ²	>740	El Goresy and Kullerud (1969); Vogel (1968); Bell et al. (1970)
Cu-Fe-S	see text			
Cu-Fe-Bi-S				Sugaki et al. (1984)
Cu-Fe-Sn-S				Ohtsuki et al. (1981a,b)
Cu-As-Sb-S				Sugaki et al. (1982)
Cu-Fe-Zn-Sn-S				Moh (1975)
Cu-Ga-S	CuGaS ₂	gallite		Strunz et al. (1958); Ueno et al. (2005)
Cu-Ge-S				Wang (1988)
Cu-Mo-S				Grover and Moh (1969)
Cu-Ni-S	CuNi ₂ S ₆	villamaninite	503	Kullerud et al. (1969); Bouchard (1968)
Cu-Pb-S	Cu ₁₄ Pb ₂ S _{9-x}		486-528	Schuller and Wohlmann (1955); Craig and Kullerud (1968); Clark and Sillitoe (1971)
Cu-Sb-S	Cu ₃ SbS ₄ CuSbS ₂ Cu _{12+x} Sb _{4+y} S ₁₃ Cu ₃ SbS ₃	famatinite chalcocostibite tetrahedrite skinnerite	627 553 543 607	Avilov et al. (1971); Skinner et al. (1972); Tatsuka and Morimoto (1973); Karup-Møller and Makovicky (1974)
Cu-Sn-S	Cu ₂ SnS ₃			Wang (1974); Roy-Choudhury (1974)
Cu-V-S	Cu ₃ VS ₄	sulvanite		Dolanski (1974)
Cu-W-S				Moh (1973)
Cu-Zn-S	~Cu ₃ ZnS ₄			Craig and Kullerud (1973); Clark (1970c)
Cu-Zn-Cd-Sn-S		kesterite, černyite, mohite, sphalerite, wurtzite and greenockite		Osadchii (1986)
Fe-Cr-S		daubréelite		Balabin et al. (1986)
Fe-Ga-S		c, h, t ternary phases		Ueno and Scott (1994)
Fe-Ge-S	Fe ₂ GeS ₄		>800	Viaene (1968, 1972)
Fe-Mg-S	see text			
Fe-Mn-S	see text			
Fe-Mo-S	FeMo ₃ S ₄			Kullerud (1967a); Grover and Moh (1966); Lawson (1972); Grover et al. (1975)
Fe-Ni-S	see text			
Fe-Os-S				Karup-Møller and Makovicky (2002)
Fe-Pb-S				Brett and Kullerud (1967)
Fe-Pb-Bi-S				Chang and Knowles (1977)

table continued on following page

Table 1. continued from previous page

System	Compound	Mineral/(Notes)	Stability, T_{\max} (°C)	References
Fe-Pb-Sb-S	$\text{Pb}_8\text{Fe}_2\text{Sb}_{12}\text{S}_{28}$	jamesonite, etc.		Chang and Knowles (1977); Bortnikov et al. (1981)
Fe-Sb-S	FeSb_2S_4	berthierite	563	Barton (1971)
	FeSbS	gudmundite	280	Clark (1966)
Fe-Sn-S				Stemprok (1971)
Fe-Ti-S	FeTi_2S_4		>1000	Plovnick et al. (1968); Hahn et al. (1965); Keil and Brett (1974); Viaene and Kullerud (1971)
	FeTi_2S_4		540	
	$\text{Fe}_{1+x}\text{Ti}_2\text{S}_4$	heideite		
Fe-W-S				Stemprok (1971); Grover and Moh (1966)
Fe-Zn-S	see text			
Fe-Zn-Ga-S	$(\text{Zn,Fe,Ga})_{1-x}\text{S}$	sphalerite/wurtzite phases		Ueno et al. (1996)
Hg-Sb-S	HgSb_4S_8	livingstonite	451	Learned (1966); Tunell (1964); Learned et al. (1974)
Pb-Sb-S				Wang, (1973); Kitakaze et al. (1995)
Pb-S-Se-Te				Liu and Chang (1994)
Pd-Co-S				Karup-Møller (1985)
Pd-Pt-Sn				Shelton et al. (1981)

Notes: 1. three other quinary solid solutions; 2. >14 kbar; 3. c- cubic, t- tetragonal, h- hexagonal, r- rhombohedral, a- amorphous

The phase diagrams for these three systems are similar, differing principally in the presence of metal-excess sulfides and the greater thermal stability of the low-spin pyrite phases in the Co-S and Ni-S systems (Fig. 1). This section is organized into the following topics: monosulfides of Fe, Co and Ni, binary phase relations in the systems Fe-S and Ni-S, the system Fe-Co-S, and ternary phase relations in the system Fe-Ni-S.

Monosulfides of Fe, Co and Ni

Electronic configuration and magnetism. The mineral phases of end-member (or near end-member) composition are troilite (FeS) and jaipurite (Co_{1-x}S) (both with NiAs-type or derivative structures) and millerite (NiS). The NiAs-type phase $\alpha\text{-Ni}_{1-x}\text{S}$ encountered in the Ni-S system has not been reported as a mineral: in synthesis experiments, it inverts to millerite at the stoichiometric composition, but persists as a metastable phase at room temperature on quenching. The crystal structures, electrical and magnetic properties and energy band diagrams of NiAs-type and derivative phases have been extensively studied using conventional laboratory techniques (e.g., Vaughan and Craig 1978; Gopalakrishnan et al. 1979; King and Prewitt 1982; Anzai 1997; Raybaud et al. 1997; Hobbs and Hafner 1999), but details remain controversial. The NiAs-type substructure (space group $P6_3/mmc$) of metal monosulfides has the metal (M) and S atoms in six-fold coordination to nearest neighbors; the metal atom is in octahedral coordination with S (site symmetry $\bar{3}m$), and S is in trigonal prismatic coordination with the metal ($\bar{6}m2$). The metal and S atoms form alternate layers normal to the c -axis, with the S layers hexagonal closest packed and metals in octahedral interstices. A key feature of the NiAs-type structure is the sharing of MS_6 octahedral faces along the c -axis which permits both a direct M - M interaction via either metal $3d(t_{2g})$ or metal $3d(e_g)$ orbitals and an indirect M - S - M interaction via hybridized S $3p$ (or S $3d$) and metal $3d(e_g)$ orbitals. At high-temperature, metal-deficient monosulfides ($M_{1-x}\text{S}$) have vacancies in metal positions which are randomly distributed in individual layers of metal atoms normal to c -axis. The $3d$ electron

(a)

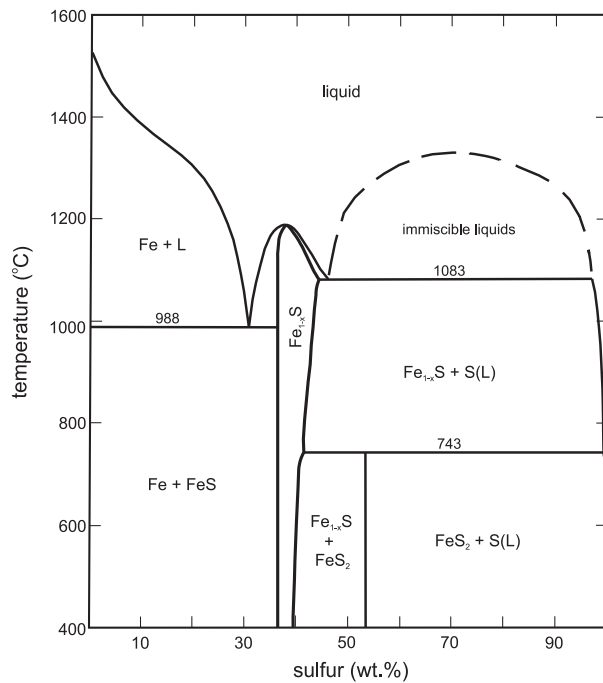
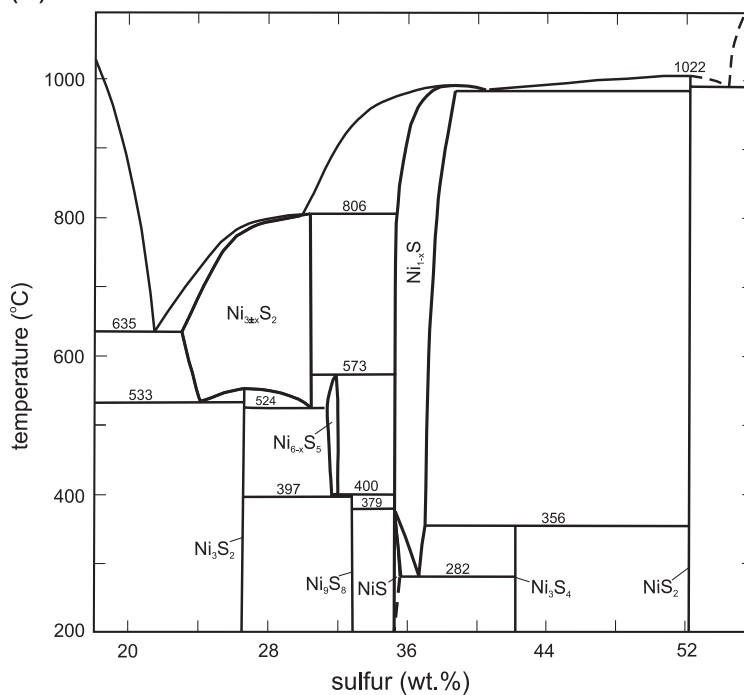


Figure 1. (a) Phase relations in the Fe-S system above 400 °C (after Kullerud et al. 1969); and (b) phase relations in the Ni-S system above 200 °C and from 18 to 56 wt% sulfur (after Kullerud and Yund 1962; Fleet 1988). All phases and phase assemblages coexist with vapor.

(b)



configurations of divalent Fe, Co and Ni monosulfides with the NiAs-type or derivative structure are well understood from the magnetic behavior of these compounds. Stoichiometric FeS is antiferromagnetic at room temperature (*RT*; troilite), but paramagnetic above 147 °C. Iron has the high spin $t_{2g}^4 - e_g^2$ configuration with the majority spin (\uparrow) t_{2g}^α and e_g^α bands filled, minority spin (\downarrow) t_{2g}^β band half filled and minority spin (\downarrow) e_g^β band empty. Co_{1-x}S is Pauli paramagnetic at room temperature, and Co has the low spin $t_{2g}^6 - e_g^1$ electronic configuration, with majority spin (\uparrow) t_{2g}^α and minority spin (\downarrow) t_{2g}^β bands filled, majority spin (\uparrow) e_g^α band half filled and minority spin (\downarrow) e_g^β band empty. α -NiS is paramagnetic at room temperature and antiferromagnetic below -13 °C (White and Mott 1971; Townsend et al. 1971), and Ni has the high spin $t_{2g}^6 - e_g^2$ configuration, with majority spin (\uparrow) t_{2g}^α and e_g^α and minority spin (\downarrow) t_{2g}^β bands filled, and the minority spin (\downarrow) e_g^β band empty.

Stoichiometric FeS (troilite) is a small band gap semiconductor, but the nature of this band gap and of the metallic behavior above 147 °C is controversial (Marfunin 1979; King and Prewitt 1982; Sakkopoulos et al. 1984; Tossell and Vaughan 1992; Shimada et al. 1998), because electron delocalization through overlap of the half-filled t_{2g}^β and empty e_g^β bands is prohibited by symmetry. Goodenough (1967) recognized that trigonal distortion of the face-shared FeS_6 octahedra could split the t_{2g}^β levels below 147 °C into narrow bands parallel (Γ_1) and normal (Γ_{II}) to the *c*-axis, and thus directly account for the energy gap; partial overlap of the (Γ_1) and (Γ_{II}) bands at the transition temperature would explain the metallic behavior at higher temperature. Although recent density of states (DOS) studies invoke extensive hybridization of S $3p$ and metal $3d$ states and attribute the metallic behavior to *M-S-M* π bonding. Metallic behavior in Co_{1-x}S and NiS is generally attributed to delocalization of e_g^α electrons through overlap of the e_g^α and e_g^β bands. Fujimori et al. (1990) indicated that a shift to lower X-ray photoelectron (XPS) binding energy should be expected as the metal-nonmetal transition is approached, consistent with closure of the energy band gap. Coey and Roux-Buisson (1979) pointed to a sudden decrease in the Mössbauer hyperfine field and isomer shift for $(\text{Ni}_{1-x}\text{Fe}_x)\text{S}$ ($x = 0.1-0.2$) at the temperature of the metal-nonmetal transition of NiS and discounted the possibility of this being a high-spin to low-spin transition. Nakamura et al. (1993) invoked Ni($3d$)-Co($3d$) charge transfer across the shared MS_6 octahedral faces to explain the contrasting effects of substitution by Co and Fe on the metal-nonmetal transition (at -13 °C) in NiS. Impurities and vacancies in these compounds tend to lower the metal-nonmetal transition temperature due to broadening of the S $3p$ bandwidth with decreasing S-S bond distances (Matoba et al. 1994). The effect of metal vacancies on magnetic ordering and metallic behavior of $(\text{Fe,Ni})_{1-x}\text{S}$ solid solutions has been studied by Vaughan and Craig (1974). Most studies show that metallic character increases in the sequence $\text{Co}_{1-x}\text{S} > \text{NiS} > \text{FeS}$, and is associated with progressive increase in covalence and decrease in metal $3d$ electron interaction energy. This trend correlates nicely with the progressive downward shift in the metal-nonmetal transition, from 147 °C for FeS, to -13 °C for NiS, and not detected at cryogenic temperatures for CoS.

FeS. The phase relations of stoichiometric FeS are complex. The phase stable at room temperature and pressure is troilite, which has a NiAs-type derivative structure, with space group $P6_2c$ and $a = (3)^{1/2}A$, $c = 2C$ (Bertaut 1956), where A and C are the unit-cell parameters for the hexagonal NiAs-type subcell and are approximately 3.4 and 5.9 Å, respectively. Troilite is stable up to 147 °C at 1 bar. The first order transition (known as the α transition) is well defined by changes in entropy (Robie et al. 1978), electrical conductivity (Gosselin et al. 1976a), and magnetic susceptibility (Horwood et al. 1976). The α transition has been investigated by X-ray powder diffraction (Haraldsen 1941; Grønvold and Haraldsen 1952; Taylor 1970c), neutron powder diffraction (Andresen 1960), and selected area electron diffraction (Putnis 1974). All of these researchers concluded that troilite transforms to FeS with NiAs-derivative structure; Putnis (1974) reporting a $2A, 1C$ superstructure. On the other hand, single-crystal X-ray diffraction study revealed instead a MnP-type phase with space group $Pnma$ and a diffraction pattern very similar to that of a NiAs-type phase, corresponding to $a = C$, $b = A$

and $c = (3)^{1/2}A$ (cf. Tremel et al. 1986). However, this tritwinned MnP structure was apparently excluded by detailed study of the α transition in Keller-Besrest and Collin (1990a,b). *In situ* single-crystal X-ray diffraction pointed to a 2A,1C structure in space group $P6_3mc$. Later, Kruse (1992) investigated the α transition in a natural troilite with ~ 0.17 wt% Cr using *in situ* X-ray diffraction and Mössbauer spectroscopy, and assuming the high-temperature phase to be of MnP type. Like Keller-Besrest and Collin (1990b), he found that the transformation of troilite takes place over a wide interval in temperature, of at least 40 °C: also, the reverse transition was sluggish. Above the α transition, a second order, spin-flip transition occurs at about 167 °C (Andresen and Torbo 1967; Gosselin et al. 1976b; Horwood et al. 1976), and is marked by change in the direction of the magnetic spins from parallel to normal to c -axis. Kruse (1992) observed that this magnetic spin flip transition required several weeks for completion at 156 °C. The final transition of FeS is to the ideal NiAs-type structure with the 1A,1C subcell. This first-order transition coincides with the Néel transition at about 327 °C. Thus, the loss of correlation of spin states appears to be associated with complete disorder and relaxation of the Fe and S sub-lattices. Unit-cell parameters for the subcell structure from *in situ* cooling neutron powder diffraction are $a = 3.5308(2)$, $c = 5.779(10)$ Å, measured just above the Néel transition (at 340 °C; Tenailleau et al. 2005). The 1A,1C subcell structure persists up to the low-pressure melting point. Melting of Fe_{1-x}S begins at about 1080 °C for the stoichiometric composition, and is complete at 1190 °C at 52 at% S (Figs. 1a and 2). The Néel temperature (327 °C at 1 bar) increases linearly with increase in pressure by 3.2 ± 0.1 °C/kbar, measured up to 8.5 kbars (Anzai and Ozawa 1974), whereas the α transition temperature (147 °C at 1 bar) decreases by -0.8 ± 0.1 °C/kbar up to 11 kbars (Ozawa and Anzai 1966). Note that, elsewhere, the three low-pressure FeS polymorphs [troilite, 2A,1C (or MnP) and 1A,1C] may be referred to as the α , β and γ phases, respectively: β and γ are also used to discriminate between low-temperature, ordered (or partially ordered) hexagonal pyrrhotite and high-temperature, disordered 1A,1C pyrrhotite.

FeS at high pressure. The high-pressure phase relations of FeS are actively researched, largely because of the interest in predicting the sulfide mineralogy and melting in the core of Mars and Earth. Two structural phase transitions have been observed experimentally with increasing pressure at room temperature (Karunakaran et al. 1980; King and Prewitt 1982; Fei et al. 1995; Kusaba et al. 1997; Nelmes et al. 1999; Marshall et al. 2000; Kobayashi et al. 2005). Troilite is stable to 3.4 GPa (Pichulo 1979) where it transforms to an MnP-type structure (King and Prewitt 1982). The next transition is at 6.7 GPa to a monoclinic phase (“FeS III” in Urakawa et al. 2004, and other studies) with a 24 atom unit cell (Nelmes et al. 1999) and b -axis parallel to a -axis of troilite and c -axis of MnP. This $\text{MnP} \rightleftharpoons$

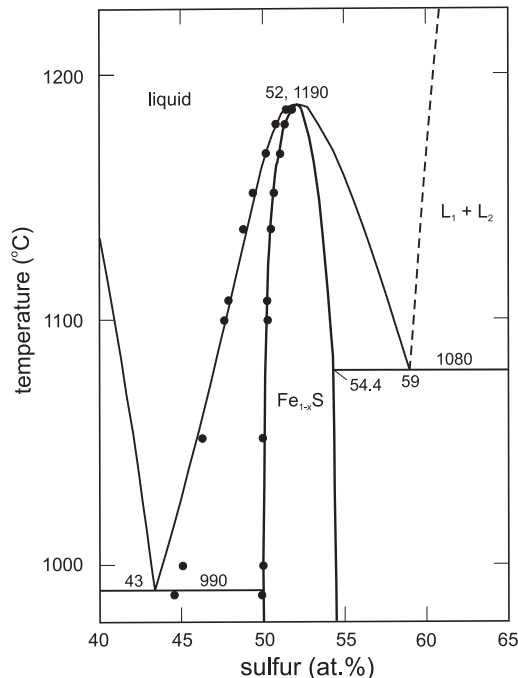


Figure 2. Calculated melting relations for high-temperature iron monosulfide (Fe_{1-x}S): dots are experimental values of Burgmann et al. (1968) (after Chuang et al. 1985).

FeS III transition is marked by a volume reduction of 9% (6% in Kusaba et al. 1997), a large decrease in ca for the equivalent NiAs-type subcell (i.e., C/A), and the disappearance of the magnetic moment (King and Prewitt 1982; Rueff et al. 1999). Kobayashi et al. (1997) suggested that collapse of the magnetic moment in the Fe atom is related to electron delocalization associated with a distinct change in the $3d$ electron configuration of the Fe atoms. Takele and Hearn (1999) confirmed that the troilite and MnP structures have a high-spin configuration whereas the monoclinic phase adopts a magnetically quenched low-spin state. Above 7 GPa, FeS III transforms with increasing temperature first to a $2A,1C$ hexagonal superstructure (labeled FeS IV and perhaps equivalent to the low-pressure $2A,1C$ phase of Putnis 1974), and then to the NiAs-type subcell $1A,1C$ structure (FeS V; Fei et al. 1995; Kusaba et al. 1998). A cubic CsCl-type phase (with Fe and S in eight-fold coordination) was predicted to be stable at the very high pressures of the Earth's inner core (>330 GPa; Sherman 1995; Martin et al. 2001). Temperature-pressure phase diagrams are given in Kavner et al. (2001) and Urakawa et al. (2004; present Fig. 3); the former study used a laser-heated diamond anvil cell and the latter a large volume multianvil apparatus, and both studies were made *in situ* using synchrotron X-ray diffraction. Note that Urakawa et al. (2004) did not encounter the MnP (FeS II) phase, which was earlier reported to be stable in between troilite and FeS III at room temperature (e.g., King and Prewitt 1982; Fei et al. 1995; Marshall et al. 2000).

Fe-S phase relations

Numerous diverse studies have contributed to our understanding of the Fe-S system (e.g., Jensen 1942; Rosenqvist 1954; Kullerud and Yoder 1959; Kullerud 1961, 1967a; Arnold 1962; Carpenter and Desborough 1964; Toulmin and Barton 1964; Clark 1966b; Burgmann et al. 1968; Nakazawa and Morimoto 1971; Rau 1976; Sugaki and Shima 1977; Sugaki et al. 1977; Kissin and Scott 1982; Barker and Parks 1986; Chuang et al. 1985; Fig. 1a). The central portion of the phase diagram is dominated by the broad field of pyrrhotites ($Fe_{1-x}S$) which extends from complete melting at 1190 °C and 52 at% S to below room temperature, and from 50 at% S to a maximum width at pyrite breakdown at 55 at% S ($x = 0.18$; Toulmin and Barton 1964). There are no Fe-excess sulfides above the low-temperature region (at low

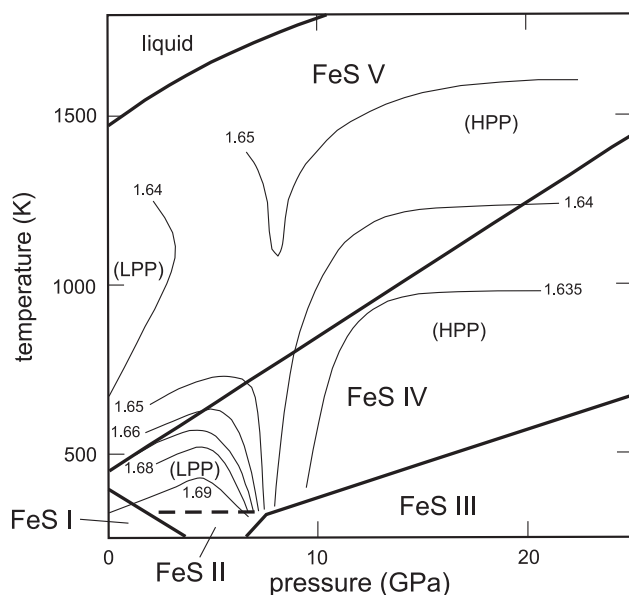


Figure 3. High-pressure phase relations of FeS obtained by *in situ* X-ray diffraction: isopleths are C/A ratio for equivalent NiAs-type subcell; FeS I is troilite; FeS III is monoclinic phase; FeS IV is $2A,1C$ phase; and FeS V is disordered NiAs-type FeS (e.g., $1A,1C$, FeS^{HT}); LPP and HPP are low- and high-pressure phases, respectively, of earlier studies (after Urakawa et al. 2004).

pressure), and the eutectic in the Fe-FeS portion (for coexisting α -iron + FeS + liquid) is at 990 °C and 43 at% S. Details of the melting relationships in this central region are shown in Figure 2. The composition of Fe_{1-x}S coexisting with pyrite (i.e., the pyrrhotite-pyrite solvus) is defined by the experiments of Arnold (1962) and Toulmin and Barton (1964; present Fig. 4). The breakdown of pyrite to $\text{Fe}_{1-x}\text{S} + \text{S}_2$ occurs at 743 °C (742 °C in Chuang et al. 1985).

Sulfur fugacity and activity of FeS. In what has become a classic study, Toulmin and Barton (1964) determined the $f(\text{S}_2)$ versus temperature (T) curve for the univariant assemblage pyrrhotite + pyrite + vapor from 743-325 °C. The fugacity of S_2 was measured using the electrometallurgical method, which is based on the reaction:



Note that their data were only in moderate agreement with later electrochemical measurements at 185-460 °C (Schneeberg 1973; Lusk and Bray 2002), when extrapolated into the lower-temperature range. Toulmin and Barton (1964) also developed the following equation to interrelate the composition of pyrrhotite, $f(\text{S}_2)$ and T :

$$\log f(\text{S}_2) = (70.03 - 85.83N_{\text{FeS}})(1000/T - 1) + 39.30(1 - 0.9981N_{\text{FeS}})^{1/2} - 11.91 \quad (2)$$

where N_{FeS} is the mole fraction of FeS in the system FeS- S_2 . They then mapped the field for pyrrhotite with isopleths of N_{FeS} in a plot of $\log f(\text{S}_2)$ vs. $(1000/T)$ (Fig. 5). The activity of FeS in pyrrhotite was extracted by application of the Gibbs-Duhem equation. Note, however, that here the activity of FeS in Fe_{1-x}S relates to mixing of FeS and S_2 , but the primary interaction leading to nonideality of the $(\text{Fe}, \square)\text{S}$ solid solution (and departure from Raoult's law) is clearly that of Fe atoms and vacancies on the Fe sublattice of the NiAs-type structure. Chuang et al. (1985) handled this problem reasonably well in their thermodynamic analysis of the Fe-S system by considering mixtures of FeS, S, Fe vacancies, and Fe interstitials. Their calculated values for the activity of S in high-temperature pyrrhotite up to 1101 °C compared favorably with values from several experimental studies, including Burgmann et al. (1968) and Rau (1976).

Low-temperature iron sulfides. The low-temperature phase relations for bulk compositions between FeS (or Fe-excess FeS; Fe_{1+x}S) and FeS_2 are complex and little understood due to inconsistency between laboratory products and natural assemblages. The

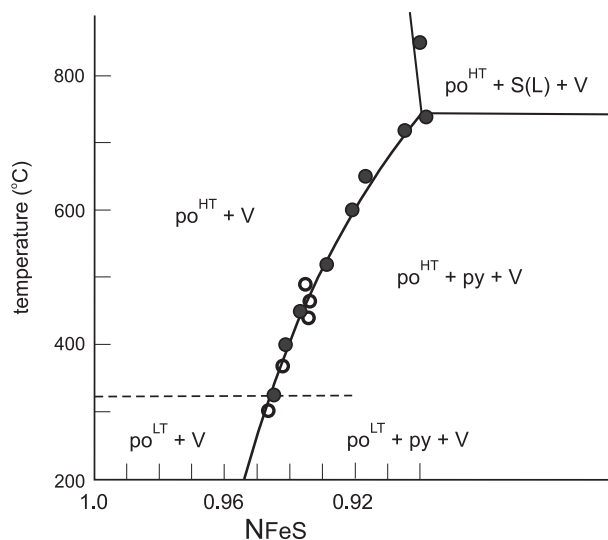


Figure 4. Pyrrhotite-pyrite solvus from low-pressure experiments; filled circles are Arnold (1962); open circles are Toulmin and Barton (1964); N_{FeS} is mole fraction of FeS in the system FeS- S_2 (after Toulmin and Barton 1964).

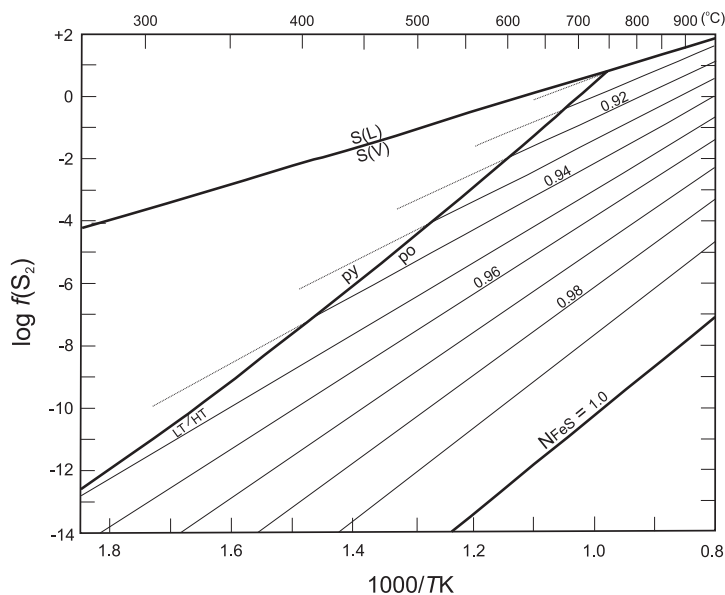


Figure 5. Composition of pyrrhotite in the Fe-S system as a function of temperature and sulfur fugacity, $f(S_2)$ (after Toulmin and Barton 1964).

latter are generally assumed to better reflect mineral stability, whereas synthesis experiments are plagued by sluggish reactions and metastability. Troilite and hexagonal and monoclinic pyrrhotites all have structures based on the NiAs-type structure.

The literature on the structure, phase relations, physical properties and mineralogy of the low-temperature NiAs-type phases is very extensive (e.g., Fleet 1968, 1971; Ward 1970; Scott and Kissin 1973; Craig and Scott 1974; Kissin 1974; Morimoto et al. 1975a,b; Power and Fine 1976; Sugaki et al. 1977; Vaughan and Craig 1978; Kissin and Scott 1982; Pósfai and Dódonny 1990; Lusk et al. 1993; Li and Franzen 1996; Li et al. 1996; Farrell and Fleet 2001; Powell et al. 2004; Tenaillieu et al. 2005). Superstructure phases of the 1A,1C NiAs-type substructure arise by the clustering of Fe atoms in the troilite structure and the ordering of Fe atoms and vacancies in individual (001) layers in the more metal-deficient compositions. As reviewed above, troilite forms spontaneously on quenching below 147 °C at the stoichiometric composition (FeS), by the triangular clustering of Fe atoms (Bertaut 1953, 1956), giving a hexagonal unit cell with $a = A(3)^{1/2}$, $c = 2C$.

There appear to be numerous low-temperature superstructures based on the commensurate and incommensurate ordering of Fe atoms and vacancies in $Fe_{1-x}S$ compositions. Although there is some correlation between superstructure type and Fe-S composition, there are significant discrepancies between laboratory products and natural hexagonal and monoclinic pyrrhotites. Most of these pyrrhotite superstructures have a unit cell with $a = 2A$, or an incommensurate modulation of $2A$, and various patterns of order in the c -axis direction. Experimental products were classified by Nakazawa and Morimoto (1971) into the following superstructure types:

NC for intermediate pyrrhotite compositions below about 200 °C, and characterized by a hexagonal $2A,NC$ unit cell, where N is generally non-integral with values from 3.0 to 6.0. Superstructure reflections occur as satellites to the subcell reflections as well as in reciprocal lattice rows reflecting doubling of the A dimension.

NA for more S-rich intermediate compositions near and above 200 °C, and characterized additionally by non-integral spacings in the *a*-axis direction, with N varying from about 40 to 90.

MC limited to S-rich compositions near 300 °C, and characterized by a similar diffraction pattern to NC, with N varying from 3.0 to 4.0, but without the satellite reflections.

4C monoclinic pyrrhotite of near Fe_7S_8 composition.

Nakazawa and Morimoto (1971) additionally recognized a field of 1C phases (undifferentiated high-temperature 1A, 1C and low-temperature 2A, 1C phases) and a 2C phase (troilite). The NC, NA and MC superstructure types have hexagonal diffraction symmetry. Their characteristic single-crystal X-ray diffraction patterns are depicted in Nakazawa and Morimoto (1971) and Craig and Scott (1974), and a representative phase diagram is given in the present Figure 6. Only structures with the ideal Fe_7S_8 composition have been determined in any detail; i.e., synthetic hexagonal 3C (Fleet 1971; a quench product, and broadly equivalent to NA type) and natural monoclinic 4C (Tokonami et al. 1972).

Integral NC superstructures are generally restricted to natural assemblages. As representative natural pyrrhotites, Lennie and Vaughan (1996) list $\sim\text{Fe}_7\text{S}_8$ (monoclinic 4C), Fe_9S_{10} (intermediate hexagonal pyrrhotite 5C), $\text{Fe}_{10}\text{S}_{11}$ (intermediate hexagonal pyrrhotite 11C), $\text{Fe}_{11}\text{S}_{12}$ (intermediate hexagonal pyrrhotite 6C), and $\sim\text{Fe}_9\text{S}_{10}\text{-Fe}_{11}\text{S}_{12}$ (intermediate hexagonal pyrrhotite non-integral, or incommensurate, NC). These five pyrrhotite superstructure types occur as important minerals in sulfide ores of “magmatic” origin and as accessory minerals in ultramafic and mafic rocks, as well as in metamorphosed massive sulfides and some hydrothermal ores.

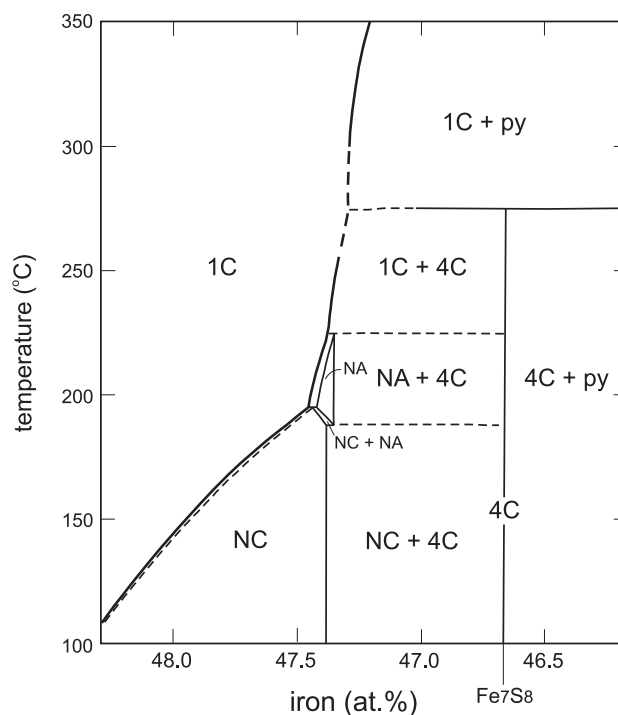
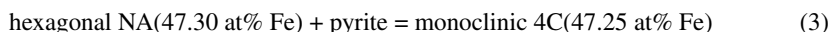


Figure 6. Schematic phase diagram for pyrrhotite superstructures encountered in laboratory studies (after Sugaki et al. 1977).

Pyrrhotite phase relations below 350 °C have been investigated systematically by Nakazawa and Morimoto (1971), Scott and Kissin (1973), Kissin (1974), Sugaki et al. (1977), and Kissin and Scott (1982). The observations of Nakazawa and Morimoto (1971) were based on *in situ* high-temperature X-ray diffraction, whereas those of Kissin (1974), Scott and Kissin (1973) and Kissin and Scott (1982) were based on room-temperature measurements of crystals grown by hydrothermal recrystallization both *in situ* and via transport reactions in 5 *m* aqueous solutions of NH₄I. Sugaki et al. (1977) grew crystals by the thermal gradient hydrothermal transport method, but based their phase diagram (Fig. 6) largely on *in situ* X-ray diffraction measurements.

The stability fields of the pyrrhotite superstructures lie, very generally, on the S-rich side of the low-temperature extension of the hexagonal pyrrhotite-pyrite solvus (cf. Figs. 4 and 6). The field of the 1C phases extends down to near, or below, 100 °C at about 48.6 at% Fe. Interestingly the onset of vacancy ordering in laboratory equilibrated pyrrhotites is anticipated by discontinuities in A and C subcell parameter plots for Fe_{1-x}S compositions quenched from 700 °C (Fleet 1968). Between 48.6 at% Fe and stoichiometric FeS, the literature phase diagrams show a wedge-like field of troilite + 1C. There is overall inter-laboratory agreement on the pyrrhotite phase relations. Kissin and Scott (1982) found that a discontinuity in the hexagonal pyrrhotite-pyrite solvus at 308 °C marked the upper stability of the MC superstructure. The onset of the NA superstructure occurred further down the solvus at 262 °C, and monoclinic 4C pyrrhotite became stable at 254 °C through the peritectic reaction:



At lower temperatures, hexagonal pyrrhotite is separated from the field of monoclinic 4C pyrrhotite by a narrow miscibility gap. Hexagonal NC pyrrhotite appeared at and below 209 °C. The integral 6C, 11C and 5C superstructures of intermediate pyrrhotite were thought to form in nature only below about 60 °C, and the field of coexisting troilite + 1C hexagonal pyrrhotite extended from 147 °C at the stoichiometric FeS composition to about 60-70 °C at 48.3 at% Fe. Sugaki et al. (1977) and Sugaki and Shima (1977) had earlier reported similar results for assemblages of troilite and hexagonal NC and NA and monoclinic 4C pyrrhotites, but did not observe a field of stability for MC pyrrhotite (Fig. 6). Sugaki et al. (1977) found that the monoclinic 4C phase reacted out at a slightly higher temperature (275 ± 5 °C) than in Kissin and Scott (1982). Revising Kissin and Scott (1982), the monoclinic 4C phase was not detected by Lusk et al. (1993) in experiments on phase relations in the Fe-Zn-S system between 325-150 °C. Therefore, they concluded that in nature monoclinic pyrrhotite may become stable somewhere around 140 °C.

Troilite and hexagonal NC phases are antiferromagnetic (Schwarz and Vaughan 1972), monoclinic 4C pyrrhotite is ferrimagnetic (Nakazawa and Morimoto 1971), and the high-temperature 1A,1C subcell phase is paramagnetic (e.g., Vaughan and Craig 1978; Kruse 1990). Magnetic ordering (i.e., the Néel temperature) and ordering of vacancies in Fe_{1-x}S both occur near 250-300 °C (Power and Fine 1976) on cooling, but these ordering events are clearly composition-dependent, and their details remain obscure (e.g., Li and Franzen 1996). Hysteresis of magnetic and electrical properties and phase transitions and transformations is commonly encountered in heating-cooling experiments with nonstoichiometric phases (Nakazawa and Morimoto 1971; Schwarz and Vaughan 1972; McCammon and Price 1982). Li and Franzen (1996) attributed hysteresis in their synthetic and natural pyrrhotites heated above 550 °C to loss of S. Powell et al. (2004) recently confirmed that, at the ideal Fe₇S₈ composition, the magnetic transition is accompanied by a structural transformation from vacancy-ordered monoclinic 4C to vacancy disordered hexagonal 1C.

Of interest here is that a vacancy- and magnetically-ordered hexagonal 3C pyrrhotite is obtained by quenching Fe₇S₈ and more S-rich compositions from well within the field of

1A,1C pyrrhotite (e.g., 500-700 °C; Fleet 1968, 1982). This 3C phase is clearly metastable in the Fe-S system. However, the hexagonal 3C type superstructure is stable in the Fe-Se system at the Fe_7Se_8 composition (Okazaki 1959, 1961). Both hexagonal 3C Fe_7Se_8 and triclinic 4C Fe_7Se_8 (which is equivalent to monoclinic 4C Fe_7S_8) are vacancy ordered and ferrimagnetic and have nearly identical Curie temperatures (189 °C for 3C and 187 °C for 4C). The low-temperature 4C selenide transforms to 3C over the temperature interval 240 to 298 °C, and magnetic and vacancy disordering of 3C occurs over the interval 360 to 375 °C. A similar 4C→3C→1C transformation sequence was suggested for pyrrhotites of Fe_7S_8 composition by Li and Franzen (1996) but this was not supported by later study (Powell et al. 2004).

The other low-temperature binary Fe-S phases are, in the main, either metastable or of questionable stability (Lennie and Vaughan 1996) and include:

1. synthetic iron-pentlandite (Fe_9S_8 ; $a = 10.5 \text{ \AA}$; Nakazawa et al. 1973)
2. cubic Fe_{1+x}S ($x = 0.03\text{-}0.10$; sphalerite-type, $a = 5.425 \text{ \AA}$; Takeno et al. 1970; Murowchick and Barnes 1986a)
3. mackinawite (Fe_{1+x}S ; $x = 0.01\text{-}0.08$; tetragonal, PbO-type, $a = 3.676$, $c = 5.032 \text{ \AA}$; Berner 1962, 1964; Nozaki et al. 1977; Takeno et al. 1982; Lennie et al. 1995b)
4. amorphous FeS/disordered mackinawite/"dorite" (Lennie and Vaughan 1996; Wolthers et al. 2003; Ritvo et al. 2003)
5. smythite ($\sim\text{Fe}_9\text{S}_{11}$, ideally $\text{Fe}_{13}\text{S}_{16}$; rhombohedral, $a = 3.47$, $c = 34.50 \text{ \AA}$; Erd et al. 1957; Rickard 1968; Fleet 1982)
6. greigite (Fe_3S_4 ; cubic, spinel-type, $a = 9.876 \text{ \AA}$; Skinner et al. 1964)
7. synthetic Fe_3S_4 (monoclinic, NiAs-derivative, $a = 5.93$, $b = 3.42$, $c = 10.64 \text{ \AA}$; Fleet 1982)
8. marcasite (FeS_2 ; $a = 4.436$, $b = 5.414$, $c = 3.381 \text{ \AA}$; Murowchick and Barnes 1986b)
9. pyrite (FeS_2 ; $a = 5.417 \text{ \AA}$).

The relative stability of these phases has been studied variously by precipitation, sulfidation and replacement in aqueous or hydrothermal media and dry heating and quenching, as well as in natural assemblages: e.g., conversion of mackinawite to greigite (Lennie et al. 1977; Taylor et al. 1979) and mackinawite to hexagonal pyrrhotite (Lennie et al. 1995a). Lennie and Vaughan (1996) concluded that the predominant sulfidation sequence at low temperature is: (cubic FeS/amorphous FeS) → mackinawite → greigite → marcasite/pyrite. On the other hand, Krupp (1994) studied textural relationships of smythite, greigite and mackinawite from the low-temperature hydrothermal Moschellandsberg mercury deposit in south-western Germany, and concluded that greigite and mackinawite were probably metastable phases, smythite was stable, and pyrrhotites may be metastable below 65 °C. Fleet (1982) found that S-rich Fe_{1-x}S compositions spontaneously precipitated smythite ($\text{Fe}_{13}\text{S}_{16}$) and monoclinic Fe_3S_4 when quenched under dry conditions from the pyrrhotite solvus and also from just above pyrite decomposition (743 °C). Monoclinic Fe_3S_4 is isomorphous with monoclinic Fe_3Se_4 and Cr_3S_4 . It also seems appropriate to note here that the cubic (Mg,Fe)S solid solution extends beyond 70 mol% FeS at the highest temperature investigated (Skinner and Luce 1970; Farrell and Fleet 2000), allowing extrapolation to $a = 5.07 \text{ \AA}$ for the unstable halite-type FeS. Both monoclinic Fe_3S_4 and halite-type FeS are potential metastable products of low-temperature experiments with Fe-S compositions.

High-pressure phases. The high-pressure phase relations in the system Fe-FeS are of current interest in connection with the composition and mineralogy of planetary cores, for which S is a leading candidate for the light element component (e.g., Svendsen et al. 1989; Boehler 1992; Sherman 1995; Liu and Fleet 2001; Sanloup et al. 2002; Secco et al. 2002; Lin et al. 2004;

Sanloup and Fei 2004). Earlier research focused on the melting behavior, with Boehler (1992) demonstrating strong depression of melting in an Fe-rich core for mixtures of Fe and FeS. A surprising development has been the discovery of the Fe-S alloys Fe_3S , Fe_2S , and Fe_3S_2 . Fe_3S was predicted as a probable core phase based on crystal chemical reasoning and first-principles density functional calculations (Sherman 1995). Subsequently, Fei et al. (1997, 2000) synthesized three Fe-S alloy phases (Fe_3S_2 , Fe_3S and Fe_2S) at subsolidus temperatures and high pressures (Fig. 7). Fe_3S has a tetragonally distorted AuCu_3 -type structure. It forms at 21 GPa and 1027 °C and is stable in the tetragonal structure up to 42.5 GPa. Lin et al. (2004) studied magnetic and elastic properties of Fe_3S up to 57 GPa at room temperature, observing a magnetic collapse at 21 GPa consistent with the high-spin to low-spin electronic transition at 20-25 GPa reported earlier. Whereas S was thought formerly to concentrate in the outer liquid core of Earth, the existence of high-pressure Fe-S alloys as probable host phases for S argues for significant amounts of S in the inner solid core (e.g., Sanloup et al. 2002). Indeed, Lin et al. (2004) concluded that the non-magnetic Fe_3S phase is a dominant component of the Martian core.

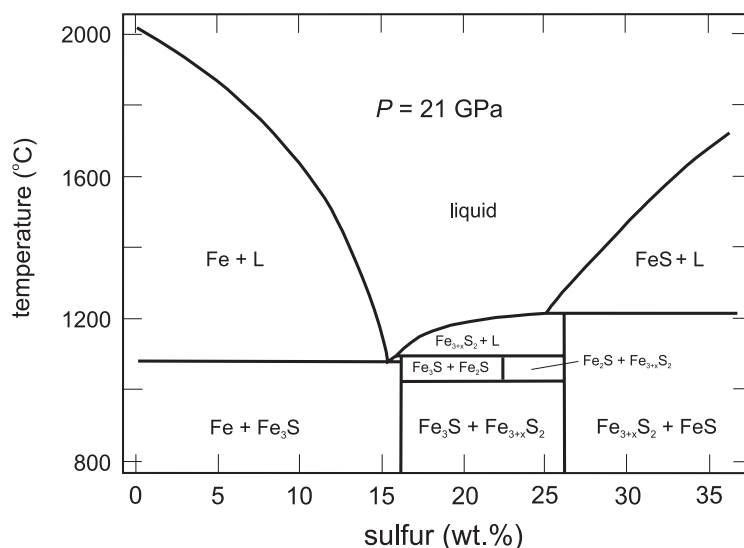


Figure 7. Melting relations in the system Fe-FeS at 21 GPa; Fe_3S , Fe_2S and $\text{Fe}_{3+x}\text{S}_2$ are new alloy phases (after Fei et al. 2000).

Ni-S phase relations

The phase diagram for the binary Ni-S system (Fig. 1b) is based on the experiments of Rosenqvist (1954) and Kullerud and Yund (1962), with additional details from Arnold and Malik (1974), Craig and Scott (1974), Sharma and Chang (1980), Lin et al. (1978), and Fleet (1988). The system includes five minerals: heazlewoodite (Ni_3S_2), godlevskite (Ni_9S_8), millerite (NiS), polydymite (Ni_3S_4), and vaesite (NiS_2); and three high-temperature fields of solid solution: $\alpha\text{-Ni}_{3\pm x}\text{S}_2$, $\text{Ni}_{6-x}\text{S}_5$ (elsewhere known as $\alpha\text{-Ni}_7\text{S}_6$), and $\alpha\text{-Ni}_{1-x}\text{S}$. End-member heazlewoodite is stable up to 565 °C, where it inverts to $\alpha\text{-Ni}_{3\pm x}\text{S}_2$, Ni_9S_8 (elsewhere known as $\beta\text{-Ni}_7\text{S}_6$; godlevskite) is stable up to about 400 °C, NiS (millerite) up to 379 °C, Ni_3S_4 (polydymite) up to 356 °C, and NiS_2 (vaesite) up to 1022 °C, the congruent melting point. The field of the NiAs-derivative phase $\alpha\text{-Ni}_{1-x}\text{S}$ extends from 999 °C down to 282 °C, being replaced at lower temperature by the assemblage millerite + polydymite.

The structures and detailed phase relations of the two metal-excess sulfides located in between NiS and Ni₃S₂ proved to be troublesome in earlier studies. The orthorhombic (space group *Bmmb*) structure of the high-temperature solid solution Ni_{6-x}S₅ was determined by Fleet (1972) for a sample of composition Ni₇S₆. Surprisingly, the structure has an ideal 6:5 stoichiometry; the commonly reported 7:6 stoichiometry being accommodated by partial occupancy of the Ni positions. Three of the Ni positions are disordered, and various superstructures (*2a, 2b, 2c*; *2a, 2b, 3c*; and *2a, 2b, 4c*; Putnis 1976; Parise and Moore 1981) have been reported. Fleet (1987, 1988) also showed that godlevskite [(Ni_{8.7}Fe_{0.3})S₈] and β-Ni₉S₈ were the same phase and the stoichiometry was pentlandite-like (9:8). However, unlike pentlandite, (Fe,Ni)₉S₈, which is a true ternary phase, their crystal structures contain three-fold clusters (Ni₃) of short Ni-Ni interactions. The greater metallic character of Ni and Co and their tendency to form *M-M* bonds, compared with Fe, results in metal-excess sulfides in both of the Ni-S and Co-S binary systems. The activity of sulfur in the metal-excess Ni-S phases has been determined using a gas equilibration technique (Lin et al. 1978). This study predated resolution of the phase relations of β-Ni₉S₈, and also separated the broad field of α-Ni_{3±x}S₂ solid solution into two phases, which they labelled β'-Ni₃S₂ and β₂-Ni₄S₃.

The system Fe-Co-S

Low-pressure phase relations and physical properties in the systems Co-S and Fe-Co-S have been fairly extensively studied (e.g., Lamprecht and Hanus 1973; Rau 1976; Wyszomirski 1976, 1977, 1980; Lamprecht 1978; Terukov et al. 1981; McCammon and Price 1982; Wieser et al. 1982; Barthelemy and Carcaly 1987; Collin et al. 1987; Raghavan 1988; Vlach 1988; Farrell and Fleet 2002). Rau (1976) and Vlach (1988) reviewed the binary Co-S phase relations and calculated equilibrium sulfur pressures. There is some inconsistency in precise temperatures between these two studies. Using Vlach (1988), the field of Co_{1-x}S extends from 1181 °C down to only 460 °C, being replaced at lower temperature by the assemblage cobalt pentlandite + Co₃S₄. Below 785 °C, the bulk-composition CoS yields cobalt pentlandite + Co_{1-x}S to 460 °C, and cobalt pentlandite + Co₃S₄ below 460 °C. Thus, stoichiometric CoS cannot be preserved at room temperature using conventional quenching procedures. Incidentally, Wyszomirski (1976) considered the existence of jaipurite, the mineral of ideal Co_{1-x}S composition, to be doubtful. Cobalt pentlandite is stable up to 834 °C, reacting to Co₄S₃ + Co_{1-x}S, and the pyrite structure phase CoS₂ is stable up to 1027 °C, reacting to Co_{1-x}S + S₂.

The *mss* phase in the ternary system, (Fe,Co)-*mss*, is continuous between Fe_{1-x}S and Co_{1-x}S down to at least 500 °C (Wyszomirski 1976; Raghavan 1988; present Fig. 8). Of interest here is that, for experiments at and above 500 °C: (1) the range in nonstoichiometry (*x*) in Co_{1-x}S is similar to that of Fe_{1-x}S and to *mss* in the system Fe-Ni-S; (2) (Fe,Co)-*mss* near FeS composition is metal-rich [>50 at% (Fe,Co)], and analogous to the area of Fe-rich *mss* reported by Misra and Fleet (1973); and, (3) the composition field of cobalt pentlandite is restricted to <0.2 atomic Fe/(Fe + Co). The Fe content of natural cobalt pentlandite is also very low in the absence of Ni, even though there is extensive solid solution between synthetic (Fe-Ni) pentlandite and cobalt pentlandite (Knop and Ibrahim 1961; Geller 1962). Misra and Fleet (1973) found that the Co content of natural pentlandite is highly variable, ranging from almost Co-free pentlandite with less than 0.1 at% Co to an Fe-free pentlandite of composition Co_{6.9}Ni_{1.3}S₈, and a Ni-free pentlandite of composition Co_{9.1}Fe_{0.2}S₈. For quenched stoichiometric (Fe_{1-x}Co_xS) compositions, the troilite phase extends to about $x = 0.17$, although this composition limit varies somewhat with heat treatment and from study to study (Terukov et al. 1981; Wieser et al. 1982; Barthelemy and Carcaly 1987; Collin et al. 1987). The more Co-rich compositions exhibit hysteresis of magnetic and electrical properties and phase behavior. McCammon and Price (1982) investigated the magnetism of (Fe,Co)_{1-x}S solid solutions quenched from 1000 °C using Mössbauer spectroscopy, observing an antiferromagnetic = paramagnetic transition between 0.69 and 0.50 atomic Fe/(Fe + Co) at 25 °C and 0.50 and 0.16

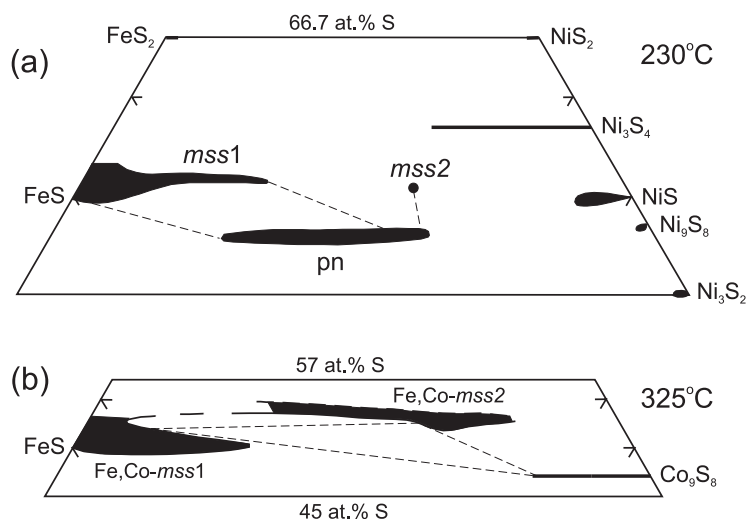


Figure 8. Partial phase relations at low temperature showing incompletely unmixed monosulfide solid solution (*mss*) in: (a) the system Fe-Ni-S at 230 °C (after Misra and Fleet 1973; Fleet 1988); and (b) the system Fe-Co-S at 325 °C (after Farrell and Fleet 2002).

atomic Fe/(Fe + Co) at 4.2 K. Thus, Fe-rich (Fe,Co)-*mss* compositions are antiferromagnetic like troilite and hexagonal pyrrhotites (Schwarz and Vaughan 1972) in the system Fe-S, but Co-rich (Fe,Co)-*mss* compositions are paramagnetic.

Farrell and Fleet (2002) observed that (Fe,Co)-*mss* unmixes abruptly below 425 °C, giving co-existing phases of Fe-rich (Fe,Co)-*mss*1, with the 1A,1C NiAs-type structure, and Co-rich (Fe,Co)-*mss*2, with the hexagonal 2A,3C structure. For bulk compositions with 52.0 at% S, the equilibrium (Fe,Co)-*mss*1 solvus is at about 0.83 atomic Fe/(Fe + Co) at 400 °C and progressively diverges toward the Fe_{1-x}S end-member composition with decrease in temperature to 0.98 atomic Fe/(Fe + Co) at 105 °C. At 400 °C, the equilibrium (Fe,Co)-*mss*2 solvus is at about 0.37 atomic Fe/(Fe + Co) and does not appear to vary significantly with decrease in temperature. There is a metastable solvus within the equilibrium miscibility gap with a critical temperature at 400 °C between 0.45 and 0.50 atomic Fe/(Fe + Co), and a narrow field of spontaneous phase-separation is centered at 0.75 atomic Fe/(Fe + Co), and results in satellite reflections to *h0l* NiAs-type subcell reflections in (Fe,Co)-*mss* quenched from high temperature (800 °C).

Ternary phase relations in the system Fe-Ni-S

The phase relations in the Fe-Ni-S system have been extensively researched largely because of their important application to Ni-Cu magmatic sulfides (e.g., Lundqvist 1947; Clarke and Kullerud 1963; Naldrett and Kullerud 1966; Naldrett et al. 1967; Kullerud et al. 1969; Shewman and Clark 1970; Craig 1971, 1973; Misra and Fleet 1973, 1974; Vaughan and Craig 1974; Mandziuk and Scott 1977; Coey and Roux-Buisson 1979; Vollstädt et al. 1980; Hsieh and Chang 1987; Naldrett 1989; Karup-Møller and Makovicky 1995, 1998; Sugaki and Kitakaze 1998; Ueno et al. 2000; Etschmann et al. 2004; Kitakaze and Sugaki 2004; Wang et al. 2005). Magmatic sulfide assemblages consist principally of pyrrhotite, chalcopyrite and pentlandite, but interest in the Fe-Ni-(Cu)-S phase relations begins with the high-temperature ternary liquid, because of the putative role of immiscible sulfide liquid in the formation of magmatic sulfide orebodies.

At 1200 °C the system is composed entirely of liquids, except for alloys along the Fe-Ni join. At high subsolidus temperatures, pyrrhotite and pentlandite in magmatic sulfide ores are

represented by (Fe,Ni) monosulfide solid solution (*mss*) (Fig. 9). Fe_{1-x}S appears on the Fe-S join at 1190 °C, and *mss* extends to the Ni-S join at 999 °C. For a number of years it was believed that the metal-excess phase pentlandite appeared only on cooling to 610 °C (Kullerud 1963). However, in a series of presentations extending from Sugaki et al. (1982) to Sugaki and Kitakaze (1998) it was demonstrated instead that a high form of pentlandite was stable between 584 ± 3 °C and 865 ± 3 °C and showed limited solid solution from $\text{Fe}_{5.07}\text{Ni}_{3.93}\text{S}_{7.85}$ to $\text{Fe}_{3.61}\text{Ni}_{5.39}\text{S}_{7.85}$, at 850 °C, including the composition point for ideal $\text{Fe}_{4.50}\text{Ni}_{4.50}\text{S}_{8.00}$. High pentlandite is cubic with $a = 5.189$ Å (at 620 °C) corresponding to $a/2$ of pentlandite. Kitakaze and Sugaki (2004) recently showed that the unit-cell of high pentlandite is the subcell of (low) pentlandite, and that the inversion of the low- and high-form solid solution in the quaternary system Fe-Ni-Co-S is of the order-disorder type. The revised phase relations of Sugaki and Kitakaze (1998) in the system Fe-Ni-S at 850 °C and a pseudobinary temperature *versus* composition section with Fe = Ni through the pentlandite and *mss* fields are given in Figures 9 and 10. The latter shows that high pentlandite crystallizes from metal-rich liquid between 865 °C and 746 °C: note that pentlandite in magmatic sulfide ores is generally understood to form by segregation or phase separation from *mss* in the subsolidus (e.g., Francis et al. 1976; Etschmann et al. 2004). The composition limits of pentlandite solid solution are $\text{Fe}_{5.95}\text{Ni}_{3.07}\text{S}_{8.00}$ to $\text{Fe}_{2.81}\text{Ni}_{6.55}\text{S}_{8.00}$ and $\text{Fe}_{6.57}\text{Ni}_{2.82}\text{S}_{8.00}$ to $\text{Fe}_{3.79}\text{Ni}_{5.45}\text{S}_{8.00}$ at 400 °C and 500 °C, respectively (Ueno et al. 2000).

Low-temperature phase relations in the *mss* region of the system Fe-Ni-S were investigated by Misra and Fleet (1973) and Craig (1973). Misra and Fleet (1973) reported that *mss* is continuous between Fe_{1-x}S and Ni_{1-x}S to below 400 °C, but is discontinuous at 300 °C, with a region of solid-solution extending from Fe_{1-x}S to about 25 at% Ni (*mss*1), a second *mss* phase (*mss*2) at about 33 at% Ni, and millerite solid-solution containing about 5 at% Fe. At 230 °C, the composition of *mss*2 had not changed appreciably, but the maximum Ni content of *mss*1 had diminished to 17 at% (Fig. 8a). Craig's (1973) results were similar, except that he found the critical temperature for unmixing to be 263 ± 13 °C, and the field of *mss*2 extended further toward the Ni-S join. Misra and Fleet (1973) noted that the Ni content near the *mss*1 solvus at 230 °C is still appreciably greater than the range in Ni content of 0.2-0.7 at% for intergrown hexagonal and monoclinic pyrrhotite coexisting with pentlandite in magmatic sulfides. These findings suggest that either the progressive chemical readjustment in magmatic sulfides persists to very low temperatures or there is a discontinuous change from *mss*1 to pyrrhotite at some lower temperature. Indeed, the initial phase separation of (Fe,Co)*mss* is discontinuous in the analogue system Fe-Co-S (Farrell and Fleet 2002). This occurs between 425-400 °C and, thereafter, the miscibility gap in (Fe,Co)-*mss* is generally similar to that for the phase separation of *mss* in the system Fe-Ni-S.

Violarite (ideally FeNi_2S_4) appears in the subsolidus at 461 °C (Craig 1971) and solid solution with the end-member thiospinel polydymite (Ni_3S_4) is thought to be complete at 356 °C. There remains some uncertainty as to whether the common association of violarite with pentlandite represents stable equilibrium (e.g., Misra and Fleet 1974) or merely metastable juxtaposition (Misra and Fleet 1973; Craig 1973): the phase relations of Craig (1973), in particular, exclude the establishment of violarite-pentlandite tie-lines.

Structural and electrical properties of *mss* in the Fe-Ni-S system have been investigated at high pressures and temperatures by Vollstädt et al. (1980) and Kraft et al. (1982).

Cu-S, Cu-Fe-S AND Cu-Fe-Zn-S SYSTEMS

The ternary system Cu-Fe-S is the road map for understanding the geology and geochemistry of Cu sulfide deposits and has been studied systematically for more than 70 years, beginning with Merwin and Lombard (1937). This early experimental study was followed by Schlegel and Schüller (1952), Hiller and Probsthain (1956), Roseboom and

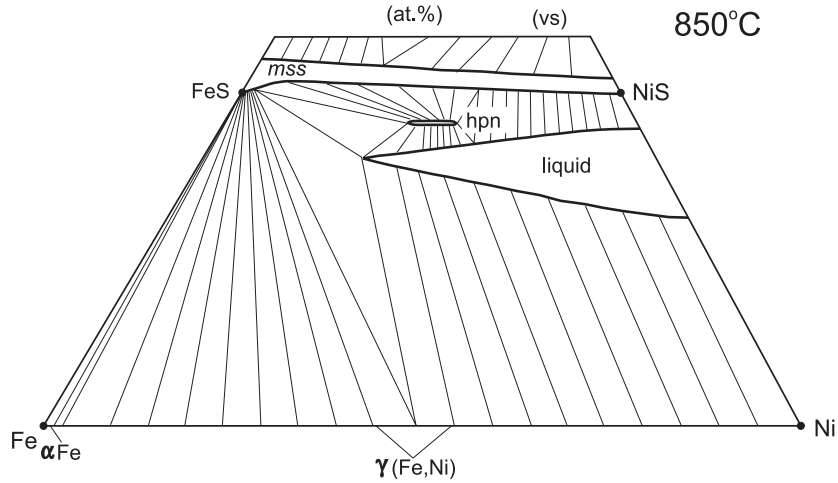


Figure 9. Phase relations in the metal-rich portion of the Fe-Ni-S system at 850 °C, showing extensive field of liquid alloy centered near the Ni₃S₂ composition point, a continuous field of *mss*, and early appearance of high pentlandite (after Sugaki and Kitakaze 1998).

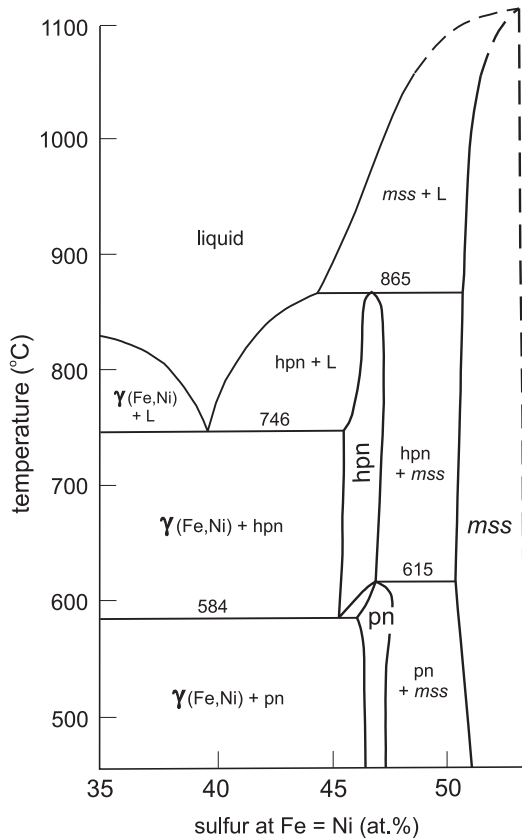


Figure 10. Partial temperature versus sulfur section at atomic Fe = Ni through Fe-Ni-S system, showing relationship of new high pentlandite phase to coexisting liquid, *mss* and pentlandite (after Sugaki and Kitakaze 1998).

Kullerud (1958), Yund (1963), Brett (1964), Morimoto and Kullerud (1966), Roseboom (1966), Yund and Kullerud (1966), Cabri (1967, 1973), Kullerud et al. (1969), Morimoto and Koto (1970), Mukaiyama and Izawa (1970), Cabri and Harris (1971), Morimoto and Gyobu (1971), Cabri and Hall (1972), MacLean et al. (1972), Barton (1973), and Sugaki et al. (1975). Since then there have been a number of studies on, variously: electrochemistry of the Cu-S join (Potter 1977) and ternary Cu-Fe-S system (Lusk and Bray 2002); digenite (Grønvold and Westrum 1980; Pósfai and Buseck 1994), bornite (Putnis and Grace 1976; Kanazawa et al. 1978; Grguric and Putnis 1998; Grguric et al. 1998) and the low-temperature phase relations of digenite-bornite solid solution (Grguric and Putnis 1999; Grguric et al. 2000), the ternary system (Wang 1984), the effects of addition of Zn to the ternary system (Wiggins and Craig 1980; Kojima and Sugaki 1984, 1985; Lusk and Calder 2004), and phase relations in the system CuS-FeS-H₂S-H₂SO₄-HCl-H₂O at magmatic temperatures and pressures (McKenzie and Helgeson 1985). However, the present state of knowledge is based largely on the flurry of studies in the sixties and seventies. Therefore, this section builds on the review of Craig and Scott (1973) and the subsequent detailed experimental work of Sugaki et al. (1975).

Phase relations in the system Cu-S

The original list of eleven minerals and phases in the Cu-S system in Craig and Scott (1974) is now expanded to fourteen (Tables 2 and 3) with the addition of the new minerals roxbyite, geerite, and spionkopite. Also, blaubleibender covellite is now recognized as the mineral yarrowite, which has a 9:8 Cu:S stoichiometry and, therefore, is distinct from covellite, and I have included villamininite as the mineral form of synthetic CuS₂, even though this pyrite-group mineral contains significant amounts of Ni, Co and Fe. Most Cu-

Table 2. Minerals and phases in the system Cu-S.

Mineral/Phase	Formula	Symmetry	Stability	References
chalcocite	Cu ₂ S	monoclinic	to 103 °C	1, 2, 3
hexagonal Cu ₂ S	Cu ₂ S	hexagonal	103 ° to ~435 °C	1, 4, 5
cubic Cu ₂ S	Cu ₂ S	cubic	~435 ° to 1129 °C	6, 7
tetragonal Cu ₂ S	Cu ₂ S	tetragonal	>1 kbar	8, 9
high digenite	Cu _{1.80+x} S ₅	cubic	83 ° to 1129 °C	6,7
djurleite	Cu _{1.97} S	orthorhombic	to 93 °C	1, 3, 10, 11
digenite	Cu _{1.80} S	cubic	76 ° to 83 °C	1, 7, 12
roxbyite	Cu _{1.78} S	monoclinic		13
anilite	Cu _{1.75} S	orthorhombic	to 76 °C	3, 11, 14, 15
geerite	Cu _{1.60} S	cubic		16
spionkopite	Cu _{1.40} S	hexagonal-R		17
yarrowite	Cu ₉ S ₈	hexagonal-R	to 157 °C	11, 17, 18, 19
covellite	CuS	hexagonal	to 507 °C	3, 20, 21
villamaninite	CuS ₂	cubic		22, 23, 24

References: 1. Roseboom (1966); 2. Evans (1971); 3. Potter and Evans (1976); 4. Buerger and Buerger (1944); 5. Wuensch and Buerger (1963); 6. Jensen (1947); 7. Morimoto and Kullerud (1963); 8. Skinner (1970); 9. Janosi (1964); 10. Morimoto (1962); 11. Potter (1977); 12. Grønvold and Westrum (1980); 13. Mumme et al. (1988); 14. Morimoto and Koto (1970); 15. Morimoto et al. (1969); 16. Goble and Robinson (1980); 17. Goble (1980); 18. Moh (1964); 19. Rickard (1972); 20. Kullerud (1965a); 21. Berry (1954); 22. Munson (1966); 23. Taylor and Kullerud (1971, 1972); 24. Bayliss (1989)

Notes: 1. cubic Cu₂S, stable between ~435-1129 °C in solid solution with high digenite, Cu_{1.80}S; 2. yarrowite –formerly blaubleibender covellite; 3. villamaninite must be the mineral form of synthetic cubic CuS₂ since both are pyrite structure compounds, even though the mineral contains high amounts of Ni, Co and Fe; 4. hexagonal-R is hexagonal-rhombohedral; 5. covellite- $a = 3.7938$, $c = 16.341$ Å; yarrowite- $a = 3.800$, $c = 67.26$ Å; villamaninite- $a = 5.694$ Å

Table 3. Crystal data for some Cu-excess Cu-S minerals and phases.

Mineral	Formula	Space Group	<i>a</i> (Å)	<i>b</i> (Å)	<i>c</i> (Å)	β (°)	Z
chalcocite	Cu ₂ S	<i>P2₁/c</i>	15.235	11.885	13.496	116.26	48
h chalcocite	Cu ₂ S	<i>P6/mmc</i>	3.95		6.75		2
djurleite	Cu _{1.97} S	<i>P2₁/c</i>	26.896	15.745	13.565	90.13	128
digenite	Cu _{1.80} S	<i>Fm3m</i>	5.57				4
roxbyite	Cu _{1.78} S	<i>C2/m</i>	53.79	30.90	13.36	90.0	512
anilite	Cu _{1.75} S	<i>Pnma</i>	7.89	7.84	11.01		16
geerite	Cu _{1.60} S	<i>F-43m</i>	5.410				4
spionkopite	Cu _{1.40} S	<i>P3m1</i>	22.962		41.429		504

Notes: 1. after Gaines et al. (1997); 2. h- hexagonal

and Cu-Fe-sulfides have crystal structures based on closest-packed arrays of S atoms, with hexagonal closest packed tending to be favored in low-temperature phases and cubic in higher-temperature phases. There is a tendency for tetrahedral coordination to predominate in structures of the ternary phases. This preference is driven by the golden rule that the number of bonding electrons available is four times the number of atoms (e.g., Wuensch 1974). The predominant 1+ oxidation state of Cu requires occupancy of interstitial metal positions for ternary compositions with atomic (Cu,Fe) > S and Cu > Fe. Along the Cu-S join, the stability of chalcocite (Cu₂S) is a direct reflection of the 1+ oxidation state (cf., the analogue formulae of Na₂S, Ag₂S and Au₂S), but now Cu is predominantly in three-fold coordination to minimize the distant Cu-Cu interactions. Covellite (CuS) accommodates the 1+ oxidation state by forming S-S bonds. All of these sulfides are metallic compounds (or small band gap semiconductors). Complexity in the compositions of the low-temperature phases in the vicinity of Cu₂S stoichiometry arises because of their alloy nature and similarity in energy of the 1+ and 2+ oxidation states of Cu for these minerals/compounds. Although not evident in laboratory experiments, there are a total of seven minerals (eight including binary digenite) with compositions extending from Cu₂S (chalcocite) to Cu_{1.40}S (spionkopite).

The binary Cu-S phase diagram (Roseboom 1966; Barton 1973) is complicated by an extensive field of high-digenite(Cu_{9+x}S₅)-high-chalcocite solid solution extending from 83 °C to 1129 °C and some uncertainty in the precise stability of digenite, as well as numerous phases of very-low-temperature (<103 °C) stability in this same composition region. The detailed phase relations are shown in Figure 11 which is after Barton (1973) and Craig and Scott (1974). There remains considerable uncertainty on the precise temperatures of phase transitions in the very-low-temperature region, with literature values varying markedly with the method of investigation. Also, there have been no studies on the stability of the new minerals roxbyite, geerite and spionkopite, and their investigation could be very demanding. As concluded from the minimal amounts of Ni, Co and Cu dissolved in pyrrhotites (discussed elsewhere), it seems that alloy-like sulfides continue to re-equilibrate toward ambient temperatures on exhumation of orebodies. Morimoto and Koto (1970) suggested that the mineral digenite (Cu₉S₅) was not stable in the binary Cu-S system, but invariably contained a small amount of Fe (~1%). Cubic low-temperature digenite only becomes a stable phase on the Cu-S join above about 70 °C. At a slightly higher, and composition dependent, temperature (76-83 °C), binary Cu-S digenite inverts to cubic high digenite (Cu_{9+x}S₅) which is isostructural with cubic high chalcocite (Morimoto and Kullerud 1963; Roseboom 1966). Chalcocite is one of four polymorphs of Cu₂S. The mineral is monoclinic (Evans 1971), and inverts to hexagonal Cu₂S at 103 °C. The cubic high form appears at 435 °C, forming continuous solid solution with cubic Cu_{9+x}S₅. A low-temperature, high-pressure polymorph has tetragonal symmetry and is stable only above

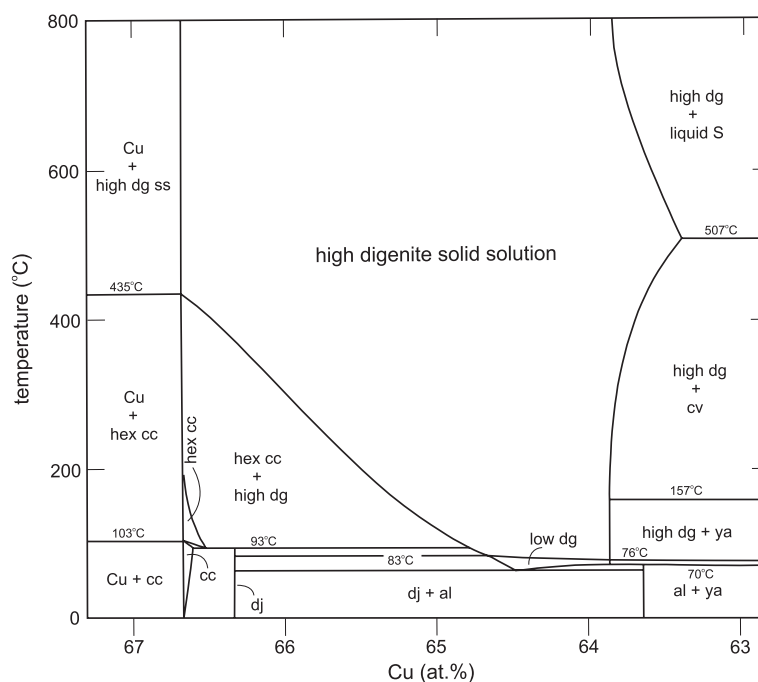


Figure 11. Partial temperature-composition phase diagram for binary Cu-S system centered on the field of high digenite solid solution: see INTRODUCTION for mineral/phase abbreviations (after Barton 1973).

~0.8 kbars (Skinner 1970). Djurleite ($\text{Cu}_{1.96}\text{S}$) is stable at and below 93 °C: it was discovered as a synthetic compound by Djurle (1958) and described as a mineral by Roseboom (1962) and Morimoto (1962). Anilite ($\text{Cu}_{1.75}\text{S}$) is stable at and below about 70 °C. The remaining Cu-S phase of intermediate composition, covellite (CuS), exhibits no solid solution and is stable on its composition point up to 507 °C where it melts incongruently to $\text{Cu}_{9+x}\text{S}_5$ + liquid sulfur.

The Cu-S phase equilibria have since been investigated using electrochemical cells from 0 °C to 250 °C over the composition range $\text{Cu/S} = 0.95\text{-}2.10$ (Potter 1977). The electrolytes were vapor-saturated aqueous cupric sulfate and cuprous chloride solutions. Two blaubleibender covellites (e.g., Moh 1971), corresponding in composition to “ideal” yarrowite and spionkopite (Table 2), low digenite, tetragonal Cu_2S , and a protodjurleite were found to be metastable. The temperatures of stable invariant points were in general agreement with literature values, as follows:

1. covellite = high digenite + liquid sulfur (507 ± 2 °C)
2. high chalcocite + Cu = high digenite + Cu (435 ± 8 °C)
3. low chalcocite + Cu = high chalcocite + Cu (103.5 ± 0.5 °C)
4. djurleite = high digenite + high chalcocite (93 ± 2 °C)
5. low chalcocite = djurleite + high chalcocite (90 ± 2 °C)
6. anilite = covellite + high digenite (75 ± 3 °C)
7. high digenite = anilite + djurleite (72 ± 3 °C)

Contradicting earlier results for anilite decomposition, Grønvold and Westrum (1980), using calorimetry and X-ray diffraction, found that the anilite to digenite transition occurred at 37 °C: coexisting covellite was not detected. The transition was rapid in the forward direction, but sluggish and initiated at 17 °C in reversal.

Phase relations in the ternary system Cu-Fe-S

There are numerous ternary Cu-Fe-S phases, and most of them lie within a broad swath of composition space between pyrrhotite on the Fe-S join and high digenite solid solution on the Cu-S join. To the list of eighteen minerals and confirmed phases in Craig and Scott (1974), I have added the new minerals putoranite ($\text{Cu}_{1.1}\text{Fe}_{1.2}\text{S}_2$), isocubanite and nukundamite, and revised the formula for idaite (Clark 1970a; Inan and Einaudi 2002) (Table 4).

Craig and Scott (1974) remarked that, although more time and effort had been expended on the Cu-Fe-S system than any other ternary sulfide system, many relationships remained enigmatic, obscured by extensive solid solutions, non-quenchable phases, and metastability. Since that time, detail has been added to the low-temperature phase relations (e.g., Sugaki et al. 1975; Wang 1984; Grguric et al. 2000; Inan and Einaudi 2002), $f(\text{S}_2)$ for selected reactions has been determined by electrochemistry (Lusk and Bray 2002), and the phase relations under hydrothermal conditions have been calculated (McKenzie and Helgeson 1985, 1987; Einaudi 1987). The phase relations in the central part of the Cu-Fe-S system at 600 °C and 350 °C are shown in Figures 12 and 13. As with the binary Cu-S join, the phase relations of many ternary Cu-Fe-S minerals remain unclear; e.g., the metal-excess chalcopyrite-like minerals

Table 4. Minerals and phases in the system Cu-Fe-S.

Mineral/ Phase	Formula	(Symmetry)/Unit cell (Å, °)	Stability	Refs.
digenite	$(\text{Cu,Fe})_9\text{S}_5$	(c) $a = 5.57$	37 ° to 77 °C	1
high digenite	$\sim(\text{Cu,Fe})_9\text{S}_5$	(c) $a = 27.85$	77 ° to 1129 °C	1
bornite	Cu_5FeS_4	(t) $a = 10.95, c = 21.86$	to 228 °C	2
Cu_5FeS_4	Cu_5FeS_4	(c) $a = n(5.5)$		2
Cu_5FeS_4	Cu_5FeS_4	(c) $a = 5.5$	228 ° to ~1100 °C	2
x-bornite	$\text{Cu}_5\text{FeS}_{4.05}$	(t) $a = 10.44, c = 21.88$	to 125 °C	3, 4
idaite	Cu_3FeS_4	(h) $a = 3.90, c = 16.95$	metastable to 265 °C	5, 6
nukundamite	$\text{Cu}_{3.38}\text{Fe}_{0.62}\text{S}_4$	(f) $a = 3.782, c = 11.187$	224 ° to 501 °C	6, 7, 8, 9
fukuchilite	Cu_3FeS_8	(c) $a = 5.604$	to ~200 °C	10, 11
talnakhite	$\text{Cu}_9\text{Fe}_8\text{S}_{16}$	(c) $a = 10.591$	to ~186 °C	12, 13
intermediate I	$\text{Cu}_9\text{Fe}_8\text{S}_{16}?$		186 ° to 230 °C	14
intermediate II	$\text{Cu}_9\text{Fe}_8\text{S}_{16}?$		230 ° to 520 °C	14
chalcopyrite	CuFeS_2	(t) $a = 5.28, c = 10.40$	to 557 °C	15, 16
mooihoekite	$\text{Cu}_9\text{Fe}_9\text{S}_{16}$	(t) $a = 10.585, c = 5.383$	to ~167 °C	14, 15
intermediate A	$\text{Cu}_9\text{Fe}_9\text{S}_{16}$		167 to 236 °C	14
putoranite	$\text{Cu}_{1.1}\text{Fe}_{1.2}\text{S}_2$	(c) $a = 5.30$		17
haycockite	$\text{Cu}_4\text{Fe}_5\text{S}_8$	(o) $a \approx b = 10.71, c = 31.56$		14, 18
<i>pc</i>			to ~200 °C	14
<i>iss</i>		(c) $a = 5.36$	20-200 ° to 960 °C	19
cubanite	CuFe_2S_3	(o) $a = 6.46, b = 11.117, c = 6.233$	to 200-210 °C	20
isocubanite	CuFe_2S_3	(c) $a = 5.303$	>200-210 °C	21

Symmetry: c- cubic, t- tetragonal, h- hexagonal, r- hexagonal-rhombohedral, o- orthorhombic

References: 1. Morimoto and Kullerud (1963); 2. Morimoto and Kullerud (1966); 3. Yund and Kullerud (1966); 4. Morimoto (1970); 5. Wang (1984); 6. Inan and Einaudi (2002); 7. Merwin and Lombard (1937); 8. Clark (1970); 9. Seal et al. (2001); 10. Kajiwara (1969); 11. Bayliss (1989); 12. Cabri and Harris (1971); 13. Hall and Gabe (1972); 14. Cabri (1973); 15. Cabri and Hall (1972); 16. Barton (1973); 17. Filimonova et al. (1980); 18. Hiller and Pobstthain (1956); 19. Kullerud et al. (1969); 20. Cabri et al. (1973); 21. Caye (1988)

Notes: 1. bornite is orthorhombic, pseudo-tetragonal- $a = 10.950, b = 21.862, c = 10.950$ Å; 2. fukuchilite may be ferroan villamaninite (Bayliss 1989); 3. *pc* is primitive cubic phase; 4. *iss* is intermediate solid solution; isocubanite is mineral form of *iss* of CuFe_2S_3 composition

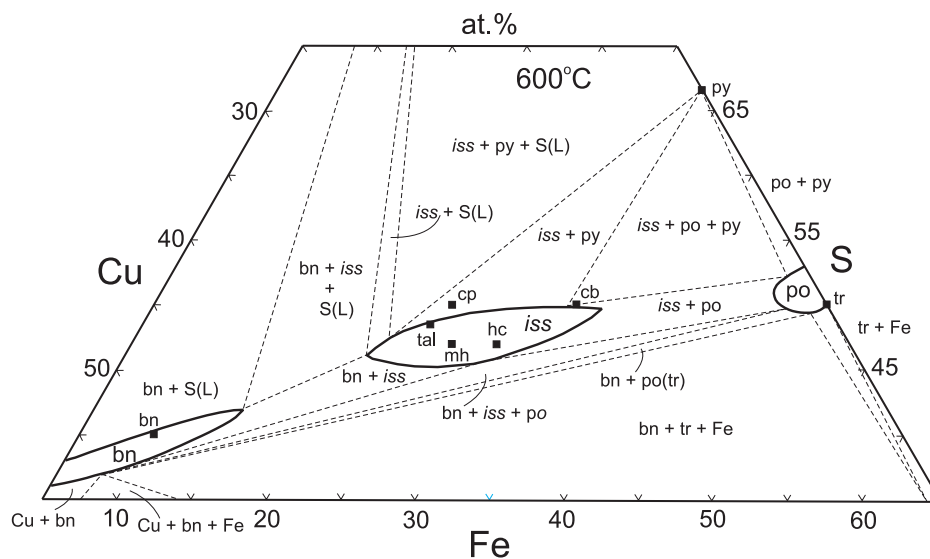


Figure 12. Phase relations in the central portion of the Cu-Fe-S system at 600 °C, highlighting extensive fields of solid solution centered on bornite, the chalcopyrite-derivative phases (*iss*), and pyrrhotite: solid squares are stoichiometric compositions for bornite, chalcopyrite, talnakhite, mooihoekite, haycockite, cubanite, troilite, and pyrite (after Cabri 1973).

talnakhite, mooihoekite, putoranite, and haycockite have not yet been associated with special composition points in the isometric solid solution (*iss*) by reversal of reaction.

Following Kullerud et al. (1969), the immiscible liquid of intermediate composition in the Cu-S system above 1105 °C extends far into the ternary system with increasing temperature, and reaches within 5 wt% of the Fe-S join at 1400 °C. Pyrrhotite appears on the Fe-S join at 1192 °C and high digenite solid solution on the Cu-S join at 1129 °C, quickly becoming a field of high digenite-high bornite solid solution extending far beyond the ideal bornite composition at 900 °C. Sphalerite-structure *iss* initially crystallizes from the central area of the liquid field at about 960 °C, and extends to the cubanite composition point by 700 °C. The 600 °C isothermal section shows the typical phase relations at intermediate temperatures (Fig. 12). The ternary phase diagram is characterized by three extensive solid solutions: (1) high digenite-high bornite; (2) *iss*; and (3) pyrrhotite. The lensoid *iss* field extends largely to metal-excess compositions. Cabri (1973) noted that it may be divided into three zones each characterized by a different quenching behavior, but this feature is not prominently recognized in other studies. Tetragonal chalcopyrite solid solution appears at 557 °C, in the *iss* + pyrite field, and remains isolated from all other Cu-Fe sulfides until temperature is decreased further. Covellite crystallizes at 507 °C and nukundamite at 501 °C. The field of *iss* shifts toward cubanite composition, and that of pyrrhotite shrinks toward the Fe-S join with further decrease in temperature.

Whereas most previous workers had studied the ternary Cu-Fe-S phase relations under dry conditions, using evacuated sealed silica glass tubes, Susaki et al. (1975) used the hydrothermal gradient transport method of Chernyshev and Anfilogov (1968) and Scott and Barnes (1971) at 350 ° and 300 °C. Consistent with previous studies, especially Cabri (1973), they found that the extensive high-temperature field of *iss* in the center of the system separated at low temperature into tetragonal chalcopyrite and a more restricted field of *iss*. At 350 °C, chalcopyrite has a narrow solid solution field extending from stoichiometric CuFeS_2 to $\text{Cu}_{0.9}\text{Fe}_{1.1}\text{S}_{2.0}$ along a line with metal/S atomic ratio of approximately 1, while *iss* extended from nearly stoichiometric

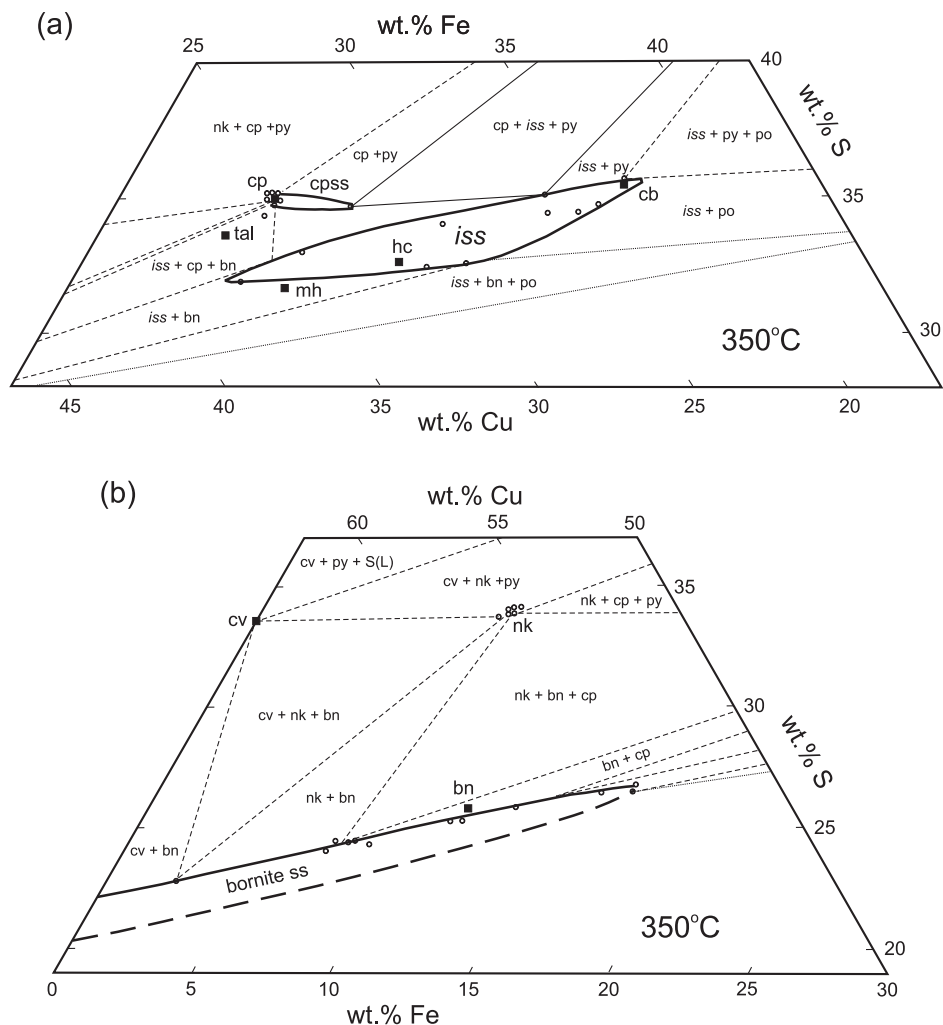


Figure 13. Detailed phase relations in the system Cu-Fe-S at 350 °C around: (a) chalcopyrite and cubanite composition; and (b) bornite composition: nk is nukundamite (idaite of earlier studies) (after Sugaki et al. 1975).

CuFe_2S_3 (cubanite composition) to $\text{Cu}_{1.2}\text{Fe}_{1.1}\text{S}_{2.0}$. Digenite-bornite solid solution extended far beyond stoichiometric Cu_5FeS_4 toward an Fe-rich composition, and the Cu/Fe atomic ratio reached 3.2 at 300 °C and 2.9 at 350 °C (Fig. 13a,b): the composition of this solid solution in equilibrium with chalcopyrite extended from about atomic Cu/Fe 4.0 to 7.5. The pyrrhotite solid solution was fairly extensive in ternary space at high temperature, but retreated rapidly toward the Fe-S join with decreasing temperature, so that the maximum Cu in pyrrhotite was only 0.6 wt% at 350 °C and 0.3 wt% at 300 °C. Nukundamite (idaite in Susaki et al. 1975) composition was very close to $\text{Cu}_{3.38}\text{Fe}_{0.6}\text{S}_4$ and exhibited no solid solution. Susaki et al. (1975) established that the nukundamite-chalcopyrite tie-line exists stably at 350 °C and 300 °C under hydrothermal conditions, and that the tie-line change from *iss*-pyrite to chalcopyrite-pyrrhotite occurred at 328 ± 5 °C, in agreement with the dry experiments of Yund and Kullerud (1966).

Chalcopyrite, talnakhite and mooihoeckite were synthesized by Cabri (1973), but he was unable to synthesize cubanite and haycockite. Synthetic talnakhite transformed at $\sim 186^\circ\text{C}$ to intermediate high-temperature phase I which, in turn, transformed at $\sim 230^\circ\text{C}$ to intermediate phase II, and then to sphalerite-structure *iss* at $520\text{--}525^\circ\text{C}$ (Table 4). Synthetic mooihoeckite transformed to intermediate high-temperature phase A at $\sim 167^\circ\text{C}$ which, in turn, transformed to *iss* at $\sim 236^\circ\text{C}$. At haycockite composition, an unquenchable high-temperature phase formed between 20° and 200°C . The transformation of cubanite to isocubanite (formerly *iss* of near-cubanite composition) occurs on heating to $200\text{--}210^\circ\text{C}$: this reaction has not been reversed.

In other studies, Wang (1984) demonstrated using dry synthesis that a ternary phase similar in composition to idaite reacted to nukundamite + chalcopyrite at 260°C . The assemblage covellite + nukundamite + chalcopyrite was replaced above 290°C by nukundamite + pyrite + bornite. Also, there was evidence of an incomplete pyrite-type solid solution [i.e., $(\text{Cu},\text{Fe})\text{S}_2$] below 325°C : note that fukuchilite (Cu_3FeS_8) may be ferroan villamaninite (Bayliss 1989). The limited compositional range of nukundamite (essentially $\text{Cu}_{3.38}\text{Fe}_{0.62}\text{S}_4$) was confirmed by Sugaki et al. (1981) in their hydrothermal synthesis of the mineral. The behavior of digenite-bornite solid solution below 265°C is dominated by two time- and temperature-dependent processes: (1) ordering of metal cations and vacancies, which leads to a variety of ordered structures (Morimoto and Kullerud 1966; Putnis and Grace 1976; Kanazawa et al. 1978; Grguric et al. 1998), and (2) rapid exsolution and coarsening which results in the formation of distinctive exsolution microtextures (Grguric and Putnis 1999). Grguric et al. (2000) revised the long-standing pseudobinary phase diagram of Morimoto and Kullerud (1966) using work of Morimoto and Gyobu (1971) and new experimental results based mainly on differential scanning calorimetry over the temperature interval $50\text{--}300^\circ\text{C}$ on a natural digenite and synthetic compositions at 5 mol% intervals along the $\text{Cu}_9\text{S}_5\text{--Cu}_5\text{FeS}_4$ join (Fig. 14). Their phase diagram shows a consolute point at Cu_5FeS_4 and 265°C , with the temperature corresponding to the tricritical intermediate-high transition in bornite. Robie et al. (1994) measured the heat capacities of synthetic bornite between 5 K and 78°C and 65°C and 488°C , and revised the Gibbs free energy of formation expressions for covellite, anilite, chalcocite, chalcopyrite, bornite, and nukundamite.

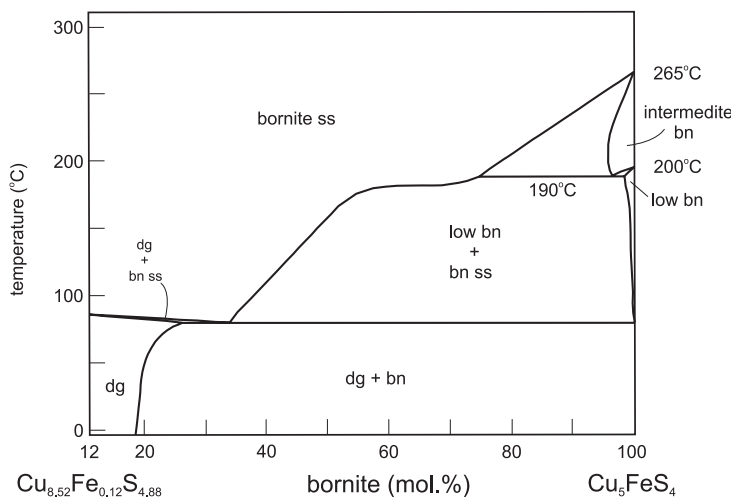
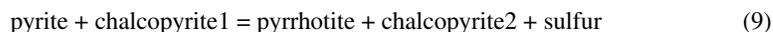
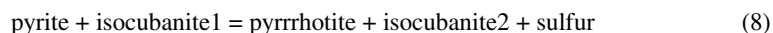
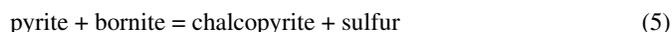
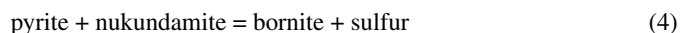


Figure 14. Revised pseudobinary phase diagram for condensed phases in the bornite-digenite solid solution series (after Grguric et al. 2000).

Sulfur fugacity in ternary Cu-Fe-S system

Merwin and Lombard (1937) achieved equilibrium in ternary Cu-Fe-S phase assemblages in the presence of vapor by independently controlling the sulfur vapor pressure. However, Barton and Toulmin (1964a,b) and Toulmin and Barton (1964) were the first to actually measure the sulfur fugacity [$f(S_2)$] in equilibrium with Cu-Fe-S and Fe-S assemblages: they used the electromotive force method and noted that the Fe-S assemblages uniquely determined $f(S_2)$. Subsequently, Schneeberg (1973) measured $f(S_2)$ directly, using the Ag/AgI/Ag_{2+x}S₂ $f(S_2)$ electrochemical cell, and investigating equilibrium sulfide assemblages in the systems Cu-Fe-S, Ni-S and Fe-S between 210-445 °C. Recently, Lusk and Bray (2002) used Schneeberg's electrochemical procedures to investigate the following seven reactions between 185-460 °C at 1 bar:



Their data for these reactions are mapped in $\log f(S_2)$ vs. $(1/T)$ space in Figure 15. The sulfur fugacities for Reactions (5) and (10) are in excellent agreement with Schneeberg (1973) at higher temperatures, but are lower than Schneeberg (1973) for Reaction (4) and reveal undetected inflections at ~221 °C and ~237 °C for Reactions (4) and (5), respectively. Also, an inflection at ~291 °C for Reaction (10) was interpreted to imply a low-temperature phase transition in hexagonal pyrrhotite.

Quaternary System Cu-Fe-Zn-S

In natural ores, chalcopyrite and sphalerite occur frequently as intimate intergrowths in the form of: (1) skeletal sphalerite crystals (sphalerite stars) in chalcopyrite, and (2) chalcopyrite dots and blebs in sphalerite. These characteristic intergrowths have been variously interpreted as products of exsolution, epitaxial growth or replacement, and mechanical mixing (see review in Kojima and Sugaki 1985). Naturally, the solubility of CuS in high-temperature sphalerite is of concern as a possible source of error for sphalerite solid solution (Zn,Fe)S geobarometers calibrated in the Fe-Zn-S system (see following section). The Cu-Fe-Zn-S system has been studied by Wiggins and Craig (1980), Kojima and Sugaki (1984, 1985) and Lusk and Calder (2004). The first two studies both investigated the low pressure phase relations from 500-800 °C using the sealed silica glass tube method. Kojima and Sugaki (1984) found that the maximum solubility of Zn in chalcopyrite at 500 °C was less than 0.9 at%, whereas the extensive field of intermediate solid solution (*iss*) dissolves considerable amounts of Zn with maximum values in Fe-rich *iss* from 12.7 at% at 800 °C to 3.3 at% at 500 °C (Fig. 16). Correspondingly, sphalerite solid solution dissolves considerable amounts of Cu, with maximum CuS contents of 10.7, 8.6 and 4.6 mol% at 800, 700 and 600 °C, respectively, in sphalerite with more than 40 mol% FeS. Thus, Kojima and Sugaki (1984) showed that entry of Cu into sphalerite was dependent on both temperature and $f(S_2)$. These phase relations were extended down to 300 °C by Kojima and Sugaki (1985), using both thermal gradient transport and isothermal recrystallization under hydrothermal conditions with an aqueous NH₄Cl solution mineralizer. The maximum Zn contents at 300 °C were 0.9 at% in chalcopyrite and 1.2 at% in *iss*. Maximum contents of CuS in sphalerite were about 2.4 mol% at the three temperatures investigated, and bore no relation to FeS^{sp} content and $f(S_2)$.

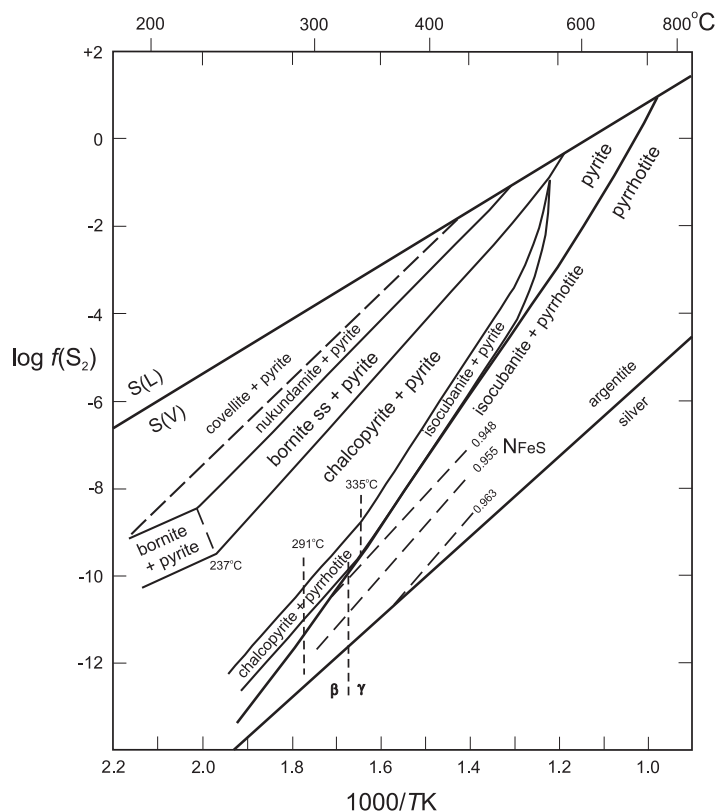


Figure 15. $\log f(S_2)$ vs. $1000/T$ map for selected reactions in the Cu-Fe-S and Fe-S systems (after Lusk and Bray 2002).

Recently, Lusk and Calder (2004) generated temperature-composition data for sphalerites and other sulfides from a sequence of reactions within the Cu-Fe-Zn-S, Fe-Zn-S and Cu-Fe-S systems at 1 bar and 250-535 °C. Two eutectic salt fluxes ($\text{NH}_4\text{Cl-LiCl}$, 50 mol% NH_4Cl , and KCl-LiCl , 41 mol% KCl ; introduced by Boorman 1967) were used routinely for crystallizing the sulfide products *in situ*, and the experiments were made in evacuated sealed Pyrex or Vycor glass capsules. Lusk and Calder (2004) superimposed the 1 bar data for equilibrium sphalerite compositions on Lusk and Bray's (2002) $\log f(S_2)$ - $(1/T)$ map for buffer reactions in the Cu-Fe-S and Fe-S systems (see Fig. 15). The FeS contents of sphalerites (mol%) were about 1.7 for pyrite + nukundamite = bornite + S^{vap} , 4.4 for pyrite + bornite = chalcocopyrite + S, 14.4 for pyrite + chalcocopyrite = isocubanite + S, 22.9 for pyrite + isocubanite1 = pyrrhotite + isocubanite2 + S, and 21.5 for pyrite = pyrrhotite + S. In general agreement with Kojima and Sugaki (1985), they found that Cu contents in sphalerite were low, ranging between about 3 and 0.5 mol% CuS, with highest values for sphalerites associated with bornites. However, the Lusk and Calder (2004) sphalerites for assemblages of high $f(S_2)$ had significantly higher FeS contents than in Czamanske (1974) and Kojima and Sugaki (1985). Lusk and Calder (2004) fitted their results and selected literature data for buffer assemblages of sphalerite with either pyrite or pyrrhotite + pyrite in the Fe-Zn-S and Cu-Fe-Zn-S systems at 250-550 °C and 1 bar to the following Equation for $f(S_2)$:

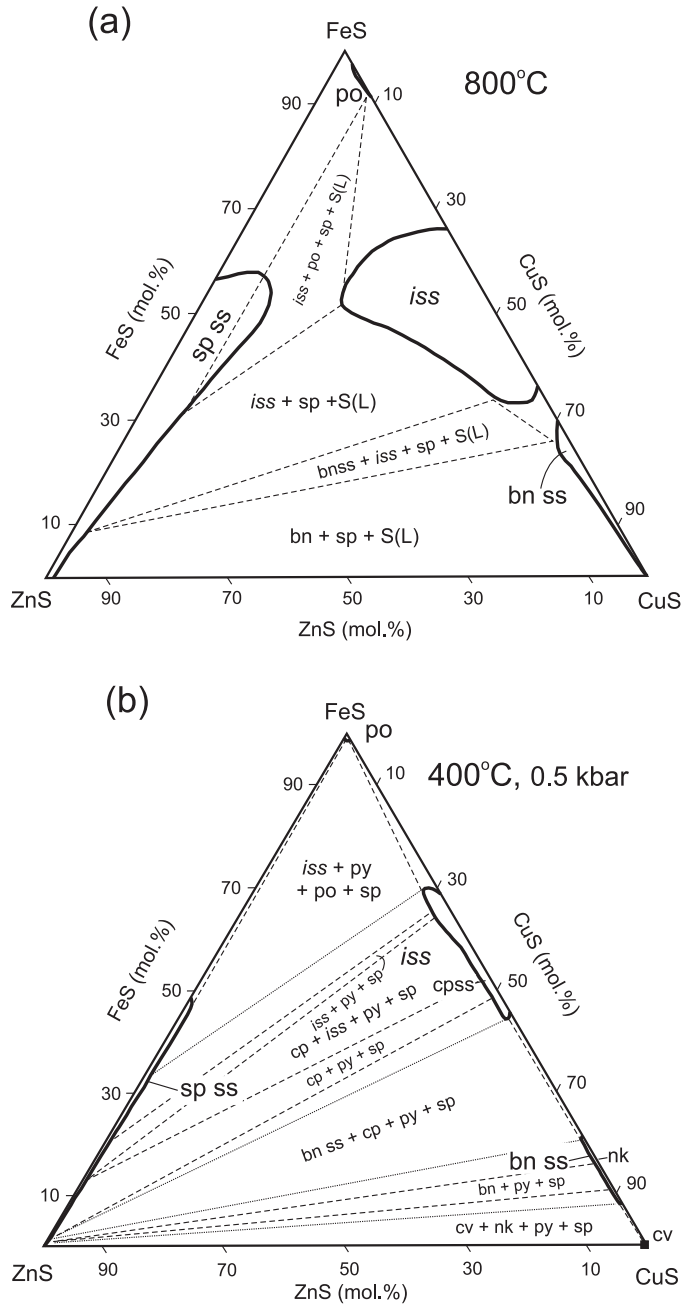


Figure 16. Isothermal phase relations in quaternary Cu-Fe-Zn-S system at: (a) 800 °C and low pressure (after Kojima and Sugaki 1984); and (b) 400 °C and 0.5 kbars, showing marked dependence of solubility of Cu in sphalerite and of Zn in intermediate solid solution (*iss*) with temperature (after Kojima and Sugaki 1985).

$$\log f(S_2) = 11.01 - 9.49 \left(\frac{1000}{T} \right) + \left[0.187 - 0.252 \left(\frac{1000}{T} \right) \right] \text{FeS}^{\text{sp}} + \left[0.35 - 0.2 \left(\frac{1000}{T} \right) \right] \text{CuS}^{\text{sp}} \quad (11)$$

where T is Kelvin, and FeS^{sp} and CuS^{sp} are mol%.

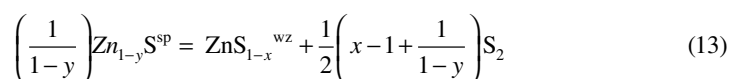
ZnS AND Fe-Zn-S SYSTEM

ZnS

Zinc monosulfide (ZnS) exhibits both polymorphism and polytypism at room pressure. Sphalerite, wurtzite and the wurtzite polytypes all have structures based on the closest packing of their constituent atoms. The Zn and S atoms form interleaved stacking sequences of closest-packed layers, and Zn is in four-fold tetrahedral coordination with S. Interestingly, sphalerite and wurtzite are readily distinguished in petrographic thin section on account of the birefringence of wurtzite and the wurtzite polytypes (e.g., Fleet 1977). Sphalerite [cubic (Zn,Fe)S solid solution] is the dominant zinc sulfide mineral in sulfide ore deposits, occurring in association with iron sulfides (pyrite, pyrrhotite, troilite) \pm Cu-Fe sulfides \pm galena. Elsewhere, sphalerite is found in a wide variety of rocks and unconsolidated lithologies, including metamorphic, hydrothermally altered and sulfidized rocks, glacial tills, iron meteorites and enstatite chondrites, which collectively represent a very wide range in temperature and pressure of formation or annealing. Zinc monosulfide is a refractory compound. Pure sphalerite structure ZnS sublimes at 1185 °C and melts congruently at 1830 °C and 3.7 atm. At room temperature, sphalerite- and wurtzite-structure ZnS invert to halite structure ZnS with Zn in six-fold octahedral coordination near 15 GPa (e.g., 15 GPa in Zhou et al. 1991; 16.2 \pm 0.4 GPa in Yagi et al. 1976). Measurements by Desgreniers et al. (2000) exclude the existence of an intermediate phase of cinnabar type structure. Desgreniers et al. (2000) also found that the halite structure is stable up to 65 GPa, where it inverts to a structure with *Cmcm* symmetry, an orthorhombic distortion of the halite structure, without significant change in volume. The low-pressure sphalerite/wurtzite equilibrium phase relations remain unclear, and their understanding has not changed substantially since the review of Craig and Scott (1974). Wurtzite is generally regarded as the stable high-temperature phase at low pressure and, indeed, wurtzite and the wurtzite polytypes readily transform to sphalerite in supergene alteration and diagenesis (e.g., Fleet 1977). The early study of Allen et al. (1913) reported a transformation temperature of 1020 °C at 1 atm, albeit based on a sluggish reversal, and this has been widely adopted in the absence of a more systematic study. However, Scott and Barnes (1972) reviewed literature values for the transition temperature ranging from 600 °C to above 1240 °C. Using hydrothermal recrystallization and gas-mixing experiments, they showed that sphalerite and wurtzite can coexist over a range of temperatures well below 1020 °C, as a function of $f(S_2)$. Scott and Barnes (1972) argued that wurtzite was deficient in S relative to sphalerite at the same T , P and $f(S_2)$, and that the sphalerite/wurtzite equilibrium was actually univariant and represented by an equation of the type:



or, more generally:



The univariant boundary was located at 500 atm from 465-517 °C over a corresponding calculated $f(S_2)$ range of $10^{-9.5}$ to $10^{-8.7}$ atm. Reversal of the transition was demonstrated from 0.28 to 0.55 kbars and about 450-470 °C in 15 *m* NaOH solutions. Direct determination of $f(S_2)$ at the transition was made by passing $H_2 + H_2S$ mixtures over ZnS powder, giving values of 10^{-5} atm at 890 °C, $10^{-5.5}$ to $10^{-6.4}$ atm at 800 °C, and $10^{-6.5}$ to $10^{-8.5}$ at 700 °C. Ueno et al. (1996) investigated the sphalerite = wurtzite transition in the system Zn-Fe-Ga-S. They found that, for a sample of composition $(Zn_{0.70}Ga_{0.30})S$, the sphalerite phase inverted to wurtzite structure near 875 °C, but the transition was sluggish in both directions and the transition temperature varied with cation composition and $f(S_2)$.

Ternary Fe-Zn-S system and geobarometry

The Fe content of sphalerite varies with the iron sulfide assemblage [i.e., with $f(S_2)$] and lithostatic pressure, and tends to be preserved during exhumation of metamorphic rocks and orebodies under dry conditions and in the post-formation thermal history of meteorites. Therefore, it is widely used for geobarometry of sphalerite-bearing ore bodies, metamorphic rocks and meteorites. The phase relations of sphalerite in the Fe-Zn-S and Cu-Fe-Zn-S systems have been studied extensively using synthesis experiments, largely to support these geobarometric applications (e.g., Kullerud 1953; Barton and Toulmin 1966; Boorman 1967; Boorman et al. 1971; Scott and Barnes 1971; Scott 1973; Scott and Kissin 1973; Czamanske 1974; Lusk and Ford 1978; Wiggins and Craig 1980; Hutchison and Scott 1983; Kojima and Sugaki 1984, 1985; Bryndzia et al. 1988; Lusk et al. 1993; Balabin and Urusov 1995; Mavrogenes et al. 2001; Lusk and Calder 2004), and thermodynamic and model calculations and field relationships (e.g., Einaudi 1968; Schwarcz et al. 1975; Scott 1976; Hutcheon 1978, 1980; Barker and Parks 1986; Banno 1988; Bryndzia et al. 1990; Toulmin et al. 1991; Balabin and Urusov 1995; Balabin and Sack 2000; Martín and Gil 2005).

The fundamental understanding of the important phase relations close to the FeS-ZnS join of the Fe-Zn-S system was provided by Barton and Toulmin (1966) using evacuated sealed silica glass tube experiments. They investigated isothermal sections at about 580, 600, 640, 700, 740, 800, and 850 °C (e.g., Fig. 17), and clearly demonstrated that the Fe content of sphalerite decreases systematically

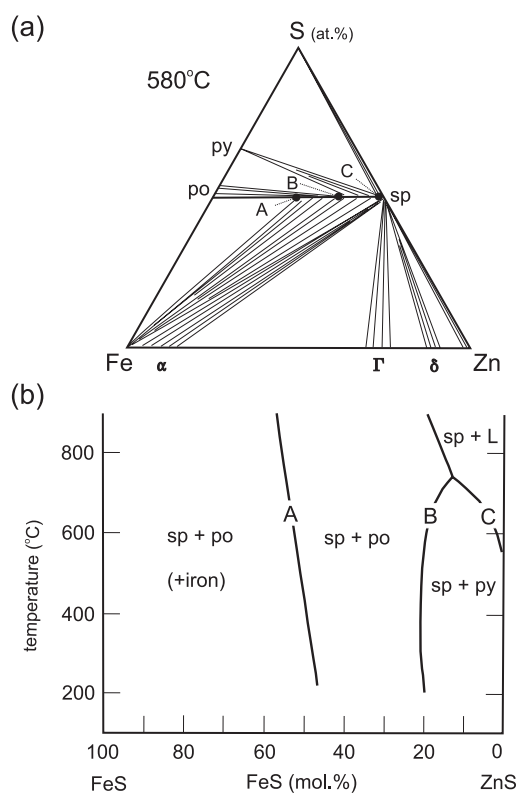


Figure 17. Sphalerite compositions determined by important reactions in the Fe-Zn-S system: (a) 580 °C isothermal section showing ternary phase relations; and (b) temperature-composition projection onto FeS-ZnS join showing sphalerites buffered by reactions A, B and C at 1 bar (after Lusk and Calder 2004).

with increase in $f(S_2)$, consistent with reactions of the type:



for coexisting sphalerite + pyrite. Sphalerite solid solutions lie essentially along the FeS-ZnS join, and neither pyrrhotite nor pyrite takes up appreciable amounts of zinc: the latter is a reflection of the strong tendency of Zn for four-fold tetrahedral coordination with anions in ionic compounds and ligands in covalently bonded compounds. Sphalerite (of various compositions) may be in equilibrium with any of the other phases in the ternary Fe-Zn-S system, and always contains Fe in Fe-bearing bulk compositions. Nevertheless, the join Fe-ZnS is nearly binary; i.e., sphalerite of nearly pure ZnS composition is in equilibrium with α -iron of nearly pure Fe composition. The principal change in the phase relations with increase in temperature is the disappearance of pyrite above 742 °C (at 1 bar).

Barton and Toulmin (1966) identified three univariant reactions, labeled A, B and C in Figure 17 and representing the buffered assemblages sphalerite + troilite (or high-temperature pyrrhotite at or near stoichiometric FeS; presently abbreviated as FeS^{HT}) + α -iron (curve A), sphalerite + hexagonal pyrrhotite (hpo) + pyrite (curve B), and sphalerite + pyrite + liquid sulfur (curve C). These univariant curves are the sphalerite solvi for the three buffered assemblages. Barton and Toulmin (1966) reported that the solvus for sphalerite coexisting with FeS^{HT} is very steep, passing through 56 mol% FeS at 850 °C and 52 mol% at 580 °C. The solvus for sphalerite coexisting with hexagonal pyrrhotite + pyrite is also steep, but concave towards the ZnS composition due mainly to the pinching out of the sphalerite + pyrite field and its replacement by sphalerite + hpo and sphalerite + liquid sulfur assemblages. The composition of sphalerite in equilibrium with hexagonal pyrrhotite + pyrite changes from 13 mol% FeS at 742 °C to 19 mol% at 580 °C. Barton and Toulmin (1966) suggested that the composition of sphalerite in these buffered assemblages might be useful in geothermometry and outlined how the effect of pressure could be estimated by correlating change in the natural logarithm of the activity coefficient for FeS in sphalerite with change in partial molar volume. This pressure correction theory has been adopted in numerous studies using the univariant curve B for sphalerite geobarometry (e.g., Scott 1973) and A for sphalerite cosmobarometry (e.g., Hutchison and Scott 1983; Balabin and Urusov 1995).

Subsequent studies (Boorman 1967; Scott and Barnes 1971) further defined the low-pressure univariant curve for the buffered assemblage sphalerite + pyrrhotite + pyrite using halide fluxes to achieve equilibrium at lower temperatures and 1 bar and 0.25 to 1 kbar, respectively. Scott (1973) extended the experimental calibration of the sphalerite geobarometer to pressures of 2.5, 5 and 7.5 kbars at 325-710 °C using hydrothermal recrystallization in aqueous alkali halide fluxes and cold sealed pressure vessels. This study established the sphalerite geobarometer as a viable method for estimating pressure of formation from assemblages of sphalerite + pyrrhotite + pyrite. However, since the solvus for this buffered assemblage was essentially independent of temperature over the temperature range of most interest (550 °C to below 300 °C; Fig. 18) it was clearly unsuitable for geothermometry. The experimental calibration was extended to about 10 kbars and 420 °C to 700 °C by Lusk and Ford (1978) using an internally heated pressure vessel and various fluxes; i.e., aqueous solutions of 4.5 M KCl or 5 M NH₄Cl or KCl-LiCl and NH₄Cl-LiCl salt mixtures (Fig. 19). The progressive decrease in FeS content of sphalerite with increase in pressure in the temperature independent region was expressed in the equation:

$$\text{FeS}^{\text{sp}} = 20.53 - 1.313P + 0.0271P^2 \quad (15)$$

where FeS^{sp} is mol% and P is kbars, and the equation was fitted to the preferred experimental results of Boorman (1967), Scott and Barnes (1971), Scott (1973), and Lusk and Ford (1978). Lusk et al. (1993) investigated sphalerite + pyrite + pyrrhotite phase relations to lower temperature (150 °C and 325 °C, and 0.4 to 5.1 kbars), using recrystallization in saturated

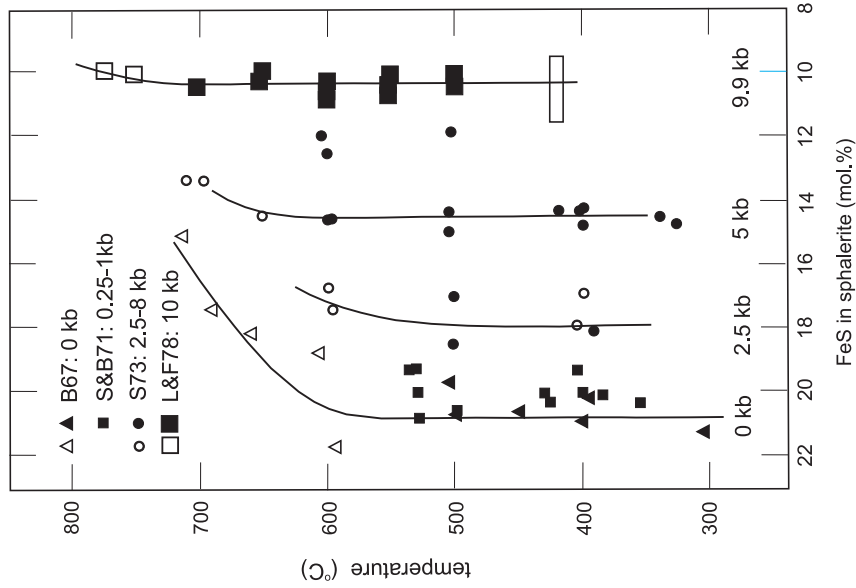


Figure 18. (left image) Experimental measurements of temperature vs. FeS content of sphalerite (FeS^{sp}) buffered along univariant curve B (Fig. 17) by the equilibrium assemblage pyrrhotite + pyrite + sulfur(vapor): B&T66 is Barton and Toulmin (1966); B67 is Boorman (1967); BS&C71 is Boorman et al. (1971); S&B71 is Scott and Barnes (1971); and LC04 is Lusk and Calder (2004) (after Lusk and Calder 2004).

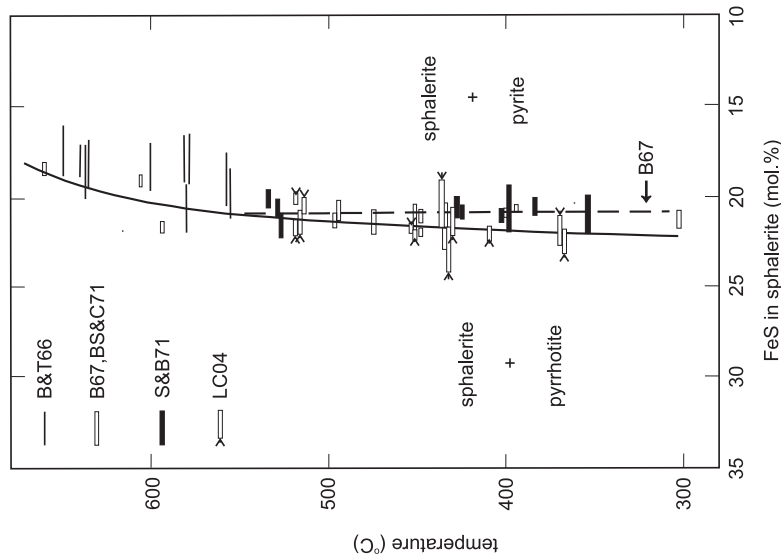


Figure 19. (right image) Experimental measurements of FeS content of sphalerite (FeS^{sp}) coexisting with hexagonal pyrrhotite + pyrite as a function of temperature and confining pressure: B67 is Boorman (1967); S&B71 is Scott and Barnes (1971); S73 is Scott (1973); and L&F78 is Lusk and Ford (1978) (after Lusk and Ford 1978).

ammonium iodide solution. Solvus isobars were deflected slightly to lower FeS^{sp} content at about 280 °C. They presented a P - T - X calibration map for sphalerite composition coexisting with hexagonal pyrrhotite and pyrite based on the data for equilibrated assemblages in the literature and their study. Although monoclinic pyrrhotite (mpo) most commonly coexists with pyrite under very-low temperature conditions in nature, it was not present in the experimental products of Lusk et al. (1993). It was suggested, therefore, that monoclinic pyrrhotite was stable under isotropic stress conditions only below 150 °C.

Univariant reaction A (Fig. 17) represents the FeS saturation limit of sphalerite coexisting with $\text{FeS}^{\text{HT}} + \alpha$ -iron (which quenches to troilite + alloy). Although the sphalerite + troilite + alloy assemblage is unknown on Earth, sphalerite does occur as a minor phase in troilite nodules of some iron meteorites as well as in a few enstatite chondrites. Therefore, the composition of sphalerite in this assemblage may be used to estimate the pressures of formation of meteorites. This “cosmobarometer” was calibrated with the 1 bar experimental data of Barton and Toulmin (1966) and additional experiments at 2.5 and 5.0 kbars between 400-800 °C using both aqueous and anhydrous alkali halide flux recrystallization techniques in Hutchison and Scott (1983). They graphed the 1 bar, 2.5 and 5.0 kbar isobars as a function of temperature and sphalerite composition (Fig. 20) and regressed the sphalerite composition data to give an equation for estimating pressure of formation, as follows:

$$P = -3.576 + 0.0551T - 0.0296T \log(\text{FeS}^{\text{sp}}) \quad (16)$$

where P is kbars, T is Kelvin, and FeS^{sp} is mol%. Unlike the sphalerite + pyrrhotite + pyrite equilibrium, the shifts in the solvus to lower values of FeS^{sp} due to the pressure effect were large (Fig. 20). Also, the measured pressure effect was larger than that calculated by Schwarcz et al. (1975). The composition of sphalerite in equilibrium with troilite + α -iron

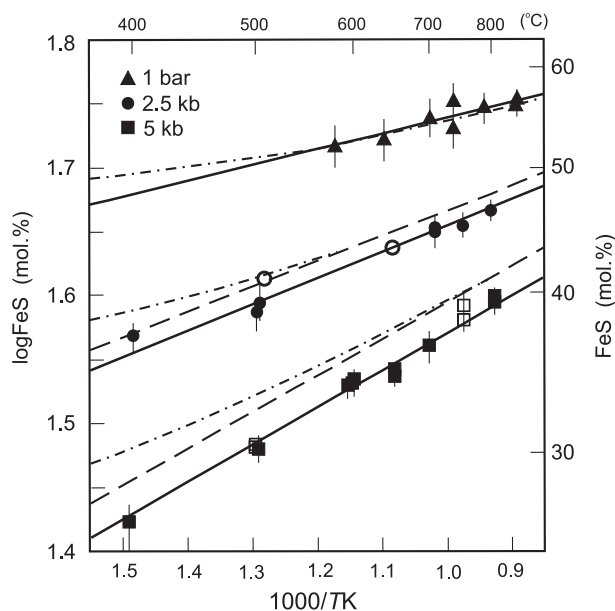


Figure 20. Experimentally determined and calculated isobars along the sphalerite + troilite (FeS^{HT}) + α -iron solvus (curve A in Fig. 17): measurements were made at 1 bar, and 2.5 and 5 kbars; dashed and dot-dashed curves are calculated isobars of Hutchison and Scott (1983) and Schwarcz et al. (1975), respectively (after Hutchison and Scott 1983).

was reinvestigated experimentally from 400-840 °C at 1 bar by Balabin and Urusov (1995). They used evacuated sealed silica glass tubes and dry sintering of pure ZnS and FeS starting materials at 660-840 °C, and an anhydrous halide flux of eutectic NaCl + KCl + PbCl₂ + FeCl₂ composition at lower temperature. Their experimental data for the FeS^{sp} saturated solvus at 1 bar were approximated by the following equation:

$$\text{FeS}^{\text{sp}} = 44.09 + 0.0125T \quad (17)$$

where FeS^{sp} is mol% and T is Kelvin. Based on an updated thermodynamic model for the sphalerite [(Zn,Fe)S] solid solution, their new 1 bar solvus (univariant curve A) was in apparent consistency with the high-pressure experimental data of Hutchison and Scott (1983).

The compositions of coexisting hexagonal pyrrhotite + sphalerite are dependent on pressure and temperature and offer the potential of a third sphalerite barometer when appropriately calibrated. This has been investigated by Bryndzia et al. (1988) who recrystallized sphalerite and hexagonal pyrrhotite in a eutectic LiCl-KCl salt flux at 450-750 °C and 1-6 kbars. Plots of the activity of FeS^{hpo} vs. activity of FeS^{sp} were linear for any given pressure, as observed in the earlier study of Barton and Toulmin (1966) at 1 bar. Thus, Bryndzia et al. (1988) concluded that the activity coefficient of FeS^{sp} (i.e., $\gamma_{\text{FeS}^{\text{sp}}}$) is a function of pressure only (Fig. 21) and, following the theory of Barton and Toulmin (1966), used the pressure dependence of $\gamma_{\text{FeS}^{\text{sp}}}$ to establish a geobarometer for coexisting sphalerite + hexagonal pyrrhotite, as follows:

$$P = 27.982 \log(\gamma_{\text{FeS}^{\text{sp}}}) - 8.549 \quad (\pm 0.5 \text{ kbars}) \quad (18)$$

(Bryndzia et al. 1990). This geobarometer resulted in an estimate of 5.8 ± 0.7 kbars for the pressure of metamorphism in the Broken Hill area, Australia, in excellent agreement with 6.0 ± 0.5 kbars for aluminosilicate mineral geobarometers applied to local granulite-grade rocks.

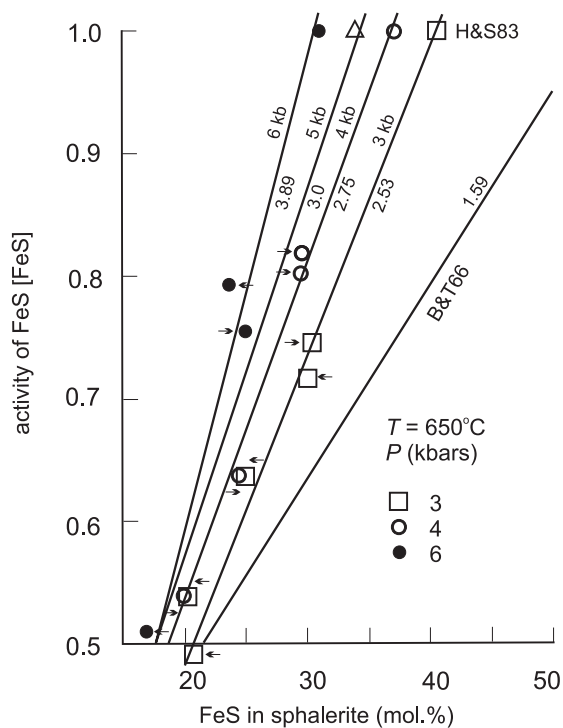


Figure 21. Activity of FeS as a function of sphalerite composition and confining pressure at 650 °C. The activity coefficient in the system FeS-S₂ (values on straight line fits) increases with increase in pressure but is essentially independent of sphalerite composition at constant pressure (after Bryndzia et al. 1988).

Calculated phase relations

Overall, the two geobarometers and the cosmobarometer have been well calibrated by the laboratory experiments and give pressure values consistent with independent estimates from nearby aluminosilicate assemblages. However, an integrated and unifying theoretical basis for these various sphalerite barometers is lacking. Thermodynamic theories for the pressure dependence of FeS^{sp} (or $\gamma_{\text{FeS}^{\text{sp}}}$) result in serious discrepancies between calculated and experimental results below 500 °C (e.g., Fig. 22) and, in the absence of a resolution for these discrepancies, Banno (1988) and Toulmin et al. (1991) regarded sphalerite pressures as tentative. Without rigorous thermodynamic support, the low-temperature experimental reversals obtained using seed crystals remain suspect.

The pronounced pressure dependence of the sphalerite solvus results from the large molar volume change for equilibria between sphalerite (Fe^{2+} in tetrahedral coordination) and pyrrhotite (Fe^{2+} in octahedral coordination). Sphalerite- and wurtzite-type structures are inefficient in respect to space filling by their constituent atoms. For hard shell atoms, the filled space in these structures is estimated as only about 50%, compared with about 70% for the corresponding halite structure compounds (Rooymans 1969). Thus, sphalerite-structure compounds are generally expected to have a relatively low-pressure stability. The relatively high-pressure stability of end-member sphalerite (up to about 15 GPa at room temperature) is anomalous for this structure type, and attributable to the very strong preference of divalent Zn for tetrahedral coordination with ligands. On the other hand, sphalerite-structure FeS is expected to behave similarly to sphalerite-structure MnS which inverts to alabandite at 0.3 GPa and room temperature. The equilibrium between sphalerite and troilite (or FeS^{tr}) in the Fe-Zn-S system may be represented by the reaction:



with an equilibrium constant $K_{\text{sp-tr}} = [\text{FeS}^{\text{tr}}]/[\text{FeS}^{\text{sp}}]$, where box brackets indicate activity. The molar volume change for this reaction at 1 bar and room temperature ($\Delta V^{\text{tr-sp}}$) is

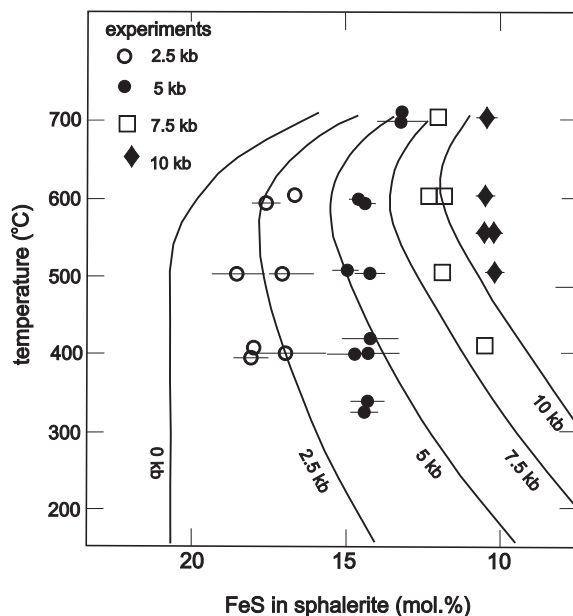


Figure 22. Calculated shifts in univariant curve B [Fig. 17; i.e., sphalerite coexisting with pyrrhotite + pyrite + sulfur(vapor)] for confining pressures of 2.5, 5, 7.5, and 10 kbars, showing marked discrepancies with experimental measurements, particularly in the low-temperature region (after Toulmin et al. 1991).

$-5.90 \text{ cm}^3/\text{mol}$ (or -0.59 J/bar ; using unit-cell data of Fleet 1975, and Yund and Hall 1968). As a first approximation, the experimental results of Barton and Toulmin (1966), Boorman (1967) and Balabin and Urusov (1995), for the 1 bar isobar for sphalerite in equilibrium with troilite (or FeS^{HT}) and α -iron, may be extrapolated to higher pressure using the isothermal pressure correction term for deviations from end-member compositions in silicate mineral geobarometers when parameterized as:

$$P = aT + b - RT \ln K/(\Delta V) \quad (20)$$

where T is Kelvin, R is the universal gas constant, K is the equilibrium constant, and the effects of thermal expansion and isothermal compression on the volume change are ignored. The change in pressure due to dilution of end-member component(s) is given by:

$$P - P_0 = -RT \ln K/(\Delta V) \quad (21)$$

where, P_0 is the reference pressure when $K = 1$ at temperature T . For the 1 bar sphalerite isobar of Balabin and Urusov (1995), the composition of sphalerite (in mole fractions of FeS ; i.e., $X_{\text{FeS}^{\text{SP}}}$) is 0.525 at 700 K and 0.565 at 1000 K. Rearranging equation (21) to:

$$P_0 - P = RT \ln K/(\Delta V) \quad (22)$$

and assuming ideal solid solution in sphalerite of composition $(\text{Zn,Fe})\text{S}$ and $[\text{FeS}^{\text{tr}}] = 1$, so that $K = 1/X_{\text{FeS}^{\text{SP}}}$, results in fictive values for the reference pressure (P_0) of -6.4 and -8.0 kbars at 700 K and 1000 K, respectively. Using these fictive values for P_0 , we calculate that, at 700 K, the solvus is shifted from $X_{\text{FeS}^{\text{SP}}} = 0.525$ at 1 bar to 0.41 at 2.5 kbars and 0.32 at 5.0 kbars and, at 1000 K, it is shifted from 0.565 at 1 bar to 0.47 at 2.5 kbars and 0.40 at 5.0 kbars. These pressure corrections shift the sphalerite solvus, respectively, toward the 2.5 and 5.0 kbars experimental isobars of Hutchison and Scott (1983). Agreement with the experimental isobars is improved by accounting for non-ideality of the $(\text{Zn,Fe})\text{S}$ solid solution. For example, using the 850 °C activity coefficients of Fleet (1975), the solvus is shifted, at 700 K, to $X_{\text{FeS}^{\text{SP}}} = 0.39$ at 2.5 kbars and 0.28 at 5.0 kbars and, at 1000 K, to $X_{\text{FeS}^{\text{SP}}} = 0.46$ at 2.5 kbars and 0.37 at 5.0 kbars. The latter set of calculated values reproduces the experimental isobars of Hutchison and Scott (1983) reasonably well (Fig. 23).

The pressure corrections of Schwarcz et al. (1975) and Hutchison and Scott (1983) for the sphalerite cosmobarometer and of Scott (1973), Hutcheon (1980) and Toulmin et al. (1991) for the sphalerite geobarometer are all based on the equation derived by Barton and Toulmin (1966) for the pressure dependence of $X_{\text{FeS}^{\text{SP}}}$:

$$\frac{dX_{\text{FeS}^{\text{SP}}}}{dP} = - \frac{(\bar{V}_{\text{FeS}^{\text{SP}}} - V_{\text{FeS}^{\text{tr}}})X_{\text{FeS}^{\text{SP}}}}{RT} \quad (23)$$

where \bar{V} is the partial molar volume of FeS^{SP} , $V_{\text{FeS}^{\text{tr}}}$ is the molar volume of pure troilite, and T is Kelvin. These authors have variously corrected for nonideality of mixing, thermal expansion and isothermal compression of coexisting $(\text{Zn,Fe})\text{S}$ and Fe_{1-x}S . The most significant discrepancy with the experimental results is the failure to reproduce the curious temperature independence of isobars for sphalerite in equilibrium with pyrrhotite and pyrite (curve B in Fig. 17) below 600 °C (e.g., Figs. 19 and 22). Balabin and Urusov (1995) used a more rigorous equation for pressure dependence of $X_{\text{FeS}^{\text{SP}}}$ in the sphalerite cosmobarometer (curve B in Fig. 17), and reevaluated the mixing properties of the sphalerite solid solution using the analytical method of Chuang et al. (1985) to solve an expanded Guggenheim-type equation for the excess free energy of mixing. Values for three coefficients and four interaction parameters were obtained by fitting a data set of experimental values for the 1 bar isobar of sphalerite in equilibrium with troilite (or FeS^{HT}) and α -iron, from Barton and Toulmin (1966) and their study. Extrapolation to 2.5 and 5.0 kbars resulted in very good agreement with selected experimental results from Hutchison and Scott (1983) (Fig. 23). Martín and Gil

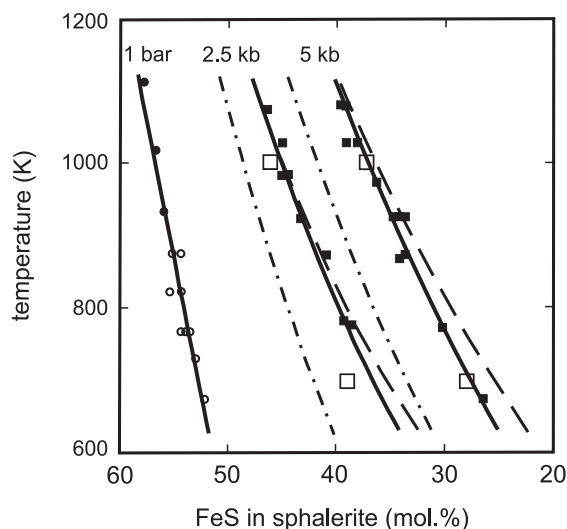


Figure 23. Experimental data of Hutchison and Scott (1983) for the high-pressure sphalerite solvus buffered by $\text{FeS}^{\text{HT}} + \alpha$ -iron (curve A in Fig. 17; i.e., the cosmobarometer) compared with solvi calculated for different models of the mixing of FeS and ZnS in sphalerite: dot-dashed curves assume ideal mixing behavior; dashed curves are a simple regular solution; solid curves are a regular solution with optimized (fitted) parameters; and open squares are values of pressure-induced shifts from 1 bar isobar calculated in present text; cf. Figure 20 (after Balabin and Urusov 1995).

(2005) followed Hutcheon (1978, 1980) in using asymmetric Margules parameters to describe the mixing in (Zn,Fe) sphalerites: this resulted in a complex analytical expression which they fitted to a database of 279 experiments. As a footnote to these theoretical pressure corrections, Fleet (1975) pointed out that the activity system used in Barton and Toulmin (1966) is a hybrid between that of Lewis and Randall (1961) and the absolute activity system of Guggenheim (1959, p. 220) and does not properly reflect mixing in the crystal lattice of sphalerite. For example, the activity of FeS^{sp} is obtained from the equality $[\text{FeS}^{\text{sp}}] = [\text{FeS}^{\text{po}}]$, in the manner of the absolute activities of Guggenheim (1959), rather than from equality of the Gibbs chemical potentials. It follows that reported values for activity coefficients have to be viewed relative to the mixing system being adopted; e.g., using the Lewis and Randall system, Fleet (1975) found that the departures of ZnS and FeS from ideal solution in sphalerite of composition (Zn,Fe)S were not very great, whereas Balabin and Urusov (1995) reported relatively large positive deviations from ideality. More recently, the cluster variation model (CVM) of Balabin and Sack (2000) predicted only moderate deviations from ideality, similar to those calculated by Fleet (1975) at 850 °C.

HALITE STRUCTURE MONOSULFIDES

The monosulfides of Mg, Ca, Mn, and Fe with the cubic halite structure occur naturally as niningerite [(Mg, Fe, Mn)S], alabandite (MnS) and oldhamite (CaS) in EH enstatite chondrite meteorites, where they appear to result from metamorphism under strongly reducing conditions (e.g., Fleet and MacRae 1987). Alabandite also occurs in low-temperature vein deposits in the Earth's crust.

Electronic structure and magnetism

As noted above, the electrical and magnetic properties of metal sulfides are strongly influenced by covalence of the metal-S bond, which results in hybridization of S $3p$ and metal $3d$ bonding states and direct or indirect metal-metal ($M-M$) bonding interactions in favourable cases. The metal and S atoms in these monosulfides are both in octahedral coordination with nearest neighbors, and there is little direct interaction between MS_6 octahedra. As reviewed in Farrell et al. (2001), the alkaline earth chalcogenides are considered to be insulators or large

band gap semiconductors. Divalent Mg differs from Ca, Mn and Fe in that there are no metal $3d$ orbitals in the energy band gap available for hybridization with S $3p$ orbitals. At room temperature and pressure, both MgS and CaS are diamagnetic and classical insulators or large indirect ($\Gamma-X$) band gap semiconductors. The band gap of 2.7 eV in MgS is bounded by S $3p$ bonding orbitals in the upper part of the valence-band (VB) and by Mg $3s \sigma^*$ (and to a lesser extent, S $3d$) antibonding orbitals in the lower part of the conduction-band (CB). In CaS, the band gap (given variously as 4.4 or 2.1 eV) lies between the S $3p$ bonding orbitals in the VB and predominantly Ca $3d$ (and to a lesser extent Ca $4s \sigma^*$) antibonding orbitals in the CB. In MnS, Mn has the high spin $t_{2g}^3-e_g^2$ electronic configuration, with the majority spin (\uparrow) t_{2g}^α and e_g^α bands filled and minority spin (\downarrow) t_{2g}^β and e_g^β bands empty. At room temperature, α -MnS (Néel temperature ~ 152 K) is antiferromagnetic. It is a diluted magnetic semiconductor and has outstanding magnetic and magneto-optical properties derived through interaction of hybridized S sp and Mn $3d$ states (Sato et al. 1997). The band gap lies between occupied Mn $3d$ states in the VB and unoccupied S $3p \sigma^*$ antibonding states hybridized with Mn $3d(e_g)$ and $3d(t_{2g}) \sigma^*$ antibonding states.

Phase relations

CaS and MgS are refractory compounds. Solid solutions within the system MgS-MnS-CaS-FeS up to about 1100 °C were investigated by Skinner and Luce (1971) using the evacuated sealed silica glass tube method. The extent of solid solution in binary systems is well displayed in their plot of cubic unit-cell edge (a) vs. composition (present Fig. 24). MgS and MnS form a completely miscible solid solution at all temperatures investigated (from 600-1000 °C), and melting was not detected up to 1100 °C. These two sulfides also displayed extensive and strongly temperature-dependent solid solutions toward FeS^{HT}, with about 74 mol% FeS in (Mn,Fe)S and 68 mol% FeS in (Mg,Fe)S at 1000 °C. Correspondingly, the high-temperature FeS phase accommodated 7.4 mol% MnS at the same temperature. However,

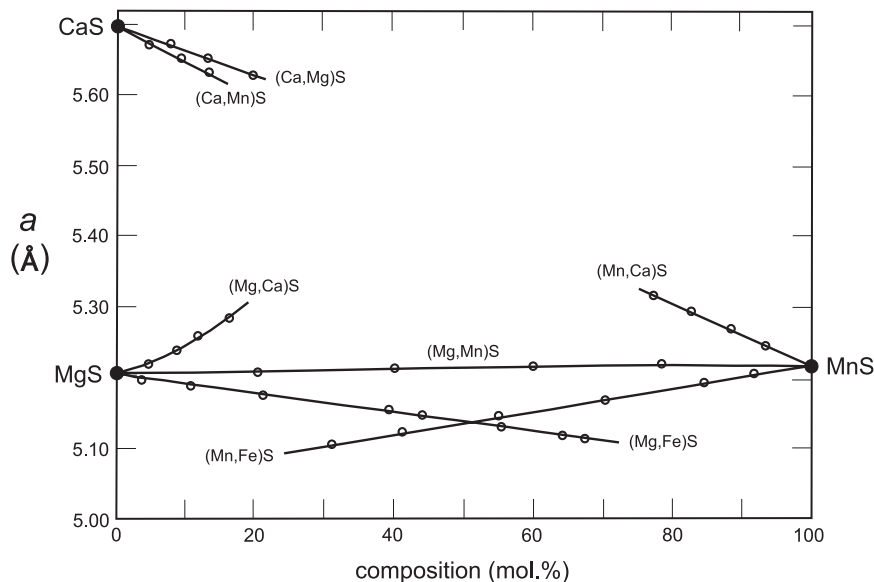


Figure 24. Effect of binary cation substitutions on unit-cell edge (a) of halite-structure monosulfides: measurements were made at room temperature on quenched experimental samples; discontinuous distributions reflect solvus limits at various temperatures investigated (after Skinner and Luce 1971).

solid solution of the ionic monosulfides MgS and CaS in NiAs-type FeS^{HT} was not detected. It is interesting to note at this point that substitution of divalent Fe into MgS results in a decrease in unit-cell edge (Fig. 24), extrapolating to $a = 5.07 \text{ \AA}$ for the hypothetical FeS end-member, compared with $a = 5.202 \text{ \AA}$ for MgS. Since the radius of Fe²⁺ is some 8% greater than that of Mg²⁺ in oxy structures (e.g., Shannon 1976), this decrease in the cell edge of the (Mg,Fe)S solid solution surely highlights the greater covalence of the Fe-S bond and hybridization of S 3*p* and metal 3*d* bonding states on the Fe atoms, compared with both MgS and Fe oxy compounds. The substitution of Mn into MgS also results in little increase in a , in spite of the significant difference in effective ionic radius for oxy structures (0.83 and 0.72 Å, respectively). However, covalence and *p-d* hybridization are diminished in MnS compared with halite-structure FeS, because of the stable 3*d*⁵ high spin electron configuration of Mn²⁺. The subsolidus regions of the CaS-MnS and CaS-MgS binary phase diagrams are both dominated by fairly symmetrical and temperature-dependent solvi. At 1000 °C, the solvus limits in Skinner and Luce (1971) were 12.7 and 72.4 mol% MnS in the former system and 25.1 and 81.9 mol% MgS in the latter, with complete miscibility anticipated at higher temperatures.

The stability of niningerite (Mg,Fe)S in enstatite chondrites was investigated by Fleet and MacRae (1987) in their experiments on the sulfidation of Mg-rich olivine under reducing conditions at 1100–1200 °C. Experimental products were niningerite, clinoenstatite, and (Fe,Ni)-*mss* (Fig. 25). Niningerite was present as bubble-like blebs that were interpreted to reflect liquid immiscibility during quenching but are now properly recognized as equilibrium crystals. The average value for the distribution coefficient for Ni/Fe exchange between niningerite solid solution (*nss*) and *mss* was 23.7 ± 2.6 . On the other hand, the values of the distribution coefficient for coexisting niningerite and troilite in four enstatite chondrites were close to unity and, thus, inconsistent with the equilibration of Ni between these two minerals.

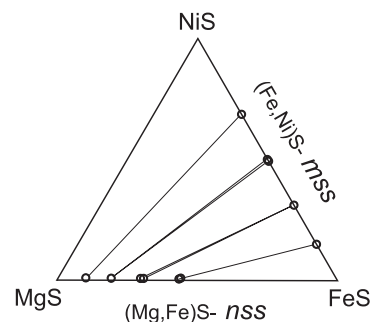


Figure 25. Compositions of coexisting niningerite (*nss*) and (Fe,Ni) monosulfide (*mss*) solid solutions from experiments on the sulfidation of Mg-rich olivine at 1200 °C (after Fleet and MacRae 1987).

ACKNOWLEDGMENTS

I thank Maggy Lengke for library work and the Natural Sciences and Engineering Research Council of Canada for financial support.

REFERENCES

- Albers W, Schol K (1961) The *P-T-X* phase diagram of the system Sn-S. Philips Research Reports 16:329-342
- Allen ET, Crenshaw JL, Merwin HE (1913) The sulfides of zinc cadmium and mercury; their crystalline forms and genetic conditions. Am J Sci Ser 4 34:341-397
- Andresen AF (1960) Magnetic phase transitions in stoichiometric FeS studied by means of neutron diffraction. Acta Chem Scand 14:919-926
- Andresen AF, Torbo P (1967) Phase transitions in Fe_xS ($x = 0.90-1.00$) studied by neutron diffraction. Acta Chem Scand 21:2841-2848
- Anzai S (1997) Effect of correlations on electronic and magnetic properties of transition metal chalcogenides. Physica B237:142-145
- Anzai S, Ozawa K (1974) Effect of pressure on the Néel and the ferromagnetic Curie temperature of FeS_{1-δ}. Phys Stat Sol 24:K31-K34
- Arnold RG (1962) Equilibrium relations between pyrrhotite and pyrite from 325 ° to 743 °C. Econ Geol 57: 72-90
- Arnold RG, Malik OP (1975) The NiS-S system above 980 °C: a revision. Econ Geol 70:176-182

- Avilov AS, Imamov RM, Muradyan LA (1971) An electron diffraction study of some phases in the Cu-Sb-S system. *Trans, Sov Phys Crystallogr* 15:616-619
- Balabin AI, Sack RO (2000) Thermodynamics of (ZnFe)S sphalerite: A CVM approach with large basis clusters. *Mineral Mag* 64:923-943
- Balabin AI, Urusov VS (1995) Recalibration of the sphalerite cosmobarometer: Experimental and theoretical treatment. *Geochim Cosmochim Acta* 59:1401-1410
- Balabin AI, Osadchiy YeG, Urusov VS, Senin VG (1986) Phase relationships involving daubreelite in the Fe-Cr-S, Mn-Fe-Cr-S, Mg-Fe-Cr-S systems at 840, 745, 660, and 550 °C. *Geochem Internat* 23:30-43
- Banno S (1988) On the sphalerite geobarometer. *Geochem J Japan* 22:129-131
- Barker WW, Parks TC (1986) The thermodynamic properties of pyrrhotite and pyrite: a re-evaluation. *Geochim Cosmochim Acta* 50:2185-2194
- Barnes HL (1973) Polymorphism and polytypism. Final Report U.S. Army Research Office (Durham) Contract No DAHCO4-69-C-0043, 38 p
- Barstad J (1959) Phase relations in the system Ag-Sb-S at 400 °C. *Acta Chem Scand* 13:1703-1708
- Barthelemy E, Carcaly C (1987) Phase relations and ageing effects in Fe_{1-x}Co_xS system. *J Solid State Chem* 66:191-203
- Barton PBJr (1969) Thermochemical study of the system Fe-As-S. *Geochim Cosmochim Acta* 33:841-857
- Barton PBJr (1971) The Fe-Sb-S system. *Econ Geol* 66:121-132
- Barton PBJr (1973) Solid solutions in system Cu-Fe-S. Part I: The Cu-S and CuFe-S joins. *Econ Geol* 68:455-465
- Barton PBJr, Toulmin PIII (1964a) The electrom-tarnish method for the determination of the fugacity of sulfur in laboratory sulfide systems. *Geochim Cosmochim Acta* 28:619-640
- Barton PBJr, Toulmin PIII (1964b) Experimental determination of the reaction chalcopyrite + sulfur = pyrite + bornite from 350 °C to 500 °C. *Econ Geol* 59:747-752
- Barton PBJr, Toulmin PIII (1966) Phase relations involving sphalerite in the Fe-Zn-S system. *Econ Geol* 61:815-849
- Baumann IH (1964) Patronite VS₄ und die Mineral-Paragenese der bituminösen Schiefer von Minasragra Peru. *Neues Jahrb Mineral, Abhdl* 101:97-108
- Bayliss P (1968) The crystal structure of disordered gersdorffite. *Am Mineral* 53:290-293
- Bayliss P (1969) Isomorphous substitution in synthetic cobaltite and ullmannite. *Am Mineral* 54:426-430
- Bayliss P (1989) Crystal chemistry and crystallography of some minerals within the pyrite group. *Am Mineral* 74:1168-1176
- Beglyaryan ML, Abrikasov HK (1959) The Bi₂Te₃-Bi₂Se₃ system. *Dokl Akad Nauk USSR* 129:135
- Bell PM, Kullerud G (1970) High pressure differential thermal analysis. *Carnegie Inst Wash, Year Book* 68:276-277
- Bell PM, El Goresy A, England JL, Kullerud G (1970) Pressure-temperature diagram for Cr₂FeS₄. *Carnegie Inst Wash, Year Book* 68:277-278
- Bell RE, Herfert RE (1957) Preparation and characterization of a new crystalline form of molybdenum disulfide. *J Am Chem Soc* 79:3351-3355
- Berner RA (1962) Tetragonal FeS a new iron sulfide. *Science* 137:669
- Berner RA (1964) Iron sulfides formed from aqueous solution at low temperatures and atmospheric pressure. *J Geol* 72:293-306
- Berry LG (1954) The crystal structure of covellite CuS and klockmannite CuSe. *Am Mineral* 39:504-509
- Bertaut EF (1953) Contribution à l'étude des structures lacunaires: la pyrrhotine. *Acta Crystallogr* 6:557-561
- Bertaut EF (1956) Structure de FeS stoechiométrique. *Bulletin Societe Francais Minéralogie et Cristallographie* 79:276-292
- Bethke PM, Barton PBJr (1971) Subsolvus relations in the system PbS-CdS. *Am Mineral* 56:2034-2039
- Bethke PM, Barton PBJr (1961) Unit-cell dimension versus composition in the systems PbS-CdS, PbS-PbSe, ZnS-ZnSe, and CuFeS₁₉₀-CuFeSe₁₉₀. *U.S. Geol Surv Prof Paper* 429B:266-270
- Bloem J, Kroger FA (1956) The *P-T-X* phase diagram of the lead-sulfur system. *Z Physikalische Chemie (München)* 7:1-14
- Boehler R (1992) Melting of the Fe-FeO and the Fe-FeS systems at high pressure: Constraints on core temperatures. *Earth Planet Sci Lett* 111:217-227
- Boer KW, Nalesnik NJ (1969) Semiconductivity of CdS as a function of S-vapor pressure during heat treatment between 500 ° and 700 °C. *Mat Res Bull* 4:153-160
- Boorman RS (1967) Subsolvus studies in the ZnS-FeS-FeS₂ system. *Econ Geol* 62:614-631
- Boorman RS, Sutherland JK, Chernyshev LV (1971) New data on the sphalerite-pyrrhotite-pyrite solvus. *Econ Geol* 66:670-675
- Bortnikov NS, Nekrasov IYa, Mozgova NN, Tsepin AI (1981) Phases and phase relations in the central portion of the system Fe-Pb-Sb-S between 300 and 500 °C in relation to lead-antimony sulphosalts. *Neues Jahrb Mineral, Abhdl* 143:37-60

- Bouchard RJ (1968) The preparation of pyrite solid solutions of the type $\text{Fe}_x\text{Co}_{1-x}\text{S}_2$, $\text{Co}_x\text{Ni}_{1-x}\text{S}_2$ and $\text{Cu}_x\text{Ni}_{1-x}\text{S}_2$. *Mat Res Bull* 3:563-570
- Brett PR (1964) Experimental data from the system Cu-Fe-S and their bearing on exsolution textures in ores. *Econ Geol* 59:1241-1269
- Brett PR, Kullerud G (1967) The Fe-Pb-S system. *Econ Geol* 62:354-369
- Brower WS, Parker HS, Roth RS (1974) Reexamination of synthetic parkerite and shandite. *Am Mineral* 59:296-301
- Bryndzia LT, Scott SD, Spry PG (1988) Sphalerite and hexagonal pyrrhotite geobarometer: Experimental calibration and application to the metamorphosed sulfide ores of Broken Hill Australia. *Econ Geol* 83:1193-1204
- Bryndzia LT, Scott SD, Spry PG (1990) Sphalerite and hexagonal pyrrhotite geobarometer: Correction in calibration and application. *Econ Geol* 85:408-411
- Buerger JJ, Buerger MH (1944) Low chalcocite. *Am Mineral* 29:55-65
- Buhlmann E (1965) Untersuchungen im System Cu-Bi-S. PhD Thesis, University of Heidelberg, Germany
- Buhlmann E (1971) Untersuchungen im System Bi_2S_3 -Cu₂S und geologische Schlussfolgerungen. *Neues Jahrb Mineral, Monat* 137-141
- Bunch TE, Fuchs LH (1969) A new mineral: brezinaite Cr_3S_4 and the Tuscon meteorite. *Am Mineral* 54:1503-1518
- Burgmann W, Urbain G, Froberg MG (1968) Iron-sulfur system in the iron monosulfide (pyrrhotite) region. *Memoires Scientifiques de la Revue de Metallurgie* 65:567-578
- Burkart-Baumann I, Ottemann J, Amstutz GC (1972) The X-ray amorphous sulfides from Cerro de Pasco Peru and the crystalline inclusions. *Neues Jahrb Mineral, Monat* 433-446
- Cabri LJ (1967) A new copper-iron sulfide. *Econ Geol* 62:910-925
- Cabri LJ (1972) The mineralogy of the platinum group elements. *Mineral Sci Engin* 4:3-29
- Cabri LJ (1973) New data on phase relations in the Cu-Fe-S system. *Econ Geol* 68:443-454
- Cabri LJ, Hall SR (1972) Mooihoekite and haycockite two new copper-iron sulfides and their relationship to chalcopyrite and talnakhite. *Am Mineral* 57:689-708
- Cabri LJ, Harris DC (1971) New compositional data on talnakhite. *Econ Geol* 66:673-675
- Cabri LJ, Harris DC, Stewart JM (1970a) Costibite (CoSbS) a new mineral from Broken Hill New South Wales. *Am Mineral* 55:10-17
- Cabri LJ, Harris DC, Stewart JM (1970b) Paracostibite (CoSbS) and nisbite (NiSb_2) new minerals from the Red Lake area Ontario Canada. *Can Mineral* 10:232-246
- Cambi L, Elli M (1965) Hydrothermal processes: III Synthesis of thiosalts derived from silver and antimony sulfides. *Chimica e l'Industria (Milan)* 47:282-290
- Canneri G, Fernandes L (1925) Contributo allo studio di alcuni minerali contenenti tallio Analise ternaica dei sistemi $\text{Ti}_2\text{S}-\text{As}_2\text{S}_3$, $\text{Ti}_2\text{S}-\text{PbS}$. *Atti della Accademia Nazionale dei Lincei Classe di Scienze Fisiche Matematiche e Naturali Rendiconti* 1:671-676
- Carpenter RH, Desborough GA (1964) Range in solid solution and structure of naturally occurring troilite and pyrrhotite. *Am Mineral* 49:1350-1365
- Caye R, Cervelle B, Cesbron F, Oudin E, Picot P, Pillard F (1988) Isocubanite a new definition of the cubic polymorph of cubanite CuFe_2S_3 . *Mineral Mag* 52:509-514
- Chang LLY (1963) Dimorphic relations in Ag_3SbS_3 . *Am Mineral* 48:429-432
- Chang LLY, Bever JE (1973) Lead sulphosalt minerals: Crystal structures stability relations and paragenesis. *Mineral Sci Engin* 5:181-191
- Chang LLY, Knowles CR (1977) Phase relations in the systems $\text{PbS}-\text{Fe}_{1-x}\text{S}-\text{Sb}_2\text{S}_3$ and $\text{PbS}-\text{Fe}_{1-x}\text{S}-\text{Bi}_2\text{S}_3$. *Can Mineral* 15:374-379
- Chang LLY, Wu D, Knowles CR (1988) Phase relations in the system $\text{Ag}_2\text{S}-\text{Cu}_2\text{S}-\text{PbS}-\text{Bi}_2\text{S}_3$. *Econ Geol* 83:405-418
- Chernyshev LV, Anfilogov VN (1968) Subsolidus phase relations in the ZnS-FeS- FeS_2 system. *Econ Geol* 63:841-844
- Chevreton M, Sapet A (1965) Structure de V_3S_4 et de quelques sulfures ternaires isotopes. *Comptes Rendus de l'Académie des Sciences, Paris* 261:928-930
- Chuang Y-Y, Hsieh K-C, Chang YA (1985) Thermodynamics and phase relationships of transition metal-sulfur systems: Part V A reevaluation of the Fe-S system using an associated solution model for the liquid phase. *Metall Trans* 16B:277-285
- Clark AH (1966a) Heating experiments on gudmundite. *Mineral Mag* 35:1123-1125
- Clark AH (1966b) Stability field of monoclinic pyrrhotite. *Trans, Inst Mining Metall (London)* B75:B232-B235
- Clark AH (1970a) An occurrence of the assemblage native sulfur-covellite- $\text{Cu}_{55x}\text{Fe}_x\text{S}_{65x}$. Aucanquilcha, Chile. *Am Mineral* 55:913-918
- Clark AH (1970b) Compositional differences between hexagonal and rhombohedral molybdenite. *Neues Jahrb Mineral, Monat* 1:33-38

- Clark AH (1970c) Cuprian sphalerite and a probable copper zinc sulfide, Cachiyuyo de Llampos, Copiapo, Chile. *Am Mineral* 55:1021-1025
- Clark AH (1970d) Supergene metastibnite from Mina Alacrán, Pampa Larga, Copiapo, Chile. *Am Mineral* 55:2104-2106
- Clark AH (1971) Molybdenite 2H₁ molybdenite 3R and jordisite from Carrizal Alto, Atacama, Chile. *Am Mineral* 56:1832-1835
- Clark AH (1974) Hypogene and supergene cobalt-copper sulfides, Carrizal Alto, Atacama, Chile. *Am Mineral* 59:302-306
- Clark AH, Sillitoe RH (1971) Cuprian galena solid solutions Zapallar Mining district, Atacama, Chile. *Am Mineral* 56:2142-2145
- Clark LA (1960a) The Fe-As-S system: Phase relations and applications. *Econ Geol* 55:1345-1381, 1631-1652
- Clark LA (1960b) The Fe-As-S system: Variations of arsenopyrite composition as functions of T and P. *Carnegie Inst Wash, Year Book* 59:127-130
- Clark LA, Kullerud G (1963) The sulfur-rich portion of the Fe-Ni-S system. *Econ Geol* 58:853-885
- Coe JMD, Roux-Buisson H (1979) Electronic properties of (Ni_{1-x}Fe_x)S solid solutions. *Mat Res Bull* 14:711-716
- Collin G, Gardette MF, Comes R (1987) The Fe_{1-x}Co_xS system (x < 0.25); transition and the high temperature phase. *J Phys Chem Solids* 48:791-802
- Corral JA (1964) Recovery of the high pressure phase of cadmium sulfide. *J Appl Phys* 35:3032-3033
- Craig JR (1967) Phase relations and mineral assemblages in the Ag-Bi-Pb-S system. *Mineralium Deposita* 1:278-306
- Craig JR (1971) Violarite stability relations. *Am Mineral* 56:1303-1311
- Craig JR (1973) Pyrite-pentlandite assemblages and other low temperature relations in the Fe-Ni-S system. *Am J Sci* 273-A:496-510
- Craig JR, Kullerud G (1968) Phase relations and mineral assemblages in the copper-lead-sulfur system. *Am Mineral* 53:145-161
- Craig JR, Kullerud G (1973) The Cu-Zn-S system. *Mineralium Deposita* 8:81-91
- Craig JR, Scott SD (1974) Sulfide phase equilibria. *Rev Mineral* 1:CS-1-CS-110
- Craig JR, Skinner BJ, Francis CA, Luce FD, Makovicky E (1974) Phase relations in the As-Sb-S system. *Trans, Am Geophys Union* 55:483
- Cubicciotti D (1962) The bismuth-sulfur phase diagram. *J Phys Chem* 66:1205-1206
- Cubicciotti D (1963) Thermodynamics of liquid bismuth and sulfur. *J Phys Chem* 67:118-123
- Curlook W, Pidgeon LM (1953) The Co-Fe-S system. *Can Mining Metall Bull* 493(56):297-301
- Czamanske GK (1969) The stability of argentopyrite and sternbergite. *Econ Geol* 64:459-461
- Czamanske GK (1974) The FeS content of sphalerite along the chalcopyrite-pyrite-sulfur fugacity buffer. *Econ Geol* 69:1328-1334
- Czamanske GK, Larson RR (1969) The chemical identity and formula of argentopyrite and sternbergite. *Am Mineral* 54:1198-1201
- Delafosse D, Can Huang Van (1962) Étude du système Ni-Co-S a température élevée. *Comptes Rendus de l'Académie des Sciences, Paris* 254:1286-1288
- Desgreniers S, Beaulieu L, Lepage I (2000) Pressure-induced structural change in ZnS. *Phys Rev B* 61:8726-8733
- Dickson FW, Tunell G (1959) The stability relations of cinnabar and metacinnabar. *Am Mineral* 44:471-487
- Dickson FW, Radtke AS, Weissberg BG, Heropoulos C (1974) Solid solutions of antimony arsenic and gold in stibnite (Sb₂S₃) orpiment (As₂S₃) and realgar (As₂S₂). *Econ Geol* 70:591-594
- Djurle S (1958) An X-ray study of the system Ag-Cu-S. *Acta Chem Scand* 12:1427-1436
- Dolanski J (1974) Sulvanite from Thorpe Hills, Utah. *Am Mineral* 59:307-313
- D'sugi J, Shimizu K, Nakamura T, Onodera A (1966) High pressure transition in cadmium sulfide. *Rev Phys Chem Japan* 36:59-73
- DuPreez JW (1945) A thermal investigation of the parkerite series. *University of Stellenbosch* 22:A 97-104
- Einaudi MT (1968) Sphalerite-pyrrhotite-pyrite equilibria- A re-evaluation. *Econ Geol* 63:832-834
- Einaudi MT (1987) Phase relations among silicates copper iron sulfides and aqueous solutions at magmatic temperatures-A discussion. *Econ Geol* 82:497-502
- El Goresy A, Kullerud G (1969) Phase relations in the system Cr-Fe-S. *In: Meteorite research* D. Millman PM (ed) Reidel, p 638-656
- Erd RC, Evans HT, Richter HD (1957) Smythite a new iron sulfide and associated pyrrhotite from Indiana. *Am Mineral* 42:309-333
- Etschmann B, Pring A, Putnis A, Grguric BA, Studer A (2004) A kinetic study of the exsolution of pentlandite (NiFe)₉S₈ from the monosulfide solid solution (FeNi)S. *Am Mineral* 89:39-50
- Evans HT Jr (1971) Crystal structure of low chalcocite. *Nature* 232:69-70
- Farrell SP, Fleet ME (2000) Evolution of local electronic structure in cubic Mg_{1-x}Fe_xS by S K-edge XANES spectroscopy. *Solid State Commun* 113:69-72

- Farrell SP, Fleet ME (2001) Sulfur K-edge XANES study of local electronic structure in ternary monosulfide solid solution [(Fe Co Ni)_{0.923}S]. *Phys Chem Mineral* 28:17-27
- Farrell SP, Fleet ME (2002) Phase separation in (FeCo)_{1-x}S monosulfide solid solution below 450 °C with consequences for coexisting pyrrhotite and pentlandite in magmatic sulfide deposits. *Can Mineral* 40: 33-46
- Farrell SP, Fleet ME, Stekhin IE, Soldatov A, Liu X (2001) Evolution of local electronic structure in alabandite and niningerite solid solutions [(MnFe)S (MgMn)S (MgFe)S] using sulfur K- and L-edge XANES spectroscopy. *Am Mineral* 87:1321-1332
- Fei Y, Bertka CM, Finger LW (1997) High-pressure iron-sulfur compound Fe₃S₂ and melting relations in the Fe-FeS system. *Science* 275:1621-1623
- Fei Y, Li J, Bertka CM, Prewitt CT (2000) Structure type and bulk modulus of Fe₃S a new iron-sulfur compound. *Am Mineral* 85:1830-1833
- Fei Y, Prewitt CT, Mao HK, Berka CM (1995) Structure and density of FeS at high-pressure and high-temperature and the internal structure of Mars. *Science* 268:1892-1894
- Filimonova AA, Evstigneeva TL, Laputina IP (1980) Putoranite and nickeloan putoranite- new minerals of the chalcopyrite group. *Zapiski Vsesoyuznogo Mineralogicheskogo Obshchestva* 109:335-341
- Fleet ME (1968) On the lattice parameters and superstructures of pyrrhotites. *Am Mineral* 53:1846-1855
- Fleet ME (1971) The crystal structure of a pyrrhotite (Fe₇S₈). *Acta Crystallogr B* 27:1864-1867
- Fleet ME (1972) The crystal structure of α-Ni₇S₆. *Acta Crystallogr B* 28:1237-1241
- Fleet ME (1973) The crystal structure of parkerite (Ni₃Bi₂S₂). *Am Mineral* 58:435-439
- Fleet ME (1975) Thermodynamic properties of (ZnFe)S solid solutions at 850 °C. *Am Mineral* 60:466-470
- Fleet ME (1977) The birefringence-structural state relation in natural zinc sulfides and its application to the schalenblende from Pribram. *Can Mineral* 15:303-308
- Fleet ME (1982) Synthetic smythite and monoclinic Fe₃S₄. *Phys Chem Mineral* 8:241-246
- Fleet ME (1987) Structure of godlevskite Ni₉S₈. *Acta Crystallogr C* 43:2255-2257
- Fleet ME (1988) Stoichiometry structure and twinning of godlevskite and synthetic low-temperature Ni-excess nickel sulphide. *Can Mineral* 26:283-291
- Fleet ME, MacRae ND (1987) Sulfidation of Mg-rich olivine and the stability of niningerite in enstatite chondrites. *Geochim Cosmochim Acta* 51:1511-1521
- Francis CA, Fleet ME, Misra KC, Craig JR (1976) Orientation of exsolved pentlandite in natural and synthetic nickeliferous pyrrhotite. *Am Mineral* 61:913-920
- Franzen HF, Smeggil J, Conard BR (1967) The group IV di-transition metal sulfides and selenides. *Mat Res Bull* 2:1087-1092
- Fujimori A, Namatame H, Matoba M, Anzai S (1990) Photoemission study of the metal-nonmetal transition in NiS. *Phys Rev B* 42:620-623
- Gaines RV (1957) Luzonite famatinite and some related minerals. *Am Mineral* 42:766-779
- Gaines RV, Skinner HCW, Foord EE, Mason B, Rosenzweig A (1997) Dana's New Mineralogy. John Wiley
- Gammon JB (1966) Some observations on minerals in the system CoAsS-FeAsS. *Norsk Geol Tids* 46:405-426
- Geller S (1962) Refinement of the crystal structure of Co₉S₈. *Acta Crystallogr* 15:1195-1198
- Goble RJ (1980) Copper sulfides from Alberta: yarrowite Cu₉S₈ and spionkopite Cu₃₉S₂₈. *Can Mineral* 18: 511-518
- Goble RJ, Robinson G (1980) Geerite Cu₁₆₀S a new copper sulfide from Dekalb Township, New York. *Can Mineral* 18:519-523
- Godovikov AA, Il'yasheva NA (1971) Phase diagram of a bismuth-bismuth sulfide-bismuth selenide system. *Materialy po Geneticheskoi i Eksperimental'noi Mineralogii* 6:5-14
- Godovikov AA, Pütsyn AB (1968) Syntheses of Cu-Bi-sulfides under hydrothermal conditions. *Eksperimental'noi Issled Mineralogii* 6:29-41
- Godovikov AA, Kochetkova KV, Lavrent'ev YuG (1970) Bismuth sulfotellurides from the Sokhondo deposit. *Geologiya i Geofizika* 11:123-127
- Goodenough JB (1967) Description of transition metal compounds: application to several sulfides. *In: Propertés thermodynamiques physiques et structurales des dérivés semi-metalliques*. Paris: Centre National de la Recherche Scientifique, p 263-292
- Gopalakrishnan J, Murugesan T, Hegde MS, Rao CNR (1979) Study of transition-metal monosulphides by photoelectron spectroscopy. *J Phys C: Solid State Phys* 12:5255-5261
- Gosselin JR, Townsend MG, Tremblay RJ (1976a) Electric anomalies at the phase transition in iron monosulfide. *Solid State Commun* 19:799-803
- Gosselin JR, Townsend MG, Tremblay RJ, Webster AH (1976b) Mössbauer effect in single-crystal Fe_{1-x}S. *J Solid State Chem* 17:43-48
- Graeser S (1964) Über Funde der neuen rhombohedrichen MoS₂ - Modifikation (Molybdanit - 3R) und von Tungstenit in den Alpen Schweiz. *Mineral Petrogr Mitt* 44:121-128
- Graeser S (1967) Ein Vorkommen von Lorandite (TlAsS₂) in der Schweiz. *Contrib Mineral Petrol* 16:45-50

- Graf R B (1968) The system $\text{Ag}_3\text{AuS}_2\text{-Ag}_2\text{S}$. *Am Mineral* 53:496-500
- Grguric BA, Putnis A (1998) Compositional controls on phase transition temperatures in bornite: a differential scanning calorimetry study. *Can Mineral* 36:215-227
- Grguric BA, Putnis A (1999) Rapid exsolution behaviour in the bornite-digenite series: implications for natural ore assemblages. *Mineral Mag* 63:1-14
- Grguric BA, Harrison RJ, Putnis P (2000) A revised phase diagram for the bornite-digenite join from *in situ* neutron diffraction and DSC experiments. *Mineral Mag* 64:213-231
- Grguric BA, Putnis A, Harrison RJ (1998) An investigation of the phase transitions in bornite (Cu_5FeS_4) using neutron diffraction and differential scanning calorimetry. *Am Mineral* 83:1231-1239
- Grønsvold F, Haraldsen H (1952) The phase relations of synthetic and natural pyrrhotites (Fe_{1-x}S). *Acta Chem Scand* 6:1452-1469
- Grønsvold F, Westrum EF (1980) The anilite/low-digenite transition. *Am Mineral* 65:574-575
- Grønsvold F, Haraldsen H, Kjekshus A (1960) On the sulfides selenides and tellurides of platinum. *Acta Chem Scand* 14:1879-1893
- Grover B, Moh GH (1966) Experimentelle untersuchungen des quaternären systems Kupfer-Eisen Molybdän-Schwefel. Referat 44 Jahrestagung der Deutschen Mineralogischen Gesellschaft, München
- Grover B, Moh GH (1969) Phasen gleichgewichtsbeziehungen im system Cu-Mo-S in Relation zu natürlichen Mineralien. *Neues Jahrb Mineral, Monat* 529-544
- Grover B, Kullerud G, Moh GH (1975) Phase equilibrium conditions in the ternary iron-molybdenum-sulfur system in relation to natural minerals and ore deposits. *Neues Jahrb Mineral, Abhdl* 124:246-272
- Guggenheim EA (1959) *Thermodynamics* 4th ed. North-Holland
- Hahn H, Harder B, Brockmüller W (1965) Untersuchungen der ternären Chalcogenide X Versuche zur Umsetzung von Titan sulfiden mit sulfiden Zweiwertiger Übergangsmetalle. *Z. Anorganische und Allgemeine Chemie* 288:260-268
- Hall HT (1966) The systems Ag-Sb-S Ag-As-S and Ag-Bi-S: Phase relations and mineralogical significance. PhD Dissertation, Brown University
- Hall HT (1968) Synthesis of two new silver sulfosalts. *Econ Geol* 63:289-291
- Hall SR, Gabe EJ (1972) The crystal structure of talnakhite $\text{Cu}_{18}\text{Fe}_{16}\text{S}_{32}$. *Am Mineral* 57:368-380
- Hansen M, Anderko K (1958) *Constitution of Binary Alloys*. McGraw-Hill
- Haraldsen H (1941) The high-temperature transformations of iron(II) sulphide mixed crystals. *Z Anorganische und Allgemeine Chemie* 246:195-226
- Hayase K (1955) Minerals of bismuthinite-stibnite series with special reference to horobetsuite from the Horobetsu Mine. *Mineral J Japan* 1:188-197
- Hiller JE, Probsthain K (1956) Thermische und röntgenographische Untersuchungen am Kupferkies. *Z Kristallogr* 108:108-129
- Hobbs D, Hafner J (1999) Magnetism and magneto-structural effects in transition-metal sulphides. *J Phys: Cond Matt* 11:8197-8222
- Horwood JL, Townsend MG, Webster AH (1976) Magnetic susceptibility of single-crystal Fe_{1-x}S . *J Solid State Chem* 17:35-42
- Hsieh K-C, Chang YA (1987) Thermochemical description of the ternary iron-nickel-sulfur system. *Can Metall Quart* 26:311-327
- Hurlbut CS (1957) The wurtzite-greenockite series. *Am Mineral* 42:184-190
- Hutcheon I (1978) Calculation of metamorphic pressure using the sphalerite-pyrrhotite-pyrite equilibrium. *Am Mineral* 63:87-95
- Hutcheon I (1980) Calculated phase relations for pyrite-pyrrhotite-sphalerite: correction. *Am Mineral* 65:1063-1064
- Hutchison MN, Scott SD (1983) Experimental calibration of the sphalerite cosmobarometer. *Geochim Cosmochim Acta* 47:101-108
- Inan EE, Einaudi MT (2002) Nukundamite ($\text{Cu}_{338}\text{Fe}_{062}\text{S}_4$)-bearing copper ore in the Bingham porphyry deposit Utah: Result of upflow through quartzite. *Econ Geol* 97:499-515
- Janosi A (1964) La structure du sulfure cuivreux quadratiques. *Acta Crystallogr* 17:311-312
- Jellinek F (1957) The structures of the chromium sulphides. *Acta Crystallogr* 10:620-628
- Jensen E (1942) Pyrrhotite: Melting relations and composition. *Am J Sci* 240:695-709
- Jensen E (1947) Melting relations of chalcocite. *Norske Videnskaps- Akademi Oslo Avhandl I Mat-Naturw Klasse* 6, 14 p
- Kajiwaraya Y (1969) Fukuchilite Cu_3FeS_3 a new mineral from the Hanawa mine Akita prefecture. *Mineral J Japan* 5:399-416
- Kanazawa Y, Koto K, Morimoto N (1978) Bornite (Cu_5FeS_4): stability and crystal structure of the intermediate form. *Can Mineral* 16:397-404
- Karakhanova MI, Pushinkin AS, Novoselova AV (1966) Phase diagram of the tin-sulfur system. *Izvestiya Akademii Nauk USSR Neorganicheskie Materialy* 2:991-996

- Karunakaran C, Vijayakumar V, Vaidya SN, Kunte NS, Suryanarayana S (1980) Effect of pressure on electrical resistivity and thermoelectric power of FeS. *Mat Res Bull* 15:201-206
- Karup-Møller S (1972) New data on pavonite gustavite and some related sulphosalt minerals. *Neues Jahrb Mineral, Monat* 19-38
- Karup-Møller S (1985) The system Pd-Co-S at 1000 800 600 and 400 °C. Fourth Internat Platinum Symp, *Can Mineral* 23:306
- Karup-Møller S, Makovicky E (1974) Skinnerite Cu_3SbS_3 a new sulfosalt from the Ilimaussag alkaline intrusion, South Greenland. *Am Mineral* 59:889-895
- Karup-Møller S, Makovicky E (1995) The phase system Fe-Ni-S at 725 °C. *Neues Jahrb Mineral, Monat* 1-10
- Karup-Møller S, Makovicky E (1998) The phase system Fe-Ni-S at 900 °C. *Neues Jahrb Mineral, Monat* 373-384
- Karup-Møller S, Makovicky E (2002) The system Fe-Os-S at 1180 °, 1100 ° and 900 °C. *Can Mineral* 40:499-507
- Kato A (1959) Ikunolite a new bismuth mineral from the Ikuno Mine, Japan. *Mineral J Japan* 2:397-407
- Kavner A, Duffy TS, Shen G (2001) Phase stability and density of FeS at high pressures and temperatures: implications for the interior structure of Mars. *Earth Planet Sci Lett* 185:25-33
- Keighin CW, Honea RM (1969) System Ag-Sb-S from 600 to 200 °C. *Mineralium Deposita* 4:153-171
- Keil K, Brett R (1974) Heiderite $(\text{FeCr})_{1+x}(\text{TiFe})_2\text{S}_4$ a new mineral in the Bustee enstatite achondrite. *Am Mineral* 59:465-470
- Keil K, Snetsinger KG (1967) Niningerite a new meteorite sulfide. *Science* 155:451-453
- Keller-Besrest F, Collin G (1990a) Structural aspects of the α transition in off-stoichiometric iron sulfide $(\text{Fe}_{1-x}\text{S})$ crystals. *J Solid State Chem* 84:211-225
- Keller-Besrest F, Collin G (1990b) Structural aspects of the α transition in stoichiometric iron sulfide (FeS): identification of the high-temperature phase. *J Solid State Chem* 84:211-225
- King HE Jr, Prewitt CT (1982) High-pressure and high-temperature polymorphism of iron sulfide (FeS). *Acta Crystallogr B* 38:1877-1887
- Kirkinskiy VA, Ryaposov AP, Yakushev VG (1967) Phase diagram for arsenic tri-sulfide up to 20 kilobars. *Isvest Akad Nauk USSR* 3:1931-1933
- Kissin, SA (1974) Phase relations in a portion of the Fe-S system. PhD Thesis, University of Toronto
- Kissin SA, Scott SD (1982) Phase relations involving pyrrhotite below 350 °C. *Econ Geol* 77:1739-1754
- Kitakaze A, Sugaki A (2004) The phase relations between $\text{Fe}_{45}\text{Ni}_{45}\text{S}_8$ and Co_9S_8 in the system Fe-Ni-Co-S at temperatures from 400 ° to 1100 °C. *Can Mineral* 42:17-42
- Kitakaze A, Sugaki A, Shima H (1995) Study of the minerals on the PbS-Sb₂S₃ join; Part 1, Phase relations above 400 °C. *Mineral J Japan* 17:282-289
- Klemm DD (1962) Untersuchungen Über die Mischkristall bildung im Dreieck diagramm FeS_2 - CoS_2 - NiS_2 und ihre Beziehungen zum Aufbau der natürlichen "Bravoite". *Neues Jahrb Mineral, Monat* 76-91
- Klemm DD (1965) Synthesen und Analysen in den Dreieckdiagrammen FeAsS - CoAsS - NiAsS und FeS_2 - CoS_2 - NiS_2 . *Neues Jahrb Mineral, Abhdl* 103:205-255
- Klominsky J, Rieder M, Kieft C, L Mraz (1971) Heyrovskyite $6(\text{Pb}_{0.86}\text{Bi}_{0.08}(\text{AgCu})_{0.04})\text{Sb}_2\text{S}_3$ from Hurky, Czechoslovakia; new mineral of genetic interest. *Mineralium Deposita* 6:133-147
- Knop O, Ibrahim MA (1961) Chalcogenides of the transition elements. II. Existence of the π phase in the M_9S_8 section of the system Fe-Co-Ni-S. *Can J Chem* 39:297-317
- Kobayashi H, Kamimura T, Ohishi Y, Takeshita N, Mori N (2005) Structural and electrical properties of stoichiometric FeS compounds under high pressure at low temperature. *Phys Rev B* 71:014110/1-014110/7
- Kobayashi H, Sato M, Kamimura T, Sakai M, Onodera H, Kuroda N, Yamaguchi Y (1997) The effect of pressure on the electronic states of FeS and Fe_7S_8 studied by Mössbauer spectroscopy. *J Phys: Cond Matt* 9:515-527
- Kojima S, Sugaki A (1984) Phase relations in the central portion of the Cu-Fe-Zn-S system between 800 ° and 500 °C. *Mineral J Japan* 12:15-28
- Kojima S, Sugaki A (1985) Phase relations in the Cu-Fe-Zn-S system between 500 ° and 300 °C under hydrothermal conditions. *Econ Geol* 80:158-171
- Kracek FC (1946) Phase relations in the system sulfur-silver and the transitions in silver sulfide. *Trans, Am Geophys Union* 27:364-374
- Kraft A, Stiller H, Vollstädt H (1982) The monosulfide solid solution in the Fe-Ni-S system; relationship to the Earth's core on the basis of experimental high-pressure investigations. *Phys Earth Planet Int* 27:255-262
- Krestovnikov AN, Mendelevich AY, Glazov VM (1968) Phase equilibria in the Cu_2S - Ag_2S system. *Inorganic Mat* 4:1047-1048
- Kretschmar U, Scott SD (1976) Phase relations involving arsenopyrite in the system Fe-As-S and their application. *Can Mineral* 14:364-386
- Krupp RE (1994) Phase relations and phase transformations between the low-temperature iron sulfides mackinawite, greigite and smythite. *Eur J Mineral* 6:265-278

- Kruse O (1990) Mössbauer and X-ray study of the effects of vacancy concentration in synthetic hexagonal pyrrhotites. *Am Mineral* 75:755-763
- Kruse O (1992) Phase transitions and kinetics in natural FeS measured by X-ray diffraction and Mössbauer spectroscopy at elevated temperatures. *Am Mineral* 77:391-398
- Kullerud G (1953) The FeS-ZnS system a geological thermometer. *Norsk Geol Tids* 32:61-147
- Kullerud G (1961) Two-liquid field in the Fe-S system. *Carnegie Inst Wash, Year Book* 60:174-176
- Kullerud G (1963) Thermal stability of pentlandite. *Can Mineral* 7:353-366
- Kullerud G (1965a) Covellite stability relations in the Cu-S system. *Freiberger Forschungshefte B* 186C:145-160
- Kullerud G (1965b) The mercury-sulfur system. *Carnegie Inst Wash, Year Book* 64:193-195
- Kullerud G (1967a) The Fe-Mo-S system. *Carnegie Inst Wash, Year Book* 65:337-342
- Kullerud G (1967b) Sulfide studies. *In: Researches in Geochemistry*, Vol 2. Abelson PH (ed) John Wiley and Sons, p 286-321
- Kullerud G (1969) The lead-sulfur system. *Am J Sci* 267-A:233-267
- Kullerud G, Yoder HS (1959) Pyrite stability relations in the Fe-S system. *Econ Geol* 54:533-572
- Kullerud G, Yund RA (1962) The Ni-S system and related minerals. *J Petrol* 3:126-175
- Kullerud G, Yund RA, Moh GH (1969) Phase relations in the Cu-Fe-S, Cu-Ni-S and Fe-Ni-S systems. *In: Magmatic ore deposits*. Wilson HDB (ed) *Econ Geol Mono* 4, p 323-343
- Kusaba K, Syono Y, Kikegawa T, Simomura O (1997) Structure of FeS under high pressure. *J Phys Chem Solids* 58:241-246
- Kusaba K, Syono Y, Kikegawa T, Simomura O (1998) Structures and phase equilibria of FeS under high pressure and temperature. *In: Properties of Earth and Planetary Materials at High Pressure and Temperature*. AGU, Washington DC, p 297-305
- Kutoglu A (1969) Rönt genographische und thermische Untersuchungen in Quasibinären system PbS-As₂S₃. *Neues Jahrb Mineral, Monat* 68-72
- Kuznetsov VG, Sokolova MA, Palkina KK, Popova ZV (1965) System cobalt-sulfur. *Izvest Akad Nauk USSR Neorgan Mat* 1:675-689
- Lamprecht G (1978) Phase relations within the Co-Ni-S system below 1000 °C. *Neues Jahrb Mineral, Monat* 176-191
- Lamprecht G, Hanus D (1973) Phase equilibrium relations in the ternary system Co-Ni-S. *Neues Jahrb Mineral, Monat* 236-240
- Lange W, Schlegel H (1951) Die Zustandbilder des Systeme Eisen-Antimon-Schwefel und Kobalt-Antimon-Schwefel. *Z Metall* 42:257-268
- Larimer JW (1968) An experimental investigation of oldhamite CaS and the petrologic significance of oldhamite in meteorites. *Geochim Cosmochim Acta* 32:965-982
- Lawson AC (1972) Lattice instabilities in superconducting ternary molybdenum sulfides. *Mat Res Bull* 7:773-776
- Le Bihan M-Th (1963) Étude structurale de quelques sulfures de plomb et d'arsenic naturels du gisement de Binn. *Mineral Soc Am Spec Paper* 1:149-152
- Learned RE (1966) The solubilities of quartz quartz-cinnabar and cinnabar-stibnite in sodium sulfide solutions and their implications for ore genesis. PhD Thesis, University of California, Riverside
- Learned RE, Tunnell G, Dickson FW (1974) Equilibria of cinnabar stibnite and saturated solutions in the system HgS-Sb₂S₃-Na₂S-H₂O from 150 ° to 250 °C at 100 bars with implications concerning ore genesis. *J Res U.S. Geol Surv* 2:457-466
- Lennie AR, Vaughan DJ (1996) Spectroscopic studies of iron sulfide formation and phase relations at low temperatures. *In: Mineral spectroscopy: A tribute to Roger G Burns*. *Spec Publ Geochem Soc* 5:117-131
- Lennie AR, England KER, Vaughan DJ (1995a) Transformation of synthetic mackinawite to hexagonal pyrrhotite: A kinetic study. *Am Mineral* 80:960-967
- Lennie AR, Redfern SAT, Champness PE, Stoddart CP, Schofield PF, Vaughan DJ (1997) Transformation of mackinawite to greigite; an in situ X-ray powder diffraction and transmission electron microscope study. *Am Mineral* 82:302-309
- Lennie AR, Redfern SAT, Schofield PF, Vaughan DJ (1995b) Synthesis and Rietveld crystal structure refinement of mackinawite tetragonal FeS. *Mineral Mag* 59:677-683
- Leonard BF, Desborough GA, Page NJ (1969) Ore microscopy and chemical composition of some lavrites. *Am Mineral* 54:1330-1346
- Lewis GN, Randall M (1961) *Thermodynamics*, 2nd ed. McGraw-Hill
- Li F, Franzen HF (1996) Ordering, incommensuration, and phase transitions in pyrrhotite, Part II: A high-temperature X-ray powder diffraction and thermomagnetic study. *J Solid State Chem* 126:108-120
- Li F, Franzen HF, Kramer MJ (1996) Ordering, incommensuration, and phase transitions in pyrrhotite, Part I: A TEM study of Fe₇S₈. *J Solid State Chem* 124:264-271
- Lin J-F, Fei Y, Sturhahn W, Zhao J, Mao H, Hemley RJ (2004) Magnetic transition and sound velocities of Fe₃S at high pressure: implications for Earth and planetary cores. *Earth Planet Sci Lett* 226:33-40

- Lin RY, Hu DC, Chang YA (1978) Thermodynamics and phase relations of transition metal-sulfur systems: II The nickel-sulfur system. *Metall Trans B* 9B 531-538
- Liu H, Chang LLY (1994) Phase relations in the system PbS-PbSe-PbTe. *Mineral Mag* 58:567-578
- Liu M, Fleet ME (2001) Partitioning of siderophile elements (W Mo As Ag Ge Ga and Sn) and Si in the Fe-S system and their fractionation in iron meteorites. *Geochim Cosmochim Acta* 65:671-682
- Lundqvist D (1947) X-ray studies in the ternary system Fe-Ni-S. *Arkiv Kemi Mineral Geol* 24A, No 22, 12p
- Lusk J, Bray DM (2002) Phase relations and the electrochemical determination of sulfur fugacity for selected reactions in the Cu-Fe-S and Fe-S systems at 1 bar and temperatures between 185 and 460 °C. *Chem Geol* 192:227-248
- Lusk J, Calder BOE (2004) The composition of sphalerite and associated sulfides in reactions of the Cu-Fe-Zn-S, Fe-Zn-S and Cu-Fe-S systems at 1 bar and temperatures between 250 and 535 °C. *Chem Geol* 203: 319-345
- Lusk J, Ford CE (1978) Experimental extension of the sphalerite geobarometer to 10 kbar. *Am Mineral* 63: 516-519
- Lusk J, Scott SD, Ford CE (1993) Phase relations in the Fe-Zn-S system to 5 kbars and temperatures between 325 ° and 150 °C. *Econ Geol* 88:1880-1903
- MacLean WH, Cabri LJ, Gill JE (1972) Exsolution products in heated chalcopyrite. *Can J Earth Sci* 9:1305-1317
- Makovicky E (2002) Ternary and quaternary phase systems with PGE. *In: The geology geochemistry, mineralogy and mineral beneficiation of platinum-group elements*. CIM Special Volume 54. Cabri LJ (ed) Can Inst Mining Metall Petroleum, p 131-175
- Mandziuk ZL, Scott SD (1977) Synthesis, stability and phase relations of argentian pentlandite in the system Ag-Fe-Ni-S. *Can Mineral* 15:349-364
- Marfunin AS (1979) *Physics of Minerals and Inorganic Compounds*. Springer-Verlag
- Mariano AN, Warekois EP (1963) High pressure phases of some compounds of groups II-VI. *Science* 142: 672-673
- Markham NL (1962) Plumbian ikonolite from Kingsgate, New South Wales. *Am Mineral* 47:1431-1434
- Marshall WG, Nelmes RJ, Loveday JS, Klotz S, Besson JM, Hamel G, Parise JB (2000) High-pressure diffraction study of FeS. *Phys Rev B* 61:11201-11204
- Martín JD, Gil ASI (2005) An integrated thermodynamic mixing model for sphalerite geobarometry from 300 to 850 °C and up to 1 GPa. *Geochim Cosmochim Acta* 69:995-1006
- Martin P, Price GD, Vočadlo L (2001) An *ab initio* study of the relative stabilities and equations of state of FeS polymorphs. *Mineral Mag* 5:181-191
- Maske S, Skinner BJ (1971) Studies of the sulfosalts of copper. I. Phases and phase relations in the system Cu-As-S. *Econ Geol* 66:901-918
- Matoba M, Anzai S, Fujimori A (1994) Effect of early transition-metal (M=Ti V and Cr) doping on the electronic structure of charge-transfer type compound NiS studied by thermoelectric power and X-ray photoemission measurements. *J Phys Soc Japan* 63:1429-1440
- Mavrogenes JA, MacIntosh IW, Ellis DJ (2001) Partial melting of the Broken Hill galena-sphalerite ore: experimental studies in the system PbS-Fe-S-Zn-S-(Ag₂S). *Econ Geol* 96:205-210
- McCammon CA, Price DC (1982) A Mössbauer effect investigation of the magnetic behaviour of (Fe Co)S_{1+x} solid solutions. *J Phys Chem Solids* 43:431-437
- McKenzie WF, Helgeson HC (1985) Phase relations among silicates copper iron sulfides and aqueous solutions at magmatic temperatures. *Econ Geol* 80:1965-1973
- McKenzie WF, Helgeson HC (1987) Phase relations among silicates copper iron sulfides and aqueous solutions at magmatic temperatures – a reply. *Econ Geol* 82:501-502
- Merwin HE, Lombard RH (1937) The system Cu-Fe-S. *Econ Geol* 32:203-284
- Miller RO, Dacheille F, Roy R (1966) High pressure phase equilibrium studies of CdS and MnS by static and dynamic methods. *J Appl Phys* 37:4913-4918
- Misra KC, Fleet ME (1973) The chemical compositions of synthetic and natural pentlandite assemblages. *Econ Geol* 68:518-539
- Misra KC, Fleet ME (1974) Chemical composition and stability of violarite. *Econ Geol* 69:391-403
- Moh GH (1964) Blaubleibender covellite. *Carnegie Inst Wash, Year Book* 63:208-209
- Moh GH (1969) The tin-sulfur system and related minerals. *Neues Jahrb Mineral, Abhdl* 111:227-263
- Moh GH (1971) Blue-remaining covellite and its relations to phases in the sulfur-rich portion of the copper sulfur system at low temperatures. *Mineral Soc Japan Spec Paper* 1:226-232
- Moh GH (1973) Das Cu-W-S system und seine Mineralien sowie ein neues Tungstenit vorkommen in Kipushi/Katanga. *Mineralium Deposita* 8:291-300
- Moh GH (1975) Tin-containing mineral systems: Part II. Phase relations and mineral assemblages in the Cu-Fe-Zn-Sn-S system. *Chemie der Erde* 34:1-61
- Moh GH, Berndt F (1964) Two new natural tin sulfides Sn₂S₃ and SnS₂. *Neues Jahrb Mineral, Monat* 94-95

- Moore DE, Dixon FW (1973) Phases of the system Sb_2S_3 - As_2S_3 . *Trans. Am Geophys Union* 54:1223-1224
- Mootz D, Puhl H (1967) Crystal structure of Sn_2S_3 . *Acta Crystallogr* 23:471-476
- Morimoto N (1962) Djurleite, a new copper sulphide mineral. *Mineral J Japan* 3:338-344
- Morimoto N (1970) Crystal-chemical studies on the Cu-Fe-S system. *In: Volcanism and ore genesis*. Tatsumi T (ed) University of Tokyo Press
- Morimoto N, Clark LA (1961) Arsenopyrite crystal-chemical relations. *Am Mineral* 46:1448-1469
- Morimoto N, Gyobu A (1971) The composition and stability of digenite. *Am Mineral* 56:1889-1909
- Morimoto N, Koto K (1970) Phase relations of the Cu-S system at low temperatures: stability of anilite. *Am Mineral* 55:106-117
- Morimoto N, Kullerud G (1962) The Mo-S system. *Carnegie Inst Wash, Year Book* 61:143-144
- Morimoto N, Kullerud G (1963) Polymorphism in digenite. *Am Mineral* 48:110-123
- Morimoto N, Kullerud G (1966) Polymorphism on the Cu_9S_5 - Cu_5FeS_4 join. *Z Kristallogr* 123:235-254
- Morimoto N, Gyobu A, Mukaiyama H, Izawa E (1975a) Crystallography and stability of pyrrhotites. *Econ Geol* 70:824-833
- Morimoto N, Gyobu A, Tsukuma K, Koto K (1975b) Superstructure and nonstoichiometry of intermediate pyrrhotite. *Am Mineral* 60:240-248
- Morimoto N, Koto K, Shimazaki Y (1969) Anilite Cu_7S_5 a new mineral. *Am Mineral* 54:1256-1268
- Mukaiyama H, Izawa E (1970) Phase relations in the Cu-Fe-S system the copper-deficient part. *In: Volcanism and Ore Genesis*. Tatsumi T (ed) University of Tokyo Press, p 339-355
- Mumme WG, Sparrow GJ, Walker GS (1988) Roxbyite a new copper sulphide mineral from the Olympic Dam deposit, Roxby Downs, South Australia. *Mineral Mag* 52:323-330
- Munson RA (1966) Synthesis of copper disulfide. *Inorg Chem* 5:1296-1297
- Murowchick JB, Barnes HL (1986a) Formation of cubic FeS. *Am Mineral* 71:1243-1246
- Murowchick JB, Barnes HL (1986b) Marcasite precipitation from hydrothermal solutions. *Geochim Cosmochim Acta* 50:2615-2629
- Nagao I (1955) Chemical studies on the hot springs of Nasu. *Nippon Kageke Zasshi* 76:1071-1073
- Nakamura M, Fujimori A, Sacchi M, Fuggle JC, Misu A, Mamori T, Tamura H, Matoba M, Anzai S (1993) Metal-nonmetal transition in NiS induced by Fe and Co substitution: X-ray-absorption spectroscopic study. *Phys Rev B* 48:16942-16947
- Nakazawa H, Osaka T, Sakaguchi K (1973) A new cubic iron sulphide prepared by vacuum deposition. *Nature, Phys Sci* 242:13-14
- Nakazawa K, Morimoto N (1971) Phase relations and superstructures of pyrrhotite $Fe_{1-x}S$. *Mat Res Bull* 6:345-358
- Naldrett AJ (1989) *Magmatic Sulfide Deposits*. Oxford Monographs on Geology and Geophysics, No 14, Clarendon Press
- Naldrett AJ, Kullerud G (1966) Limits of the $Fe_{1-x}S$ - $Ni_{1-x}S$ solid solution between 600 °C and 250 °C. *Carnegie Inst Wash, Year Book* 65:320-327
- Naldrett AJ, Craig JR, Kullerud G (1967) The central portion of the Fe-Ni-S system and its bearing on pentlandite exsolution in iron-nickel sulfide ores. *Econ Geol* 62:826-847
- Nelmes RJ, McMahon MI, Belmonte SA, Parise JB (1999) Structure of the high-pressure phase III of iron sulphide. *Phys Rev B* 59:9048-9052
- Nozaki H, Nakazawa H, Sakaguchi K (1977) Synthesis of mackinawite by vacuum deposition method. *Mineral J Japan* 8:399-405
- Ohtsuki T, Kitakaze A, Sugaki A (1981b) Synthetic minerals with quaternary components in the system Cu-Fe-Sn-S: Synthetic sulfide minerals (X). *Science Reports, Tohoku University, Series 3. Mineral Petrol Econ Geol* 14:269-282
- Ohtsuki T, Sugaki A, Kitakaze A (1981a) Three new phases in the system Cu-Fe-Sn-S: Synthetic sulfide minerals, XI. *Science Reports, Tohoku University, Series 3. Mineral Petrol Econ Geol* 15:79-87
- Okazaki A (1959) The variation of superstructure in iron selenide Fe_7Se_8 . *J Phys Soc Japan* 14:112-113.
- Okazaki A (1961) The superstructures of iron selenide Fe_7Se_8 . *J Phys Soc Japan* 16:1162-1170
- Ontoev DO (1964) Characteristic features of bismuth mineralization in some tungsten deposits of Eastern Transbaikal. *Trudy Mineral Muz Akad Nauk USSR* 15:134-153
- Osadchii EG (1986) Solid solutions and phase relations in the system Cu_2SnS_3 - ZnS - CdS at 850 ° and 700 °C. *Neues Jahrb Mineral, Abhdl* 155:23-38
- Otto HH, Strunz H (1968) Zur Kristallchemie synthetischer Blei - Wismut - Spiessglanze. *Neues Jahrb Mineral, Abhdl* 108:1-19
- Ozawa K, Anzai S (1966) Effect of pressure on the α -transition point of iron monosulphide. *Phys Stat Sol* 17:697-700
- Parise JB, Moore FH (1981) A superstructure of α - Ni_7S_6 and its relationship to heazlewoodite (Ni_3S_2) and millerite (NiS). *Twelfth Internat Conf Crystallogr, Collected Abstracts*, C-182

- Peacock MA, McAndrew J (1950) On parkerite and shandite and the crystal structure of $\text{Ni}_3\text{Pb}_2\text{S}_2$. *Am Mineral* 35:425-439
- Pearce CI, Patrick RAD, Vaughan DJ (2006) Electrical and Magnetic properties of sulfides. *Rev Mineral Geochem* 61:127-180
- Pettit FS (1964) Thermodynamic and electrical investigations on molten antimony sulfide. *J Chem Phys* 38:9-20
- Pichulo RO (1979) Polymorphism and phase relations in iron(II) sulfide (troilite) at high pressure. PhD Thesis, Columbia University
- Plovnick RH, Vlasse M, Wold A (1968) Preparation and structural properties of some ternary chalcogenides of titanium. *Inorg Chem* 7:127-129
- Pósfai M, Buseck PR (1994) Djurleite digenite and chalcocite: intergrowths and transformations. *Am Mineral* 79:308-315
- Pósfai M, Dódony I (1990) Pyrrhotite superstructures. Part I: Fundamental structures of the NC (N = 2, 3, 4 and 5) type. *Eur J Mineral* 2:525-528
- Potter RWII (1973) The systematics of polymorphism in binary sulfides: I. Phase equilibria in the system mercury-sulfur. II. Polymorphism in binary sulfides. PhD Thesis, Pennsylvania State University
- Potter RWII (1977) An electrochemical investigation of the system copper-sulfur. *Econ Geol* 72:1524-142
- Potter RWII, Evans HTJr (1976) Definitive X-ray powder data for covellite anilite djurleite and chalcocite. *J Res U.S. Geol Surv* 4:205-212
- Powell AV, Vaqueiro P, Knight KS, Chapon LC, Sánchez RD (2004) Structure and magnetism in synthetic pyrrhotite Fe_7S_8 : A powder neutron-diffraction study. *Phys Rev B* 70:014415-1-014415-12
- Power LF, Fine HA (1976) The iron-sulphur system part 1: the structures and physical properties of the compounds of the low-temperature phase fields. *Mineral Sci Engin* 8:106-128
- Putnis A (1974) Electron-optical observations on the α -transition in troilite. *Science* 186:439-440
- Putnis A (1976) Observations of transformation behavior in Ni_7S_6 by transmission electron microscopy. *Am Mineral* 61:322-535
- Putnis A, Grace J (1976) The transformation behaviour of bornite. *Contrib Mineral Petrol* 55:311-355
- Radtke AS, Taylor CM, Heropoulos C (1973) Antimony-bearing orpiment, Carlin gold deposit, Nevada. *J Res U.S. Geol Surv* 1:85-87
- Radtke AS, Taylor CM, Dickson FW, Heropoulos C (1974) Thallium bearing orpiment, Carlin Gold deposit, Nevada. *J Res U.S. Geol Surv* 2:341-342
- Radtke AS, Taylor CM, Erd RC, Dickson FW (1974) Occurrence of lorandite TlAsS_2 at the Carlin gold deposit, Nevada. *Econ Geol* 69:121-124
- Raghavan V (1988) The Co-Fe-S system. *In: Phase diagrams of ternary iron alloys, Part 2. Indian Institute of Metals, Calcutta*, p 93-106
- Rau H (1965) Thermodynamische Messungen an SnS. *Berichte der Bunsen-Gesellschaft* 69:731-736
- Rau H (1976) Range of homogeneity and defect energetics in Co_{1-x}S . *J Phys Chem Solids* 37:931-934
- Raybaud P, Hafner J, Kresse G, Toulhoat H (1997) Ab initio density functional studies of transition-metal sulphides: II. Electronic structure. *J Phys: Cond Matt* 9:11107-11140
- Richardson FD, Jeffes JHE (1952) The thermodynamics of substances of interest in iron and steel making: III. Sulphides. *J Iron Steel Inst* 171:165-175
- Rickard DT (1968) Synthesis of smythite- rhombohedral Fe_3S_4 . *Nature* 218:356-357
- Rickard DT (1972) Covellite formation in low temperature aqueous solution. *Mineralium Deposita* 7:180-188
- Ritvo G, White GN, Dixon JB (2003) A new iron sulfide precipitated from saline solutions. *Soil Sci Soc Am J* 67:1303-1308
- Robie RA, Hemingway BS, Fisher JR (1978) Thermodynamic properties of minerals and related substances at 29815 K and 1 bar (10^5 Pascals) pressure and at higher temperatures. *Geol Surv Bull* 1452, U.S. Govt Printing Office, Washington DC
- Robie RA, Seal RRII, Hemingway BS (1994) Heat capacity and entropy of bornite (Cu_5FeS_4) between 6 and 760 K and the thermodynamic properties of phases in the system Cu-Fe-S. *Can Mineral* 32:945-956
- Roland GW (1968) Synthetic trechmannite. *Am Mineral* 53:1208-1214
- Roland GW (1970) Phase relations below 575 °C in the system Ag-As-S. *Econ Geol* 65:241-252
- Rooymans CJM (1969) The behaviour of some groups of chalcogenides under very-high-pressure conditions. *In: Advances in High Pressure Research. Vol. 2. Bradley RS (ed) Academic Press, London*, p 1-100
- Rösch H, Hellner E (1959) Hydrothermale untersuchungen am system $\text{PbS-As}_2\text{S}_3$. *Naturwissenschaften* 46:72
- Roseboom EH (1962) Djurleite Cu_{106}S a new mineral. *Am Mineral* 47:1181-1183
- Roseboom EH (1966) An investigation of the system Cu-S and some natural copper sulfides between 25 ° and 700 °C. *Econ Geol* 61:641-672
- Roseboom EH, Kullerud G (1958) The solidus in the system Cu-Fe-S between 400 °C and 800 °C. *Carnegie Inst Wash, Year Book* 57:222-227
- Rosenqvist T (1954) A thermodynamic study of the iron cobalt and nickel sulfides. *J Iron Steel Inst* 176:37-57

- Roy R Majumdar AJ, Hulbe CW (1959) The Ag_2S and Ag_2Se transitions as geologic thermometers. *Econ Geol* 54:1278-1280
- Roy-Choudhury K (1974) Experimental investigations on the solid solution series between Cu_2SnS_3 and $\text{Cu}_2\text{ZnSnS}_4$ (kesterite). *Neues Jahrb Mineral, Monat* 432-434
- Rueff JP, Kao CC, Struzhkin VV, Badro J, Shu J, Hemley RJ, Mao HK (1999) Pressure-induced high-spin to low-spin transition in FeS evidenced by X-ray emission spectroscopy. *Phys Rev Lett* 82:3284-3287
- Sack RO, Ebel DS (2006) Thermochemistry of sulfide mineral solutions. *Rev Mineral Geochem* 61:265-364
- Sakkopoulos S, Vitoratos E, Argyreas T (1984) Energy-band diagram for pyrrhotite. *J Phys Chem Solids* 45: 923-928
- Salanci B (1965) Untersuchungen am System Bi_2S_3 -PbS. *Neues Jahrb Mineral, Monat* 384-388
- Salanci B, Moh GH (1969) Die experimentelle Untersuchung des pseudobinären Schnittes PbS- Bi_2S_3 innerhalb des Pb-Bi-S systems in Beziehung zu natürlichen Blei - Bismut - Sulfosalzen. *Neues Jahrb Mineral, Abhdl* 112:63-95
- Sanloup C, Fei Y (2004) Closure of the Fe-S-Si liquid miscibility gap at high pressure. *Phys Earth Planet Int* 147:57-65
- Sanloup C, Guyot F, Gillet P, Fei Y (2002) Physical properties of liquid Fe alloys at high pressure and their bearings on the nature of metallic planetary cores. *J Geophys Res* 107(B11):2272-2280
- Sato H, Mihara T, Furuta A, Tamura M, Mimura K, Happo N, Taniguchi M, Ueda Y (1997) Chemical trend of occupied and unoccupied Mn 3d states in MnY (Y=S SeTe). *Phys Rev B* 56:7222-7231
- Schenck R, von der Forst P (1939) Gleichgewichtsstudien an erzbildenden Sulfiden II. *Z Anorganische und Allgemeine Chemie* 240:145-157
- Schenck R, Hoffman I, Knepper W, Vogler H (1939) Gleichgewichtsstudien über erzbildende Sulfide, I. *Z Anorganische und Allgemeine Chemie* 240:178-197
- Schlegel H, Schüller A (1952) Die Schmelz- und Kristallisations-gleichgewichte im System Cu-Fe-S und ihre Bedeutung für Kupfergewinnung. *Freiberger Forschungshefte B* No 2:1-32
- Schneeberg EP (1973) Sulfur fugacity measurements with the electrochemical cell $\text{Ag}/\text{AgI}/\text{Ag}_{2+},\text{Sf}(\text{S}_2)$. *Econ Geol* 68:507-517
- Schüller A, Wholmann E (1955) Betekinitite ein neues Blei-Kupfer-Sulfid aus dem Mansfelder Rücken. *Geologie* 4:535-555
- Schwarz HP, Scott SD, Kissin SA (1975) Pressures of formation of iron meteorites from sphalerite compositions. *Geochim Cosmochim Acta* 39:1457-1466
- Schwarz EJ, Vaughan DJ (1972) Magnetic phase relations of pyrrhotite. *J Geomag Geoelect* 24:441-458
- Scott SD (1973) Sphalerite geothermometry and geobarometry. *Econ Geol* 66:653-669
- Scott SD (1976) Application of the sphalerite geobarometer to regionally metamorphosed terrains. *Am Mineral* 61:661-670
- Scott SD, Barnes HL (1969) Hydrothermal growth of single crystals of cinnabar (red HgS). *Mat Res Bull* 4: 897-904
- Scott SD, Barnes HL (1971) Experimental calibration of the sphalerite geobarometer. *Econ Geol* 68:466-474
- Scott SD, Barnes HL (1972) Sphalerite-wurtzite equilibria and stoichiometry. *Geochim Cosmochim Acta* 36: 1275-1295
- Scott SD, Kissin SA (1973) Sphalerite composition in the Zn-Fe-S system below 300 °C. *Econ Geol* 68:75-479
- Seal RRII, Inan EE, Hemingway BS (2001) The Gibbs free energy of nukundamite ($\text{Cu}_{338}\text{Fe}_{062}\text{S}_4$): A correction and implications for phase equilibria. *Can Mineral* 39:1635-1640
- Secco RA, Rutter MD, Balog SP, Liu H, Rubie DC, Uchida T, Frost D, Wang Y, Rivers M, Sutton SR (2002) Viscosity and density of Fe-S liquids at high pressure. *J Phys: Cond Matt* 14:1325-11330
- Shannon RD (1976) Revised effective ionic radii and systematic studies of interatomic distances in halides and chalcogenides. *Acta Crystallogr A* 32:751-767
- Sharma RC, Chang YA (1980) Thermodynamics and phase relationships of transition metal-sulfur systems: IV. Thermodynamic properties of the nickel-sulfur liquid phase and calculation of Ni-S phase diagram. *Metall Trans B* 11B:139-146
- Shelton KL, Merewether PA, Skinner BJ (1981) Phases and phase relations in the system Pd-Pt-Sn. *Can Mineral* 19:599-605
- Sherman DM (1995) Stability of possible Fe-FeS and Fe-FeO alloy phases at high pressure and the composition of the Earth's core. *Earth Planet Sci Lett* 132:87-98
- Shewman RW, Clark LA (1970) Pentlandite phase relations in the Fe-Ni-S system and notes on the monosulfide solid solution. *Can J Earth Sci* 7:67-85
- Shimada K, Mizokawa T, Mamiya K, Saitoh T, Fujimori A, Ono K, Kakizaki A, Ishii T, Shirai M, Kamimura T (1998) Spin-integrated and spin-resolved photoemission study of Fe chalcogenides. *Phys Rev B* 57: 8845-8853
- Shunk FA (1969) *Constitution of Binary Alloys*, Supplement No 2. McGraw-Hill

- Silverman MS (1964) High-temperature high-pressure synthesis of a new bismuth sulfide. *Inorg Chem* 3:1041
- Skinner BJ (1966) The system Cu-Ag-S. *Econ Geol* 61:1-26
- Skinner BJ (1970) Stability of the tetragonal polymorph of Cu_2S . *Econ Geol* 65:724-730
- Skinner BJ, Luce FD (1971) Solid solutions of the type $(\text{CaMgMnFe})\text{S}$ and their use as geothermometers for the enstatite chondrites. *Am Mineral* 56:1269-1296
- Skinner BJ, Erd RC, Grimaldi FS (1964) Greigite the thio-spinel of iron; a new mineral. *Am Mineral* 49:543-555
- Skinner BJ, Jambor JL, M Ross (1966) Mckinstryite a new copper-silver sulfide. *Econ Geol* 61:1383-1389
- Skinner BJ, Luce FD, Makovicky E (1972) Studies of the sulfosalts of copper. III. Phases and phase relations in the system Cu-Sb-S. *Econ Geol* 67:924-938
- Snetsinger KG (1971) Erlichmanite (OsS_2), a new mineral. *Am Mineral* 56:1501-1506
- Somanchi S (1963) Subsolidus phase relations in the systems Ag-Sb and Ag-Sb-S. MS Thesis, McGill University
- Springer G (1969) Naturally occurring compositions in the solid solution series Bi_2S_3 - Sb_2S_3 . *Mineral Mag* 37:295-296
- Springer G, LaFlamme JHG (1971) The system Bi_2S_3 - Sb_2S_3 . *Can Mineral* 10:847-853
- Stemprok M (1967) The Bi-Mo-S system. *Carnegie Inst Wash, Year Book* 65:336-337
- Stemprok M (1971) The Fe-W-S system and its geological application. *Mineralium Deposita* 6:302-312
- Strunz H, Geier BH, Seeliger E (1958) Gallit CuGaS_2 das erste selbständige Gallium-Mineral und seine Paragenese in Tsumeb. *Neues Jahrb Mineral, Monat* 85-96
- Stubbles JR, Birchenall CS (1959) A redetermination of the lead-lead sulfide equilibrium between 585 °C and 920 °C. *Trans, AIMME* 215:535-538
- Sugaki A, Kitakaze A (1998) High form of pentlandite and its thermal stability. *Am Mineral* 83:133-140
- Sugaki A, Shima H (1972) Phase relations of the Cu_2S - Bi_2S_3 system. *Technical Reports of Yamaguchi University*, p 45-70
- Sugaki A, Shima H (1977) On solvuses of solid solutions among troilite hexagonal and monoclinic pyrrhotites below 300 °C - Studies on pyrrhotite group minerals (3)- *Science Reports, Tohoku University, Series 3*, 13:147-163
- Sugaki A, Kitakaze A, Hayashi K (1984) Hydrothermal synthesis and phase relations of the polymetallic sulfide system, especially on the Cu-Fe-Bi-S system. *In: Materials Science of the Earth's Interior. Terra Science*, p 545-583
- Sugaki A, Kitakaze A, Hayashi T (1982) High-temperature phase of pentlandite. *Annual Meeting of the Mineralogical Society of Japan, Abstracts* 22 (in Japanese)
- Sugaki A, Kitakaze A, Kitazawa H (1985) Synthesized tin and tin-silver sulfide minerals: Synthetic sulfide minerals (XIII). *Science Reports, Tohoku University, Series 3. Mineral Petrol Econ Geol* 16:199-211
- Sugaki A, Kitakaze A, Shimizu Y (1982) Phase relations in the Cu_3AsS_4 - Cu_3SbS_4 join. *Science Reports, Tohoku University, Series 3. Mineral Petrol Econ Geol* 15:257-271
- Sugaki A, Shima H, Kitakaze A (1972) Synthetic sulfide minerals (IV). *Technical Reports of Yamaguchi University* 1:71-77
- Sugaki A, Shima H, Kitakaze A, Harada H (1975) Isothermal phase relations in the system Cu-Fe-S under hydrothermal conditions at 350 °C and 300 °C. *Econ Geol* 70:806-823
- Sugaki A, Shima H, Kitakaze A, Fukuoka M (1977) Hydrothermal synthesis of pyrrhotites and their phase relation at low temperature - Studies on the pyrrhotite group minerals (4)- *Science Reports, Tohoku University, Series 3*, 13:165-182
- Sugaki A, Shima H, Kitakaze A, Mizota T (1981) Hydrothermal synthesis of nukundamite and its crystal structure. *Am Mineral* 66:398-402
- Suhr N (1965) The Ag_2S - Cu_2S system. *Econ Geol* 50:347-250
- Sutarno, Knop O, Reid KIG (1967) Chalcogenides of the transition elements. V. Crystal structures of the disulfides and ditellurides of ruthenium and osmium. *Can J Chem* 45:1391-1400
- Svendsen B, Anderson WW, Ahrens TJ, Bass JD (1989) Ideal Fe-FeS, Fe-FeO phase relations and Earth's core. *Phys Earth Planet Int* 55:154-186
- Takele S, Hearne GR (1999) Electrical transport magnetism and spin-state configurations of high-pressure phases of FeS. *Phys Rev B* 60:4401-4403
- Takeno S, Moh GH, Wang N (1982) Dry mackinawite syntheses. *Neues Jahrb Mineral, Abhdl* 144:297-301
- Takeno S, Zōka H, Nihara T (1970) Metastable cubic iron sulfide- with special reference to mackinawite. *Am Mineral* 55:1639-1649
- Tatsuka K, Morimoto N (1973) Composition variation and polymorphism of tetrahedrite in the Cu-Sb-S system below 400 °C. *Am Mineral* 58:425-434
- Taylor LA (1969) The significance of twinning in Ag_2S . *Am Mineral* 54:961-963
- Taylor LA (1970a) The system Ag-Fe-S: Phase equilibria and mineral assemblages. *Mineralium Deposita* 5:41-58

- Taylor LA (1970b) The system Ag-Fe-S: Phase relations between 1200 ° and 700 °C. *Metall Trans* 1:2523-2529
- Taylor LA (1970c) Low-temperature phase relations in the Fe-S system. *Carnegie Inst Wash, Year Book* 68: 259-270
- Taylor LA, Kullerud G (1971) Pyrite-type compounds. *Carnegie Inst Wash, Year Book* 69:322-325
- Taylor LA, Kullerud G (1972) Phase equilibria associated with the stability of copper disulfide. *Neues Jahrb Mineral, Monat* 458-463
- Taylor P, Rummery TE, Owen DG (1979) On the conversion of mackinawite to greigite. *J Inorg Nucl Chem* 41:595-596
- Tenaillon C, Etschmann B, Wang H, Pring A, Grguric BA, Studer A (2005) Thermal expansion of troilite and pyrrhotite determined by *in situ* cooling (873 to 373 K) neutron powder diffraction measurements. *Mineral Mag* 69:205-216
- Terukov EI, Roth S, Krabbes G, Oppermann H (1981) The magnetic properties of cobalt-doped iron sulphide $Fe_{1-y}Co_yS$ ($y \leq 0.13$). *Phys Stat Sol A* 68:233-238
- Tokonami M, Nishiguchi K, Morimoto N (1972) Crystal structure of a monoclinic pyrrhotite (Fe_7S_8). *Am Mineral* 57:1066-1080
- Tossell JA, Vaughan DJ (1992) *Theoretical Geochemistry: Applications of Quantum Mechanics in the Earth and Mineral Sciences*. Oxford University Press
- Toulmin PIII (1963) Proustite-pyrargyrite solid solutions. *Am Mineral* 48:725-736
- Toulmin PIII, Barton PB Jr (1964) A thermodynamic study of pyrite and pyrrhotite. *Geochim Cosmochim Acta* 28:641-671
- Toulmin PIII, Barton PB Jr, Wiggins LB (1991) Commentary on the sphalerite geobarometer *Am Mineral* 76: 1038-1051
- Townsend MG, Tremblay R, Horwood JL, Ripley LJ (1971) Metal-semiconductor transition in single crystal hexagonal nickel sulphide *J Physics C: Solid State Phys* 4 598-606
- Trail RJ, Boyle RW (1955) Hawleyite isometric cadmium sulfide a new mineral *Am Mineral* 40 555-559
- Tremel W, Hoffmann R, Silvestre J (1986) Transitions between NiAs and MnP type phases: An electronically driven distortion of triangular (3^6) nets. *J Am Chem Soc* 108:5174-5187
- Tunnell G (1964) Chemical processes in the formation of mercury ores and ores of mercury and antimony. *Geochim Cosmochim Acta* 28:1019-1037
- Ueno T, Scott SD (1994) Phase relations in the system Ga-Fe-S at 900 °C and 800 °C. *Can Mineral* 32:203-210
- Ueno T, Ito S-I, Nakatsuka S, Nakano K, Harada T, Yamazaki T (2000) Phase equilibria in the system Fe-Ni-S at 500 °C and 400 °C. *J Mineral Petrol Sci* 95:145-161
- Ueno T, Nagasaki K, Horikawa T, Kawakami M, Kondo K (2005) Phase equilibria in the system Cu-Ga-S at 500° and 400 °C. *Can Mineral* 43:1643-1651
- Ueno T, Scott SD, Kojima S (1996) Inversion between sphalerite and wurtzite-type structures in the system Zn-Fe-Ga-S. *Can Mineral* 34:949-958
- Urakawa S, Someya K, Terasaki H, Katsura T, Yokoshi S, Funakoshi K-I, Utsumi W, Katayama Y, Sueda Y-I, Irifune T (2004) Phase relationships and equations of state for FeS at high pressures and temperatures and implications for the internal structure of Mars. *Phys Earth Planet Int* 143-144:469-479
- Urazov GG, Bol'shakov KA, Federov PI, Vasilevskaya II (1960) The ternary bismuth-iron-sulfur system (a contribution to the theory of precipitation smelting of bismuth). *Russian J Inorg Chem* 5:303-307
- Valverde DN (1968) Phase diagram of the Cu-Ag-S system at 300 °C. *Z Physikalische Chemie (München)* 62: 218-220
- van Hook JJ (1960) The ternary system $Ag_2S-Bi_2S_3-PbS$. *Econ Geol* 55:759-788
- Vaughan DJ, Craig JR (1974) The crystal chemistry and magnetic properties of iron in the monosulfide solid solution of the Fe-Ni-S system. *Am Mineral* 59:926-933
- Vaughan DJ, Craig JR (1978) *Mineral chemistry of metal sulfides*. Cambridge University Press
- Vaughan DJ, Rosso KM (2006) Chemical bonding in sulfide minerals. *Rev Mineral Geochem* 61:231-264
- Viaene W (1968) Le systeme Fe-Ge-S a 700 °C. *Comptes Rendus de l'Académie des Sciences Paris* 266:1543-1545
- Viaene W (1972) The Fe-Ge-S system: phase equilibria. *Neues Jahrb Mineral, Monat* 23-35
- Viaene W, Kullerud G (1971) The Ti-S and Fe-Ti-S Systems. *Carnegie Inst Wash, Year Book* 70:297-299
- Vlach KC (1988) A study of sulfur pressures and phase relationships in the Fe-FeS-Co-CoS and Fe-Cr-S systems. PhD Thesis, University of Wisconsin, Madison, Wisconsin
- Vogel R (1953) Über das System Blei silber-schwefel. *Z Metallkunde* 44:133-135
- Vogel R (1956) The system bismuth sulfide-copper sulfide and the ternary system Bi-Bi₂S₃-Cu₂S-Cu. *Z Metallkunde* 47:694-699
- Vogel R (1968) Zur Entstehung des Daubr elith im meteorischen Eisen. *Neues Jahrb Mineral, Monat* 453-463

- Vollstädt H, Seipold U, Kraft A (1980) Structural and electrical relations of monosulphide solid solution in the Fe-Ni-S system at high pressures and temperatures. *Phys Earth Planet Int* 22:267-271
- Wang H, Pring A, Ngothai Y, O'Neill B (2005) A low-temperature kinetic study of the exsolution of pentlandite from the monosulfide solid solution using a refined Avrami method. *Geochim Cosmochim Acta* 69:415-425
- Wang N (1973) Phases on the pseudobinary join lead sulfide-antimony sulfide. *Neues Jahrb Mineral, Monat* 79-81
- Wang N (1974) The three ternary phases in the system Cu-Sn-S. *Neues Jahrb Mineral, Monat* 424-431
- Wang N (1984) A contribution to the Cu-Fe-S system: the sulfidization of bornite at low temperatures. *Neues Jahrb Mineral, Monat* 346-352
- Wang N (1988) Experimental study of the copper-germanium-sulfur ternary phases and their mutual relations. *Neues Jahrb Mineral, Abhdl* 159:137-151
- Ward JC (1970) The structure and properties of some iron sulphides. *Rev Pure Appl Chem* 20:175-206
- Wehmeier FH, Laudise RA, Shieves JW (1968) The system $\text{Ag}_2\text{S}-\text{As}_2\text{S}_3$ and the growth of crystals of proustite smithite and pyrrargyrite. *Mat Res Bull* 3:767-778
- Weissberg GA (1965) Getchellite AsSbS_3 a new mineral from Humboldt County, Nevada. *Am Mineral* 50:1817-1826
- Werner A (1965) Investigations on the system Cu-Ag-S. *Z Physikalische Chemie (München)* 47:267-285
- White RM, Mott NF (1971) The metal-non-metal transition in nickel sulphide (NiS). *Phil Mag* 24:845-856
- Wieggers GA, Jellinek F (1970) The system titanium-sulfur II The structure of Ti_3S_4 and Ti_4S_5 . *J Solid State Chem* 1:519-525
- Wieser E, Krabbes G, Terukov EI (1982) Detection of the metastable simultaneous occurrence of high- and low-temperature states in $\text{Co}_y\text{Fe}_{1-y}\text{S}$ by Mössbauer spectroscopy. *Phys Stat Sol A* 72:695-699
- Wiggins LB, Craig JR (1980) Reconnaissance of the Cu-Fe-Zn-S system: sphalerite phase relationships. *Econ Geol* 75:742-751
- Williamson DP, Grimes NW (1974) An X-ray diffraction investigation of sulphide spinels. *J Phys Appl Phys* 7:1-6
- Wolthers M, Van der Gaast SJ, Rickard D (2003) The structure of disordered mackinawite. *Am Mineral* 88:2007-2015
- Wuensch BJ (1974) Determination relationships and classification of sulfide mineral structures. *Rev Mineral* 1:W-1-WW-44
- Wuensch BJ, Buerger MJ (1963) The crystal structure of chalcocite Cu_2S . *Mineral Soc Am Spec Paper* 1:164-170
- Wyszomirski P (1976) Experimental studies of the ternary Fe-Co-S system in the temperature range 500-700 °C. *Mineralogica Polonica* 7:39-49
- Wyszomirski P (1977) Phase relations in the Fe-Co-S system at 800 °C. *Mineralogica Polonica* 8:75-78
- Wyszomirski P (1980) The pure dry Fe-Co-S system at 400 °C. *Neues Jahrb Mineral, Abhdl* 139:131-132
- Yagi T, Akimoto S (1976) Pressure fixed points between 100 and 200 kbar based on the compression of sodium chloride. *J Appl Phys* 47:3350-3354
- Ying-chen J, Yu-jen T (1973) Isomorphous system $\text{RuS}_2-\text{OsS}_2-\text{IrS}_2$ and the mineral system PdS-PtS. *Geochemia* 4:262-270
- Yu WD, Gidisse PJ (1971) High pressure polymorphism in CdS CdSe and CdTe. *Mat Res Bull* 6:621-638
- Yund RA (1962) System Ni-As-S: phase relations of mineralogical significance. *Am J Sci* 260:761-782
- Yund RA (1963) Crystal data for synthetic $\text{Cu}_{55}\text{Fe}_x\text{S}_{65x}$ (idaite). *Am Mineral* 48:672-676
- Yund RA, Hall HT (1968) The miscibility gap between FeS and Fe_{1-x}S . *Mat Res Bull* 3:779-784
- Yund RA, Kullerud G (1966) Thermal stability of assemblages in the Cu-Fe-S system. *J Petrol* 7:454-488
- Yusa K, Kitakaze A, Sugaki A (1979) Synthesized bismuth-tellurium-sulfur system: Synthetic sulfide minerals. *Science Reports Tohoku University Series 3: Mineral Petrol Econ Geol* 14:121-133
- Zelikman AN, Belyaevskaya LV (1956) The melting point of molybdenite. *Zhurnal Neorganicheskoi Khimii* 1:2239-2244
- Zhou Y, Campbell AJ, Heinz DL (1991) Equations of state and optical properties of the high pressure phase of zinc sulfide. *J Phys Chem Solids* 52:821-825